DEVELOPMENT OF A MODEL TO PREDICT EFFECTS OF MICROBIAL PREDATION ON LEAD PHASE DISTRIBUTION AND TOXICITY

A Dissertation

Presented to the Faculty of the Graduate School

of Cornell University

in Partial Fulfillment of the Requirements for the Degree of

Doctor of Philosophy

by

Leslie Elizabeth Patton

January 2007

DEVELOPMENT OF A MODEL TO PREDICT EFFECTS OF MICROBIAL PREDATION ON LEAD PHASE DISTRIBUTION AND TOXICITY

Leslie Elizabeth Patton, Ph.D.

Cornell University 2007

Interactions between microbial predators and their prey can significantly influence the behavior of toxic trace metals. Metals associated with bacterial prey can be released into the dissolved phase following digestion by a predator, and/or metals can remain in the predator and potentially be transferred to the next level of the food chain. Toxic metal ions in the aqueous phase are also expected to modify the growth and predation rate of a microbial predator. A defined predator-prey system was developed to study metal behavior in simple microbial food chains using lead (Pb) as a representative metal. Desired features of this system were the ability to define the chemical speciation of dissolved metals as well as to distinguish between prey and predator-bound metals. *Pseudomonas putida* and the ciliate protozoan *Tetrahymena thermophila* were selected as representative bacterial prey and predator species, respectively. Batch reactors were used to measure microbial growth parameters, effects of prey density on predation and Pb phase distribution. A mathematical model was developed to describe predator-prey dynamics and their influence on the behavior and fate of Pb. Growth data were used to obtain model parameters, and model simulations for Pb fractionation were compared to experimental observations.

The methodological studies demonstrated successful predator-prey separation techniques with little metal loss. Results of batch reactor experiments demonstrated that some kinetic parameters related to prey consumption and growth of *T. thermophila* are altered by Pb. Upon addition of predator to prey cells in equilibrium with dissolved Pb, dissolved and prey-bound Pb became associated with the predator through ingestion and adsorption. Ingested Pb was later excreted as a bound metal associated with *T. thermophila* waste matter. Experimental observations that did not match model predictions prompted further mathematical modeling of this predator-prey system. These simulations also explored Pb behavior under other hypothetical experimental conditions such as a chemostat reactor and a pulsed Pb dosing regime. The generality of the model was demonstrated by matching the trends in experimental data reported by other investigators for a different trace metal (Cd) in a different predator-prey system.

BIOGRAPHICAL SKETCH

Leslie Patton was born and raised in a suburb of Rochester, NY. She graduated from Pittsford-Mendon high school in 1991 and attended the University of Toronto and the University of Michigan. In 1996, she received her Bachelor of Science degree in Natural Resources from Michigan. She worked for Atlantic Ecology Division of the U.S. Environmental Protection Agency and the Ceimic Corporation, both of Narragansett, RI. In 1997 she began her PhD program at Cornell University with support from a 5-year training grant from the NIEHS. Leslie now resides in Silver Spring, MD.

This dissertation is dedicated to my husband Clint Nesbitt and to my son, Brody Patton Nesbitt.

ACKNOWLEDGEMENTS

The author wishes to acknowledge and thank her major advisor, Dr. Len Lion and her committee members, Dr. Michael Shuler, Dr. Murray McBride and Dr. Beth Ahner. Also thank you to Dr. Dave Goldberg of Drexel University for help with understanding the mathematical modeling portion of this research; to lab-mate and great friend Anna Spaulding for support and friendship; and to Ashley, Rory, Moose, Zeke and Peppy, the animals who helped make it all happen.

TABLE OF CONTENTS

LIST OF FIGURES

LIST OF TABLES

CHAPTER I

INTRODUCTION

The presence and fate of trace metals in the aquatic ecosystems are of interest because of their known toxic properties. The development of a system to predict trace metal behavior can be a useful guide in establishing regulations that protect the environment from the toxic effects of metals or as an aid in the design of strategies for effective removal of metals. The bioavailability of a toxic metal is an important determinant of the extent to which the metal can adversely affect an ecosystem. Bioavailability is determined by metal speciation [1] and the phase distribution of the metal. It is the species of metal rather than its absolute concentration that has the greatest effect on toxicity and bioavailability [1]. Metal speciation and phase distribution are governed by the interactions of a host of environmental conditions including: pH, redox state, and ionic strength, as well as environmental processes: sorption, complexation, and biological interactions. An important biological influence on trace metal cycling is microbial uptake of trace metals and their subsequent movement up the food chain. The microbial community has the potential to adsorb a significant amount of metals. For example, bacterial cells provide surfaces for lead adsorption [2,3]. Dissolved extracellular polymers of bacterial origin have well-established metal binding properties [4,3]. Metal uptake by microorganisms occurs at the root of food webs and is thus expected to be important in all environments, particularly benthic communities where toxic metals are typically sequestered.

Protozoa play an important role in the regeneration of mineral nutrients in marine and freshwater aquatic ecosystems [5]. Protozoa are also abundant at sewage treatment plants where high bacterial concentrations result in high protozoan concentrations. Curds reported 5×10^4 protozoan cells/ml in activated sludge as

compared to average limnic densities of around 1 x 10^3 cells/ml [6]. In fact, protozoa have been shown to increase the overall efficiency of sewage treatment. Curds showed that activated sludge with protozoa reduced organic matter substantially over protozoa-free sludge [6]. In nature, protozoa occur primarily in the benthos- the sediment and detritus at the bottom of lakes. When bacterivorous protozoa prey upon and metabolize bacteria, which tend to assimilate rather than regenerate nutrients, they can change the bioavailability of these nutrients and anything else bound to prey cells. Microzooplankton grazing is known to regenerate macronutrients like phosphorous and nitrogen in marine environments [7] and can regenerate particulate-bound Cd and Zn to the dissolved phase [8]. It is also feasible that metals initially bound to prey cells can bioaccumulate or biomagnify. Bioaccumulation is the process by which a contaminant is passed from prey to predator and assimilated into the biomass of the predator. This phenomenon has been demonstrated in the microbial loop with Se [9], Zn, Pb and Hg [10, 11] and Cd [11]. In *biomagnification*, the contaminant bioaccumulates *and* increases in concentration with each trophic level. Biomagnification of organic contaminants and metals alike has been studied extensively, particularly in higher animals like fish, birds, and mammals. Chen et al. showed biomagnification of Hg and Mn from the microplankton to macroplankton in a fresh water system [12].

This research focuses on lead (Pb) as a representative toxic metal. The toxic concentrations of environmental lead that we contend with today are a result of centuries of anthropogenic use. Civilizations as far back as the Bronze Age mined lead, which was employed in a variety of ways that resulted in human exposure such as the use of Pb for plumbing. The most significant recent source of lead contamination to the environment is from combustion of leaded gasoline [13].

Lead in paints and solder is the cause of most childhood lead-poisoning cases. Childhood exposure to even trace Pb levels has been linked to numerous developmental disorders including decreased IQ, learning disorders, decreased heme biosynthesis, elevated hearing threshold, and decreased serum levels of vitamin D [14]. There is no threshold blood-Pb concentration at which these symptoms do not exist so setting criteria for lead in soils and water has been difficult. The US EPA has set the tap water "action level" for Pb at 15 μg/L (if more than 10% of water samples exceed this level, action must be taken). The World Health Organization sets their Pb guidance level at 10 μg/L. There is a strong positive correlation between exposure to lead- contaminated soils and blood lead levels. Generally, the blood-Pb levels rise 3-7 μg/dl for every 1000 ppm increase in soil or dust concentrations. Toxicity may occur at blood-Pb levels of 10-15 μg/dl or possibly less [14]. Pb^{2+} sequesters in bone, perhaps via ion exchange with Ca^{2+}. Thus, even after blood-Pb levels have returned to safe levels, neurobehavioral effects can still occur as stored Pb is released from bones [15].

The long-term objective of this dissertation research was to contribute to the understanding of mechanisms of trace metal cycling in engineered and natural aquatic environments. The short-term objective was to devise a laboratory-scale model that could be used to study the influence of predation on cell-bound metals. The goal for the model is to predict trace metal cycling and biological uptake in an aquatic microbial ecosystem.

The remainder of this thesis is organized in the following manner: Chapter 2 describes the development of experimental methods for culturing predator and prey species, for measuring the adsorption of lead to their surfaces, and for separation of dissolved and particulate forms of Pb. This research examined Pb adsorption to protozoa and bacteria grown both axenically and xenically in a predator-prey system.

The second chapter also explores the potential for a second route of Pb uptake into the predator called pinocytosis. This is uptake through consumption of dissolved metal. The predator ingests dissolved metal along with the water flowing through its body in conjunction with consumption of prey. Finally, this chapter addresses how fluorescent microspheres can be used in lieu of a bacterium in studying Pb uptake by predation.

Chapter 3 describes investigation of the fate of prey-bound lead in a predator-prey system. It also describes the development of a mathematical model for Pb behavior based on growth parameters of the predator and prey, Pb adsorption isotherms, and observed toxic effects of Pb on growth. Laboratory measurements contribute to the formulation of a mathematical model and the determination of model parameters that are used to produce simulations for comparison to experimental data. Explanations for data that are not fit by the model are considered.

The fourth chapter of this dissertation explores scenarios not included in the laboratory portion of the research using the model to predict outcomes. In addition, the predictive ability of a revised form of the model was tested using data from another research paper related to metal fate in a microbial predator-prey system.

References

1. Hodson PV, Borgmann U, Shear H. 1979. Toxicity of copper to aquatic biota. In Nriagu, JO, ed, *Copper in the Environment Part II Health Effects*. Wiley-Interscience, New York, NY, USA.

2. Nelson YM, Lo W, Lion LW, Shuler ML, Ghiorse WC. 1995. Lead distribution in a simulated aquatic environment: Effects of bacterial biofilms and iron oxide. *Water Res* 29: 1934-1944.

3. Chen JH, Lion LW, Ghiorse WC, Shuler ML. 1995. The mobilization of adsorbed cadmium and lead in aquifer material by bacterial extracellular polymers. *Water Res* 29 (2): 421-430.

4. Rudd T, Sterritt RM, Lester JN. 1984. Complexation of heavy metals by extracellular polymers in the activated sludge process. *J Water Pollut Control Fed* 56: 1260-1268.

5. Fenchel T. 1987. *Ecology of Protozoa*. Science-Tech Publishers, Madison, WI.

6. Curds CR. 1973. The role of protozoa in the activated-sludge process. *Am Zool* 13: 161-169.

7. Caron DA, Goldman JC. 1990. Nutrient regeneration. In: Capriulo, GM (ed.). *Ecology of marine protozoa.* Oxford Univ. Press, New York, pp. 283-306.

8. Twiss MR, Campbell PGC. 1995. Regeneration of trace metals from picoplankton by nanoflagellate grazing. *Limnol Oceanogr* 40(8): 1418-1429.

9. Sanders RW, Gilmour CC. 1994. Accumulation of selenium in a model freshwater microbial food web. *Appl Environ Microbiol* 60:2677-2683.

10. Mansouri-Aliabadi M, Sharp RE. 1985. Passage of selected heavy metals from *Sphaerotilus* (Bacteria: Chlamydobacteriales) to *Paramecium caudatum* (Protozoa: Ciliata). *Water Res* 19 (6): 697-699.

11. Twiss MR, Campbell PGC, Auclair J. 1996. Regeneration, recycling, and trophic transfer of trace metals by microbial food-web organisms in the pelagic surface waters of Lake Erie. *Limnol Oceanogr* 41(7): 1425-1437.

12. Chen C, Stemberger RS, Klaue B, Blum JD, Pickhardt PC, Folt CL. 2000. Accumulation of heavy metals in food web components across a gradient of lakes. *Limnol Oceanogr* 45 (7): 1525-1536.

13. Miller EK, Friedland AJ. 1994. Lead migration in forest soils: response to changing atmospheric inputs. *Environ Sci Technol* 28: 978-984.

14. Agency for Toxic Substances and Disease Registry (ATSDR) (1988). The nature and extent of lead poisoning in children in the United States: A report to Congress. July 1988.

15. Needleman HL, Schell A, Bellinger D, Leviton A, Allred EN. 1990. The long-term effects of exposure to low doses of lead in childhood: an 11-year follow-up report. *N Engl J Med* 322(2):83-8.

CHAPTER II

DEVELOPMENT OF A MODEL MICROBIAL PREDATOR-PREY SYSTEM SUITABLE FOR STUDIES OF THE BEHAVIOR OF TOXIC TRACE METALS[*]

Abstract

Interactions between microbial predators and their prey can significantly influence the behavior of toxic trace metals. Ingested bacterial prey-bound metals can either accumulate within a predator or be excreted and potentially reintroduced into the dissolved phase. A defined predator-prey system suitable for developing a more fundamental understanding of metal behavior in simple microbial food chains was designed and tested using lead (Pb) as a representative cationic transition metal. Desired features of this system were the ability to define the chemical speciation of dissolved metals as well as to distinguish between prey and predator-bound metals. *Pseudomonas putida* and the ciliate protozoan *Tetrahymena thermophila* were selected as representative bacterial prey and predator species, respectively. In addition, the use of fluorescent microspheres was evaluated as an experimental surrogate for bacterial prey. Filtration techniques for size-selective separation were developed so that the distribution of Pb between *T. thermophila* cells, *P. putida* cells or microspheres, and the dissolved phase could be assessed. Filtration units were selected based on their ability to perform separations with minimal metal loss at circumneutral pH. Five-micron polycarbonate filter membranes successfully separated *T. thermophila* from *P. putida* with good cell retention and low metal loss. Centrifuge filters successfully separated dissolved and particle-bound metal (<5,000 nominal molecular weight limit). Exemplary experimental results are presented and show that predation on Pb-exposed *P. putida* cells or microspheres increases uptake of lead by *T. thermophila.*

[*] Adapted from Patton LE, Shuler ML, Lion LW. 2004. Development of a model microbial predator-prey system suitable for studies of the behavior of toxic trace metals. *Environmental Toxicology and Chemistry* 23(2):292-297.

Introduction

Toxic trace metal bioavailability and toxicity are determined primarily by metal speciation and phase distribution [1,2] rather than by the absolute concentration of metal [1]. Metal speciation and phase distribution are in turn governed by the interactions of multiple environmental conditions including pH, redox state, ionic strength, and the ensuing adsorption and complexation reactions pertinent to these conditions. Although it is widely recognized that biologically mediated processes can alter solution chemistry and surfaces [3] relatively little attention has been given to the influence of microbial predation on trace metal behavior.

The microbial community has the potential to bind a significant concentration of trace metals in natural systems. Bacterial cells and extracellular polymers of bacterial origin both provide binding sites for transition metals [4,5], although this is not necessarily their ultimate fate since bacteria cells are consumed by predators in the microbial loop. The term "microbial loop" refers to the lowest part of the food web. In a pelagic or limnic ecosystem the microbial loop consists of dissolved organic matter (< 0.2 μm diameter), the picoplankton (~0.2-2.0 μm; primarily bacteria), the nanoplankton (2.0-20.0 μm; flagellates), the microplankton (20.0-200 μm; ciliated protozoa, diatoms), and the mesoplankton (>200 μm; zooplankters) [6].

Microzooplankton grazing is known to regenerate phosphorous and nitrogen in the marine environment [7] and has been shown to regenerate particulate-bound Cd and Zn to the dissolved phase [8,9]. Additionally, toxic metals including Zn, Pb and Hg [10,11] and Cd [11] have been shown to bioaccumulate in the microbial loop [12].

The objective of this study was to create a laboratory system suitable for observation and modeling of the behavior of trace metals subject to predator-prey dynamics. The experimental goal was to discern between three routes of metal uptake by a protozoan: direct adsorption, pinocytosis (uptake through endocytosis of

dissolved metal), and phagocytosis (uptake via ingestion of particle-bound metals). Phagocytosis uptake of metals includes predation on bacteria as well as uptake of inorganic colloids. The total metal body burden for the predator is expected to be a sum of these three routes of uptake, minus any excretion. Twiss and Campbell [9] developed a similar model predator-prey system using the nanoflagellate *Ochromonas danica* and the cyanobacterium *Synechococcus leopoliensis.* However unlike the research presented here, their experimental design did not account for the concurrent uptake of dissolved and prey-bound metal by the predator.

Experiments were conducted in controlled bioreactors using lead as the test metal with control of solution composition, pH, and temperature. The reactors provided a defined predator-prey system using *Pseudomonas putida* G7 as a bacterial prey and, the ciliate *Tetrahymena thermophila* as the predator. The selection of predator and prey species, the chemical composition of media, culturing, and size-selective separation techniques were all part of the development of the predator-prey model experimental system and are described in this publication.

Materials and Methods

Culturing

The minimal mineral salts medium (MMS) developed by Murgel et al. [13] and modified by Nelson et al. [14] (Table 2.1) was used to provide a solution matrix in which the speciation of test metals could be defined. The components of the MMS medium are restricted to those with defined known metal stability constants. MMS medium was designed to eliminate competing trace metals, and to prevent metal precipitation or the formation of solid phases that could adsorb added metals. The ionic strength of MMS medium was 0.05 M and the pH was 6.0. Calculations with *MINEQL+: A Chemical Equilibrium Modeling System* (Version 4 for Windows;

Table 2.1. Composition of minimal mineral salts (MMS) media.

Component	*mg/L*
$CaCl_2*2H_2O$	30
$MgSO_4*7H_2O$	35
$(NH_4)_2SO_4$	120
KNO_3	15
$NaHCO_3$	0.84
$NaNO_3$	3800
$FeSO_4$	0.015
KH_2PO_4	0.7
Pyruvate*	2000
Vitamin B-12*	0.002

*Organic ingredients were removed prior to batch experiments.

Environmental Research Software) show Pb is present primarily (92%) as the divalent cation (Pb^{2+}) and approximately 7% as $PbSO_4$ (aq) in MMS medium.

Pseudomonas putida G7 was grown on a shaker table at 150 rpm in sterile MMS at room temperature. Before Pb-adsorption experiments, *P. putida* cultures were centrifuged, rinsed three times, and resuspended in MMS medium minus the pyruvate, KH_2PO_4, vitamin B-12, and $FeSO_4$.

The predator, *Tetrahymena thermophila,* was grown in Neff media, (5.0 g/L dextrose, 2.5 g/L yeast extract, and 2.5 g/L proteose peptone). Cultures grew in an incubator at 30°C without shaking. In a manner comparable to that described above for preparation of *P. putida*, *T. thermophila* cells were rinsed three times and resuspended in simple MMS medium for lead-adsorption experiments. *T. thermophila* was also grown xenically in bioreactors with *P. putida* as its only food source.

Cell and particle separation

A variety of membrane filters were compared for separating predator from prey cells and predator cells from waste material. Filter materials tested included polyvinyl difluoride (Millipore - Billerica, MA, USA), polycarbonate track-etch (Osmonics – Minnetonka, MN, USA), and Poretics (Osmonics) polycarbonate membranes. Samples were filtered through membranes of variable pore size to obtain the best efficiency for size-selective separation of cells and/or particles. Samples containing axenic cultures of *T. thermophila* with and without *P. putida* were filtered through 14.0, 8.0, 5.0, and 3.0-μm pore sizes to retain *T. thermophila* cells and then filtrate was passed through 0.45-μm pore sized filters to separate *P. putida* cells from dissolved Pb. The volume of sample filtered was also varied to yield optimal results. Millipore Centricon Biomax Plus-20 (<5,000 nominal molecular weight limit) centrifuge filtration units were also tested for Pb-binding and filtration efficiency.

Axenic cultures of *T. thermophila* and *P. putida* were enumerated using a Coulter Counter Multisizer (aperture size 140-μm and 30-μm, respectively). *P. putida* cells from xenic cultures were enumerated using plate counts because bacteria cells could not be distinguished from *Tetrahymena* waste matter with the 30-μm aperture of the Coulter Counter.

Lead adsorption

Adsorption isotherms were measured as follows: *T. thermophila* and *P. putida* cells at stationary phase were rinsed three times and resuspended (each species separately) in reactors containing MMS and Pb at concentrations of 0.5, 1.0, 2.0, 2.5, 3.5, 4.0, 5.0-μM. Adsorption experiments were conducted in 500-mL jacketed glass beakers pre-treated with dimethyldichlorosilane to reduce Pb adsorption to glass surfaces, acid washed in 10% trace-metal grade HNO_3, and rinsed with distilled-deionized water. A constant temperature controller was used to circulate water through the reactor jackets and maintained reactor temperatures at 25 $^{+}$/- 1.0 ^{o}C. During experiments the pH was maintained at 6.0 $^{+}$/- 0.2 with pH-controllers through addition of 0.01 N NaOH and HNO_3. Cultures were constantly stirred by magnetic stir bar.

In axenic cultures, cells were exposed to Pb for 48-hours. Initial kinetic experiments revealed that a 48-hour equilibration was sufficient to provide a stable equilibrium dissolved Pb concentration. An aliquot for the measurement of total Pb was removed and acidified with trace metal grade nitric acid to a final concentration of 2.0% prior to analysis. Another aliquot of the cell culture was filter centrifuged with Centricon Biomax filters and the supernatant, which contained only dissolved Pb, was acidified with nitric acid for analysis. Lead adsorption by *P. putida* in axenic bioreactors was measured using graphite furnace atomic absorption spectrometry (GFAAS) as the difference between total and dissolved Pb. In axenic reactors

containing *T. thermophila*, adsorption to the predator was measured directly by digesting membranes with filtered cells in 10% trace metal grade HNO_3. The remainder of adsorbed Pb was assumed bound to waste matter. In xenic cultures, *T. thermophila* cells were added to reactors with equilibrated *P. putida* and Pb at the 48-hour mark. After an additional 48-hours, samples were enumerated, filtered, and analyzed for Pb by GFAAS (no matrix modifier; 20.0-μL analyte sampled; replicate analysis of Pb standards gave a coefficient of variation of <5%).

The adsorption of Pb to fluorescent carboxylated microspheres (Fluoresbrite 1.0-μm-diameter particles, Polysciences, Warrington, PA, USA), a potential proxy for bacteria cells in predator-prey reactors, was also measured. The experimental methodology was similar to that for *P. putida*, as described above.

Pinocytosis

Pinocytosis refers to the uptake of a dissolved substance by the formation of a vesicle at the surface of the cell membrane and its subsequent movement into the cell. Direct metal adsorption and pinocytosis of dissolved metal by protozoa were determined in the absence of bacterial cells to avoid interference from metal uptake by predation. Pinocytosis was measured indirectly by chelating metal before adding protozoan cells, effectively eliminating any cell surface adsorption. Under these conditions, the only significant metal uptake mechanism in an axenic culture was expected to be from pinocytosis; however, the experimental design did not eliminate other possible mechanisms of active uptake such as protein ports that may have inadvertently transported Pb. Lead uptake through "pinocytosis" by *T. thermophila* cells was measured at pH 6.0 in solution containing a 1:1 molar ratio of Na^+-ethylenediaminetetraacetic acid (EDTA) and $PbNO_3$ with Pb and EDTA

concentrations ranging from 0.5 to 3.0 μM. *T. thermophila* cells were added after Pb and EDTA had had 24-hours to equilibrate.

Results & Discussion

Culturing

The objective of this study was to create an experimental laboratory model of a microbial predator-prey system suitable for investigating the influence of predation on the behavior and fate of lead. Central to this objective was the ability to define and control the chemistry and biology of the system. The MMS medium was selected based on its design to minimize metal complexation, to eliminate the presence of competing metal species, and to prevent the formation of precipitates that potentially bind metals [13,14].

Pseudomonas putida was selected as a bacterial prey species because of its ability to grow in MMS medium and because of prior research by the authors on the metal binding properties and composition of its extracellular polymer [15]. Stationary phase suspensions of *P. putida* were able to survive with negligible mortality in MMS without a carbon source for the 48-hours used to obtain equilibrium adsorption data.

The ciliate protozoan *T. thermophila* was chosen as a representative predator species based on preliminary studies showing that it could grow and survive with *P. putida* as its only food source. It is also able to grow and survive axenically in a complex medium [16]. Like *P. putida, T. thermophila* was able to survive without a carbon source in the MMS media for the duration of adsorption experiments with a negligible loss of cells.

Fluorescent carboxylated microspheres (Fluoresbrite 1.0-μm-diameter particles) with similar physical properties (size, density) to bacterial cells were tested as a possible alternative to using bacteria as the "prey". Microscopic observation of *T.*

thermophila cells after contact with a suspension of microspheres revealed the presence of ingested fluorescent particles and indicated *T. thermophila* readily consumed these cell-sized particles (see Figure 2.1).

Cell and particle separation

Materials used to separate cells needed to successfully remove cells and at the same time not bind dissolved Pb. With the exception of Centricon Plus-20 centrifuge filtration units, all filtration hardware (filter platforms, frits, receiving units, etc) was found to bind a significant amount of Pb from MMS at pH 6.0. Therefore direct measurement of dissolved Pb in filtrate was unsuitable. Instead Pb binding to *T. thermophila* in predator-prey and predator-waste separation was measured by digesting the membranes themselves with the filtered particles. Filter membranes tested were Millipore polyvinyldiflouride, Osmonics polycarbonate track-etch, and Osmonics polycarbonate. Osmonics polycarbonate membrane filters adsorbed the lowest concentration of dissolved Pb of all membrane filters tested (Table 2.2). Dissolved Pb and particle-bound Pb were also separated cleanly with Centricon Plus-20 centrifuge filtration units with Biomax membranes (nominal molecular weight limit = 5000). Loss of lead to the Centricon filter units was always under 10%.

Separation of *T. thermophila* from bacteria or from waste products was performed using membrane filters. Although the average diameter of *T. thermophila* cells was approximately 30-μm, the cells were capable of distorting their shape and passing through 10 and 20 μm pores. As a result, small pore sized filters were required to ensure efficient cell capture. *T. thermophila* cells were observed in the filtrate from any membrane with a pore-size over 5.0-μm, even when vacuum pressure was not applied. Pb bound to axenic *P. putida* was separated from dissolved Pb using the Centricon filters.

Figure 2.1. Photomicrograph of *T. thermophila* showing ingested fluorescent microspheres inside food vacuoles.

Table 2.2. Pb loss to membrane filters.

	*Initial [Pb] = 1.0 μM**		*Initial [Pb] = 4.0 μM**	
Filter type	*% Loss*	*SD***	*% Loss*	*SD***
Polyvinyldiflouride	34.0	21.7	30.7	15.6
Polycarbonate track-etch	17.0	3.6	16.9	3.5
Polycarbonate	5.1	5.5	4.0	5.5

*Results shown are for filtration of 10-ml samples with 5.0-μm pore size.
**_SD_ = standard deviation.

In xenic reactors, distinguishing prey-bound Pb (or microsphere-bound Pb) from predator-bound Pb was not possible by physical separation with filters. As stated above, the issue of Pb adsorbing to filtration hardware precluded the usefulness of analyzing Pb in filtrate. Therefore, lead adsorption to *P. putida* or microspheres was measured before addition of *T. thermophila* to reactors and was assumed constant over the course of the predation experiment. Errors resulting from this assumption were deemed minimal because the number of prey particles remaining after 48-hours of predation was very small and the Pb associated with those particles was insignificant compared to Pb associated with *T. thermophila*.

Lead adsorption

Lead adsorption isotherms for *P. putida,* and fluorescent microspheres are given in Figure 2.2 and the isotherm for *T. thermophila*, is shown in Figure 2.3. Pb adsorption to *P. putida* and microspheres was adequately fit using a linear isotherm: $[Pb]_{adsorbed} = K * [Pb]_{equilibrium}$ with distribution coefficients (K) of 25,700 mL/g (r^2 = 0.64) and 18,600 mL/g (r^2 = 0.93) respectively, where the term $[Pb]_{equilibrium}$ refers to the concentration of total dissolved Pb at equilibrium. Other studies have seen similar results for Pb binding to *P. putida*. Pardo et al [17] measured a Pb binding constant of 26,600 mL/g at pH 6.5 after a 10 minute equilibration time. This indicates that Pb in the present study system was not binding significantly to dissolved organic carbon or other ligands/ chelators that might have been present after the 48 hours of equilibration.

Pb adsorption to *T. thermophila* obeyed a Langmuir isotherm:

$$[Pb]_{adsorbed} = \frac{\Gamma_{max} K [Pb]_{equilibrium}}{1 + K [Pb]_{equilibrium}}$$

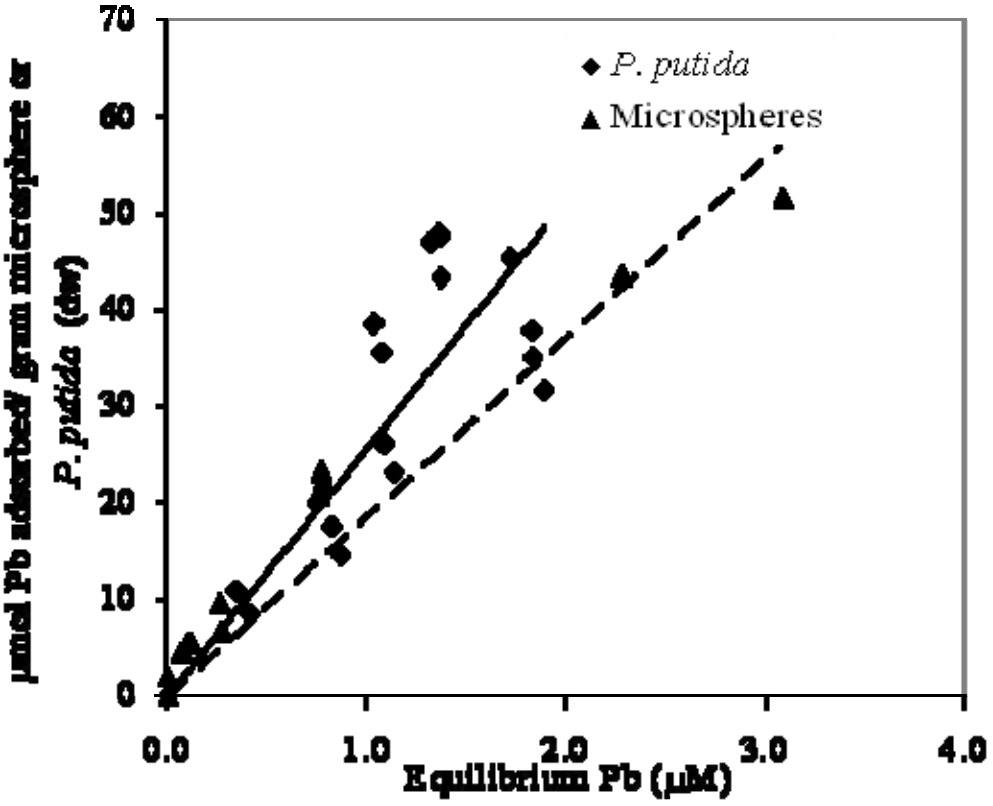

Figure 2.2. Pb adsorption isotherms for *P. putida* and fluorescent microspheres. {For P. putida: $[Pb]_{adsorbed} = 25.7 * [Pb]_{equilibrium}$; $r^2 = 0.64$; for microspheres: $[Pb]_{adsorbed} = 18.6 * [Pb]_{equilibrium}$; $r^2 = 0.93$}

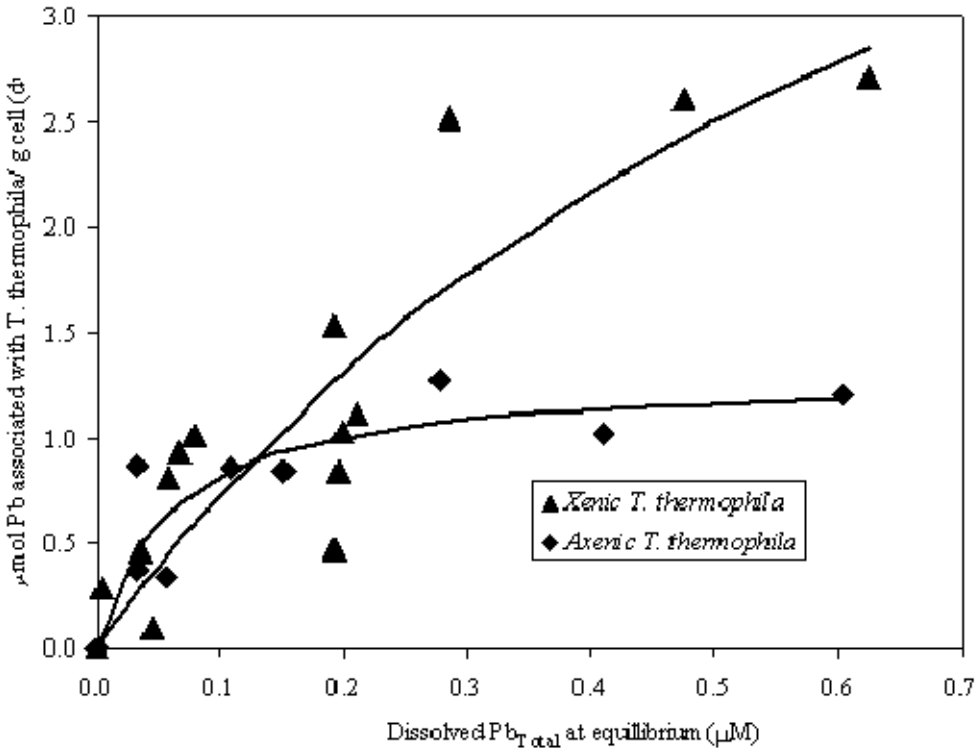

Figure 2.3. Pb adsorption isotherm for *T. thermophila*. {$[Pb]_{adsorbed} = (22.1 * [Pb]_{equilibrium})/(1 + 17.0 * [Pb]_{equilibrium})$; $r^2 = 0.75$}

where Γ_{max} = 1.30 μmol/g *T. thermophila* dry weight, and K= 17.0 L/μmole (r^2 = 0.75).

Metal uptake by pinocytosis

Figure 2.4 shows uptake of Pb by *T. thermophila* under axenic conditions when exposed to Pb^{2+} versus the Pb-EDTA chelate. These data support the hypothesis that Pb associated with *T. thermophila* is primarily the result of adsorption. The concentration of lead associated with *T. thermophila* per gram of cell dry mass was 70% less when EDTA was present in solution versus when it was absent. Based on MINEQL+ calculations, when the ratio of Pb to EDTA is 1:1 in MMS media, 99.7% of total Pb is expected to be chelated and presumed unavailable for adsorption to cells. Likewise, 99.7% of total EDTA is chelated with Pb. These results indicate that in the absence of uptake of particle-bound Pb, an upper bound of 0.40 μmol Pb/ gram cells was taken up via pinocytosis over a 48-hour time period.

Lead uptake by predation

Figure 2.5 shows the difference in Pb uptake by *T. thermophila* in xenic versus axenic cultures. The population of *T. thermophila* was $1.4x10^5$ cells/ml and stayed constant during the predation experiment. *P. putida* concentrations were initially $2.4x10^8$ cells/ml and were reduced to $2.5x10^5$ cells/ml through predation. At lower Pb concentrations, there was no discernible difference in Pb uptake by axenic and xenic cultures of *T. thermophila*. However at higher equilibrium Pb levels, there is more Pb associated with *T. thermophila* cells in cultures containing *P. putida.* While Pb uptake by *T. thermophila* levels off at higher equilibrium concentrations in axenic cultures, the body burden of Pb increases in xenic cultures, reflecting the adsorption properties of the prey that *T. thermophila* cells are ingesting. The Pb adsorption isotherm for

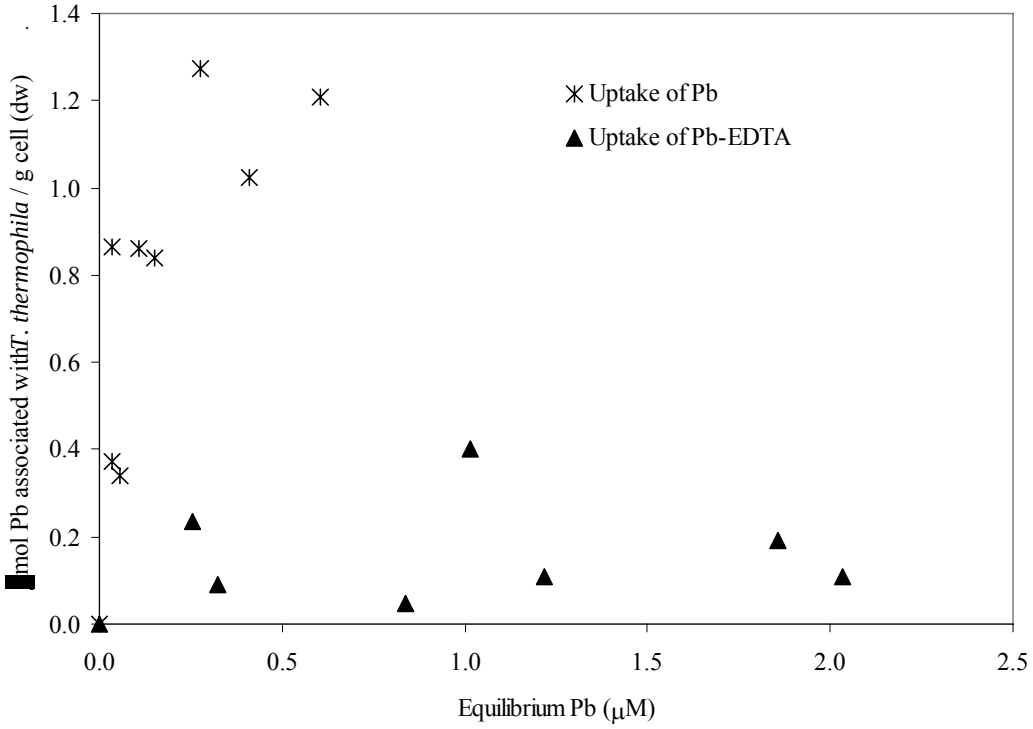

Figure 2.4. Pb associated with *T. thermophila* with and without ethylenediamine-tetraacetic acid (EDTA) chelator.

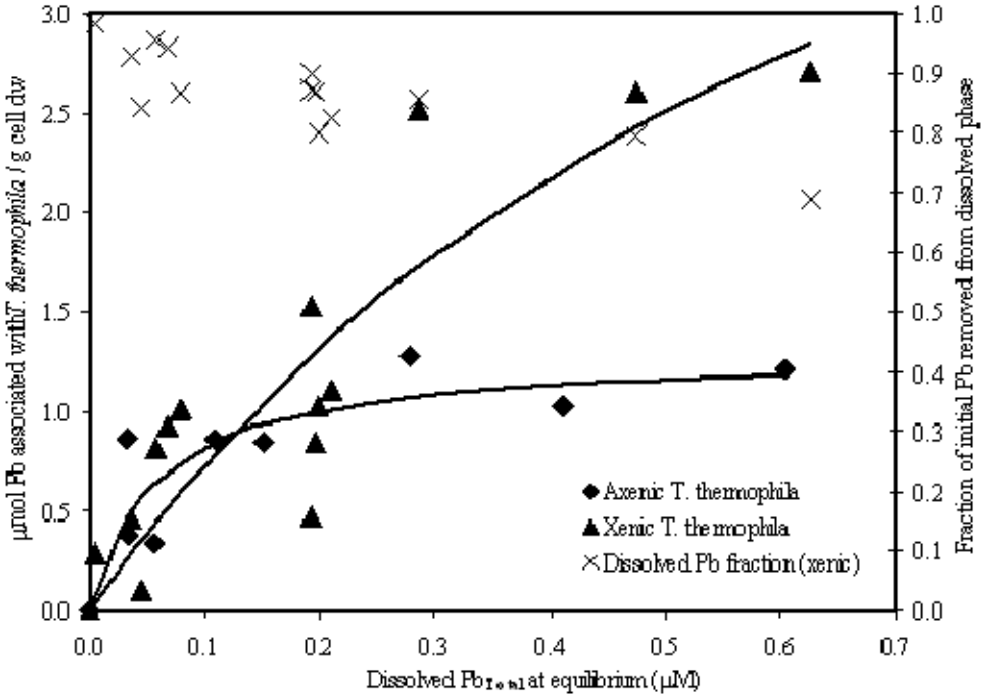

Figure 2.5. Pb associated with *T. thermophila* in axenic and xenic cultures. {$[Pb]_{xenic} = (8.3 * [Pb]_{equilibrium})/(1 + 1.3 * [Pb]_{equilibrium})$; $r^2 = 0.78$}

axenic *T. thermophila* indicates the saturation of cell surface binding sites at a dissolved Pb concentration of ~0.3 μM (Figure 2.3). Therefore, the increase in Pb associated with *T. thermophila* cells in the presence of prey (Figure 2.5) is arguably the result of internal Pb not adsorbed Pb.

Pb uptake by *T. thermophila* feeding on fluorescent microspheres is shown in Figure 2.6 and indicates a clear increase in Pb associated with the predator as a result of consumption of particle bound Pb. These results suggest that fluorescent microspheres may serve as suitable prey surrogates with respect to the trophic transfer of Pb in experimental applications where avoiding the population dynamics of the prey is desirable. Although predation on both particle types resulted in a linear increase in the Pb body burden of *T. thermophila* as a function of the equilibrium Pb concentration, *T. thermophila* took up less Pb per gram of cell dry weight when preying on *P. putida* cells versus fluorescent microspheres (Figure 2.6). The reason for this is unclear, however it is possible that some Pb in reactors with live prey cells was bound to DOC or another organic ligand present in the reactor as a result of normal metabolic processes of the bacteria cells. Pb binding to these ligands would result in less being available for adsorption to *P. putida* cells and therefore less taken up by predators via predation. In future experiments, it would be useful to measure DOC in solution or take measurements for Pb adsorbed to prey before the production of ligands becomes significant. In any case, the present experiment implicates the suitability of using fluorescent microspheres as a proxy for bacterial prey.

The results shown in Figures 2.5 and 2.6 differ somewhat from those of Twiss and Campbell [9] who reported metals in prey (Cd, Cs, Gd and Zn in *Synechococcus leopoliensis)* were primarily released to the dissolved phase by grazing of the nanoflagellate *Ochromonas danica*. Low levels of predator accumulation of Cd, Gd, and Zn were observed and attributed, in part, to adsorption of regenerated metal.

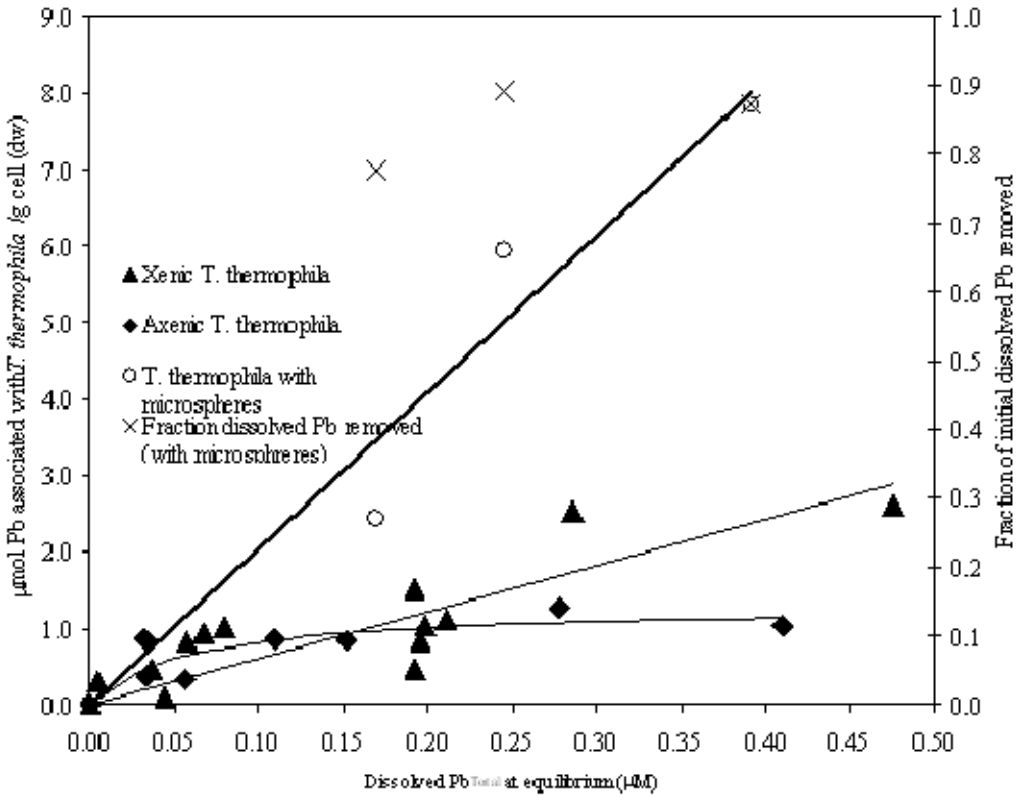

Figure 2.6. Pb associated with *T. thermophila* in the presence of microspheres and *P. putida.* {$[Pb]_{uptake\ via\ mucrospheres} = 20.4 * [Pb]_{equilibrium}$; $r^2 = 0.95$}

However, the observation of net metal release made by Twiss and Campbell was likely to have been promoted by their choice of initial conditions where added metals were available to predators solely via uptake of pre-exposed, EDTA-washed prey cells, i.e. none of the added metal was initially in the dissolved phase. In the present study, we exposed predator cells to dissolved Pb in equilibrium with prey-bound Pb and observed enhancement of predator Pb levels beyond those attributable to adsorption and pinocytosis. In addition, the level of dissolved Pb decreased in each experiment (see Figures 2.5 and 2.6) relative to the initial value indicating that metal uptake by the predator exceeded any release to solution as a consequence of predation. Thus, observations regarding the influence of predation on the phase distribution of metals depend, in part, on the experimental protocol, and conclusions should be drawn with this protocol in mind.

Summary

Methods for measuring Pb uptake in *T. thermophila* by adsorption, phagocytosis and pinocytosis have been developed. In these experiments the relative contributions of prey and predator to metal sorption were determined with size-selective filtration or centrifugation. Using these methods, it is expected that a laboratory system for measuring the behavior and fate of Pb in a microbial predator-prey community can be constructed and used for developing a mechanistic model that describes the influence of predation on Pb phase distribution and speciation. Furthermore, fluorescent microspheres are a promising proxy for bacterial prey species as their adsorption properties are similar and *T. thermophila* do not appear to prefer an actual live bacterial prey to the fluorescent microspheres. Future experiments in which the physical and chemical form of Pb is manipulated will permit a more comprehensive understanding of these variables on uptake of toxic metals by

microbial predators and the influence of microbial predation on the fate of Pb in the environment.

References

1. Hodson PV, Borgmann U, Shear H. 1979. Toxicity of copper to aquatic biota. In Nriagu, JO, ed, *Copper in the Environment Part II Health Effects*. Wiley-Interscience, New York, NY, USA.

2. Campbell PGC. 1999. Interactions between trace metals and aquatic organisms: A critique of the free-ion activity model. In Tessier A, Turner DR, eds, *Metal Speciation and Bioavailability in Aquatic Systems.* John Wiley & Sons, New York, NY, USA, pp 45-102.

3. Lion LW, Shuler ML, Hsieh KM, Ghiorse WC. 1987. Trace-metal interactions with microbial biofilms in natural and engineered systems. *CRC Crit Rev Environ Control* 17:273-306.

4. Nelson YM, Lo W, Lion LW, Shuler ML, Ghiorse WC. 1995. Lead distribution in a simulated aquatic environment: Effects of bacterial biofilms and iron oxide. *Water Res* 29:1934-1944.

5. Chen JH, Lion LW, Ghiorse WC, Shuler ML. 1995. The mobilization of adsorbed cadmium and lead in aquifer material by bacterial extracellular polymers. *Water Res* 29:421-430.

6. Sieburth JM. 1979. *Sea Microbes*. Oxford University Press, New York, NY, USA.

7. Caron DA, Goldman JC, Dennett MR. 1988. Experimental demonstration of the roles of bacteria and bacterivorous protozoa in plankton nutrient cycles. *Hydrobiologia* 159:27-40.

8. Twiss MR, Campbell PGC. 1998. Scavenging of ^{137}Cs, ^{109}Cd, ^{65}Zn, and ^{153}Gd by plankton of the microbial food web in pelagic Lake Erie surface waters. *J Gt Lakes Res* 24:776-790.

9. Twiss MR, Campbell PGC. 1995. Regeneration of trace metals from picoplankton by nanoflagellate grazing. *Limnol Oceanogr* 40:1418-1429.

10. Mansouri-Aliabadi M, Sharp RE. 1985. Passage of selected heavy metals from *Sphaerotilus* (Bacteria: Chlamydobacteriales) to *Paramecium caudatum* (Protozoa: Ciliata). *Water Res* 19:697-699.

11. Twiss MR, Campbell PGC, Auclair J. 1996. Regeneration, recycling, and trophic transfer of trace metals by microbial food-web organisms in the pelagic surface waters of Lake Erie. *Limnol Oceanogr* 41:1425-1437.

12. Sanders RW, Gilmour CC. 1994. Accumulation of selenium in a model freshwater microbial food web. *Appl Environ Microbiol* 60:2677-2683.

13. Murgel G, Lion LW, Acheson C, Shuler ML, Emerson D, Ghiorse WC. 1991. An experimental apparatus for selection of adherent microorganisms under stringent conditions. *Appl Environ Microbiol* 57:1987-1996.

14. Nelson YM, Lion LW, Ghiorse WC, Shuler ML. 1999. Production of biogenic Mn oxides by *Leptothrix discophora* SS-1 in a chemically defined growth medium and evaluation of their Pb adsorption characteristics. *Appl Environ Microbiol* 65:175-180.

15. Kachlany SC, Levery SB, Kim JS, Reuhs BL, Lion LW, Ghiorse WC. 2001. Structure and carbohydrate analysis of the exopolysaccharide capsule of *Pseudomonas putida G7. Environ Microbiol* 3:774-784.

16. Curds CR, Cockburn A. 1968. Studies on the growth and feeding of *Tetrahymena pyriformis* in axenic and monoxenic culture. *J Gen Microbiol* 54:343-358.

17. Pardo R, Herguedas M, Barrado E, Vega M. 2003. Biosorption of cadmium, copper, lead and zinc by inactive biomass of *Pseudomonas putida*. *Anal Bioanal Chem* 376:26-32.

CHAPTER III

THE BEHAVIOR OF LEAD IN A MODEL PREDATOR-PREY SYSTEM[*]

Abstract

Predation at the microbial level can affect the fate of toxic trace metals. Metals associated with bacterial prey can be released into the dissolved phase following digestion by a predator, and/or metals can remain in the predator and potentially be transferred to the next level of the food chain. Toxic metal ions in the aqueous phase are also expected to modify the growth and predation rate of a microbial predator. A model predator-prey system was developed to test the effects of Pb on cells and to help elucidate the fate of Pb in this type of interaction. Established methods that have been shown to be suitable for distinguishing dissolved, prey-bound, predator-bound, and ingested Pb were used to establish the pathway of Pb over time. Growth parameters were measured using batch reactors for the protozoan predator, *Tetrahymena thermophila,* and the bacterial prey, *Pseudomonas putida,* without Pb and at several concentrations of Pb. The effect of prey density on predation and Pb phase distribution was also investigated. Results demonstrate that some kinetic parameters related to prey consumption and growth of *T. thermophila* are altered by Pb. Upon addition of predator to prey cells in equilibrium with dissolved Pb, dissolved and prey-bound Pb become associated with the predator through ingestion and adsorption. Ingested Pb is later excreted as a bound metal associated with *T. thermophila* waste matter. A preliminary mathematical model was developed to describe predator-prey dynamics and their influence on the behavior and fate of Pb.

[*] Adapted from Patton LE, Shuler ML, Lion LW. 2005. Behavior of lead in a model microbial predator-prey system. *Environmental Toxicology and Chemistry* 24(11):2734-2741.

Growth data were used to obtain model parameters, and model simulations for Pb fractionation are compared to experimental observations.

Introduction

A mechanistic understanding of trace metal movement in the microbial loop of the food web is an important part of being able to predict the fate of toxic trace metals in engineered and natural aquatic systems. The microbial loop refers to the lowest part of the food web. In a pelagic or limnic ecosystem, the microbial loop consists of dissolved organic matter (< 0.2 μm diameter), the picoplankton (~0.2-2.0 μm; primarily bacteria), the nanoplankton (2.0-20.0 μm; flagellates), the microplankton (20.0-200 μm; ciliated protozoa, diatoms), and the mesoplankton (>200 μm; zooplankters) [1]. The presence of metal-adsorbent cellular surfaces in the microbial loop is likely to alter metal speciation and solid/solution phase distribution. Since toxic metals sorb readily to bacterial prey, the potential for metal uptake by predators and their subsequent bioaccumulation exists. Metals can also become associated with bacterial predators through direct adsorption (of dissolved metal ions) to predator surfaces and through uptake of dissolved metals (through pinocytosis, and facilitated transport) by the predator. Waste materials produced by predators can also act as adsorbents for dissolved metals, and the efflux of intracellular metals by predators may alter the physical/chemical form of the metals from which was originally ingested. In short, the process of predation of bacteria and cell-bound toxic metals may present a significant opportunity for a change in metal speciation and/or for the bioaccumulation of metals.

Understanding the effects of toxic metals on the bacteria/protozoan part of the microbial food web is also of interest in the context of waste water treatment plants. In fact, protozoa have been shown to increase the overall efficiency of sewage treatment.

Curds showed that activated sludge with protozoa reduced organic matter substantially over protozoa-free sludge [2]. Protozoan community structure can be used as an indicator of the state of waste water remediation [3]. Toxic metals, including Pb, have been shown to influence species richness and density of ciliate communities in activated sludge [4]. Studies have also shown that heavy metals can block enzymatic functioning in protozoa [5]. In nature, protozoa occur primarily in the benthos—the sediment and detritus at the bottom of lakes. When bacterivorous protozoa prey upon and metabolize bacteria, which tend to assimilate rather than regenerate nutrients, they can change the bioavailability of these nutrients and anything else bound to prey cells.

In this research, we examine metal behavior in a model predator-prey experimental system containing *Pseudomonas putida* as the bacterial prey and the protozoan *Tetrahymena thermophila* as the predator. The ciliate protozoan *T. thermophila* was chosen as a representative predator species because it can grow and survive with *P. putida* as its only food source [6]. It is also able to grow and survive axenically in a complex medium [7]. Lead adsorption parameters for *T. thermophila* have been previously determined [6]. *Pseudomonas putida* G7 was selected as a prey species because of its ability to grow in the minimal mineral salt (MMS) media employed to permit calculation of metal speciation, because of prior research by the authors on its metal binding properties, and because of its ability to serve as prey to our predator species [6].

The fate of prey-bound and dissolved toxic metals after ingestion by a bacterial predator such as *T. thermophila* is uncertain. *Tetrahymena* digests its food within food vacuoles. Once full, food vacuoles leave the oral region of the cell, fuse with the cell membrane, and what remains inside (the fecal material) is egested. It is conceivable that fecal material is the ultimate fate of metal in this microbial food web. Ingested metals may also accumulate within the predator, and be passed up the trophic levels of

the microbial loop. It is also possible that some metal desorbs from food particles during digestion and is then egested in the dissolved form. This phenomenon has been shown in protozoa ingesting iron colloids [8]. In stressed *Tetrahymena* cells, electron-rich cytoplasmic granules form and have been shown to sequester heavy metals (Cd, Zn, Cu, Pb) as a detoxification mechanism [9]. *Tetrahymena* species are also known to produce metallothioneins in response to the presence of heavy metals. These proteins have been shown to increase cellular tolerance to Cd [10].

Dissolved and predator-bound metals can alter the behavior and growth of microbial predators. For example, in *Tetrahymena pyriformis*, Cd inhibits motility [11]. Toxic metals also have resulted in both inhibitory and stimulatory effects on prey ingestion by phagocytosis as well as changes in the growth rate of bacterial predators [12]. Copper at 0.001 M was shown to stimulate the grazing rate of *T. pyriformis* but then inhibited it at concentrations above 0.002 M [13].

Experimental bioreactor systems have been developed by the authors to provide a controlled environment where predator-prey interactions can be measured in the context of well-defined metal speciation [6]. The objectives of the present study were to evaluate the fate of Pb in this model predator-prey system, to assess the effect of Pb on growth and predation rates, and to utilize experimental results to obtain model parameters that permit predictions regarding metal-microbe interactions.

Materials and Methods

Pseudomonas putida growth parameters

The minimal mineral salts medium (MMS) described in Patton et al. [6] was used to provide a solution matrix in which the speciation of test metals could be defined. The MMS medium consists of (per liter of solution): 30 mg $CaCl_2 \bullet 2H_2O$, 35 mg $MgSO_4 \bullet 7H_2O$, 120 mg $(NH_4)_2SO_4$, 15 mg KNO_3, 0.84 mg $NaHCO_3$, 3800 mg

$NaNO_3$, 0.015 mg $FeSO_4$, 0.7 mg KH_2PO_4, 2000 mg pyruvate, 0.002 mg vitamin B-12. The components of the MMS medium are restricted to those with known metal stability constants. This medium was designed to eliminate competing trace metals, and to prevent metal precipitation or the formation of solid phases that could adsorb added metals. The ionic strength of MMS was 0.05 M and the pH was six. Calculations with *MINEQL+: A Chemical Equilibrium Modeling System* (Ver 4 for Windows; Environmental Research Software, Hallowell, ME, USA) show that Pb is present primarily (92%) as the divalent cation (Pb^{2+}), and approximately 7% as $PbSO_4$ (aq) in MMS at all Pb levels used in this research.

Pseudomonas putida G7 was obtained from ATCC (Manassas, VA, USA) and was grown in MMS on a shaker table at 150 rpm at room temperature. The concentration of pyruvate and the density of bacteria cells were recorded over time. Bacterial cell density was measured as the absorbance at 600 nm. The initial concentration of pyruvate was 640 g/L. Pyruvate concentrations were measured using an enzymatic/ photometric technique [14] with a diagnostics kit (Sigma Chemical, St. Louis, MO, USA, catalog # 726-UV).

Net growth of bacteria (B) in the absence of the predator was modeled with the following relationship:

$$\frac{dB}{dt} = [(\mu_{max_B} * S)/(K_{S_B} + S)] * B - k_{d_B} B, \quad (1)$$

where μ_{maxB} is the maximum specific growth rate (/h), S is the concentration of pyruvate (g/L), and Ks_B is the saturation constant or the concentration of pyruvate present when growth rate of bacteria is at one-half the maximum (g/L), and k_{d_B} is the intrinsic death rate or maintenance coefficient of the bacteria (/h).

The μ_{max_B} was calculated from the slope of the natural logarithm of *P. putida* concentration versus time during exponential growth. The k_{d_B} was calculated as the

slope of the natural logarithm of *P. putida* concentration versus time during the death phase.

The depletion of pyruvate by bacteria was modeled as bacterial growth divided by the yield of bacteria growing on pyruvate (Y_B; *g bacteria/g pyruvate*):

$$-\frac{dS}{dt} = \frac{1}{Y_B} * \frac{\mu_{max_B} * S * B}{K_{S_B} + S} \quad (2)$$

The Y_B was calculated by plotting pyruvate concentrations against the corresponding *P. putida* concentration during exponential growth phase. The Ks_B was estimated by fitting the batch growth results for *P. putida* with the calculated growth parameters and minimizing the residual error.

Tetrahymena thermophila growth parameters

The ciliated protozoan *Tetrahymena thermophila* was used as the bacterial predator in experiments and was obtained from P. Bruns (Department of Microbiology, Cornell University, Ithaca, NY, USA; current affiliation: Howard Hughes Medical Institute, Chevy Chase, MD, USA). *Tetrahymena thermophila* was initially grown in Neff media, (5.0 g/L dextrose, 2.5 g/L yeast extract, and 2.5 g/L proteose peptone [Difco, Franklin Lakes, NJ, USA]). Cultures grew in an incubator at 30^{o}C without shaking. Before predation experiments, *P. putida* cultures were grown to stationary phase, centrifuged, rinsed three times, and resuspended in MMS without the pyruvate, KH_2PO_4, vitamin B-12, and $FeSO_4$ (referred to here as MMS-2). In a comparable manner, *T. thermophila* cells were rinsed three times and resuspended in MMS-2 containing stationary phase *P. putida* as the only carbon/energy source. Axenic control bioreactors with *P. putida* or *T. thermophila* only were run simultaneously in duplicate. The effect of initial prey density on *T. thermophila* growth parameters was investigated using three different initial concentrations of *P.*

putida: One base concentration (0.01 g/L dry wt), and suspensions with 3x and 10x the base concentration.

Populations of predator and prey were enumerated over time by different methods. Axenic *P. putida* cultures were enumerated by absorbance at 600 nm. *Tetrahymena thermophila* in both axenic and xenic cultures were enumerated using a Coulter Multisizer II (Beckman Coulter, Fullerton, CA, USA) by counting particles in the >8.0 μm size range. *Pseudomonas putida* cells from xenic cultures were enumerated using plate counts because bacterial cells could not be easily distinguished from *T. thermophila* waste material with the Coulter counter or spectrophotometer. The predator's net growth rate was modeled as:

$$\frac{dP}{dt} = [(\mu_{max_P} * B)/(Ks_P + B) - k_{d_P}] * P, \quad (3)$$

where μ_{max_P} $(/h)$ is the maximum specific growth rate of the predator (P) when $B >> Ks_P$, K_{S_P} is the *P. putida* concentration *(g/L)* when the specific growth rate is one-half the maximum, and k_{d_P} is the intrinsic predator death rate or maintenance coefficient ($/h$).

The double saturation model is an alternative approach to Monod kinetics for describing predator growth [15]. Using the double saturation model net predator growth is described as:

$$\frac{dP}{dt} = [(\mu_{\max_P} * B^2)/(Ks_P + B^2) - k_{d_P}] * P. \quad (4)$$

The double saturation model is said to better account for the dependence on substrate of the bacterial prey and the threshold prey concentration necessary for predation to occur [15]. Predator growth data were fit to the double saturation model and the Monod model, and the resulting fits were compared.

The *T. thermophila* population was sampled for a time interval sufficient to obtain a maximum growth rate (μ_{max_P}) and intrinsic death rate constant (k_{d_P}), as

described above for *P. putida*. The Ks_p was estimated by comparing the specific growth of *T. thermophila* $(\frac{dP}{dt} * \frac{1}{P})$ to both models and minimizing the residual error. To facilitate analysis, in some cases variations in *T. thermophila* data were smoothed by fitting cell concentration over time to a second order polynomial ($y=at^2+ bt +c$), and growth rates were taken as the slope of that curve.

The rate of *P. putida* consumption via predation (r_{pred}) was modeled as the protozoan growth rate divided by the yield coefficient of *T. thermophila* growing on *P. putida* (Y_P; *g/g*):

$$r_{pred} = \frac{1}{Y_P} * \frac{\mu_{max_P} * B * P}{Ks_P + B} \quad (5)$$

and Y_P was estimated by fitting the model to the data for net predator growth.

Effect of Pb and prey density on T. thermophila growth and predation

Predation experiments were conducted in 500-ml jacketed glass beakers pretreated with dimethyldichlorosilane to reduce Pb adsorption to glass surfaces. Before each use, the beakers were cleaned by washing in 10% trace-metal grade HNO_3, and rinsed with distilled-deionized water. A constant temperature controller was used to circulate water through the reactor jackets and maintain reactor temperatures at 25 $^{+}$/- 1.0 ^{o}C. During experiments, the pH was maintained at 6.0 $^{+}$/- 0.2 with pH-controllers through addition of 0.01 N NaOH and HNO_3. Cultures were constantly stirred by magnetic stir bar.

Predation experiments were conducted in reactors with initial dissolved Pb concentrations (i.e., the Pb concentration after bacteria cells had reached equilibrium with the added Pb, but prior to addition of *T. thermophila* cells) equal to 0.3 μM, 0.7 μM, and 1.8 μM (Pb_{total} = 0.4, 1.3, 2.9 μM, respectively). Control reactors contained no Pb. While directly applicable to wastewater treatment systems [4], the experimental

Pb levels are elevated relative to those observed in natural aquatic systems. Additional consideration is given below (see Results and Discussion section), with respect to the relevance of the experimental metal levels to understanding the influence of microbial predators on Pb phase distribution in aquatic systems with lower Pb concentrations.

Pseudomonas putida cells at stationary growth were added to reactors, and $PbNO_3$ was added incrementally over a 24 h period to ensure the dissolved concentration never exceeded the solubility product of Pb solid phases. After another 24 h, samples for total and dissolved Pb were taken; *P. putida* was enumerated at optical density (O.D.) 600, and *T. thermophila* was added. Axenic control reactors were also maintained. Initial *T. thermophila* counts were made with a Coulter counter, and both predator and prey species were enumerated over the course of the next 30 h.

It is expected that Pb uptake by a predator will increase (at the same total Pb level) if the prey concentration is higher, assuming that any toxic effects to growth of the increased metal uptake are outweighed by the benefits derived from an increase in the predator's food supply. In a separate experiment, the effect of initial prey densities on predation and Pb fate was studied. The initial *P. putida* concentrations were 0.01, 0.03, and 0.13 g/L, hereafter referred to as 1x, 3x, and 10x, respectively. The initial Pb_{total} concentration was 0.5 μM in all reactors except control reactors, which contained no Pb.

Total, dissolved, and predator-bound Pb were measured over time. The procedures for determining Pb speciation are described in detail by Patton and coworkers [6]. Briefly, at each time point an aliquot for the measurement of total Pb was removed and acidified with trace metal grade HNO_3 to a final concentration of 2.0% prior to analysis. Another aliquot of the cell culture was filter centrifuged with Centricon Biomax filters (Millipore Corporation, Billerica, MA, USA), (<5,000

nominal mol wt limit) and the supernatant, which contained only dissolved Pb (i.e., $Pb_{equilibrium}$), was acidified with trace metal grade nitric acid for analysis. The Pb adsorption by *P. putida* in axenic bioreactors was measured as the difference between total and dissolved Pb. In xenic reactors, Pb associated with the predator ($Pb_{predator}$ = $Pb_{ingested}$ + $Pb_{adsorbed}$) was measured directly by digesting membranes (5.0-µm pore size) with filtered cells in 10% trace metal grade HNO_3. Filtrate from 5.0-µm filters was not analyzed, because the loss of Pb to the post-filter nalgene hardware was significant. All glassware was coated with dimethyldichlorosilane to minimize loss of Pb to reactor walls. Wall loss was determined with a reactor containing Pb and no cells. The Pb concentration was measured at the beginning and end of experiments and the difference, attributable to wall loss, was consistently < 10%. All samples were analyzed for Pb by graphite furnace atomic absorption spectrometry ([GFAAS]; no matrix modifier; 20.0-µl analyte sampled; replicate analysis of Pb standards gave a coefficient of variation of <5%).

Ingested Pb was determined as the difference between $Pb_{predator}$ and the $Pb_{adsorbed}$ which was calculated using the Langmuir isotherm previously established for Pb on *T. thermophila* [6]:

$$Pb_{adsorbed_P} = \frac{K_P \Gamma_{\max} Pb_{equilibrium}}{1 + K_P Pb_{equilibrium}} \quad , \tag{6}$$

where K_P = 17.0 L/µmol and Γ_{max} =1.3 µmol/g, and $Pb_{equilibrium}$ is the concentration of dissolved Pb in µM.

The uptake of Pb by adsorption to prey was calculated using a linear Pb isotherm for *P. putida* previously established in this laboratory [6]:

$$Pb_{adsorbed_B} = K_B * Pb_{equilibrium} \tag{7}$$

where K_B was measured to be 25,755 ml/g.

The remainder of adsorbed Pb, calculated as $Pb_{Total} - (Pb_{equilibrium} + Pb_{adsorbed_B} + Pb_{predator})$, was assumed bound to waste matter produced by *T. thermophila.*

The concentration of Pb ingested by predation was modeled as the product of the predation rate and the specific sorbed metal concentration associated with *P. putida* minus Pb excreted by *T. thermophila*:

$$Pb_{ingested} = r_{pred} * \frac{Pb_{adsorbed_B}}{B} - (Pb_{ingested} * k_w) \quad (8)$$

where k_w was the excretion coefficient of Pb from *T. thermophila*. The k_w was determined from the slope of the natural logarithm of Pb associated with *T. thermophila* versus time after the prey was consumed.

Results and Discussion

P. putida growth parameters

The maximum growth rate of the bacteria (μ_{max_B}) was 0.4/h (r^2= 0.86), and the intrinsic death rate (k_{d_B}) was found to be 0.002/h (r^2= 0.79). The observed yield of bacteria growing on pyruvate (Y_B) was measured to be 0.27 g/g (r^2= 0.91). The saturation constant (Ks_B) was found by fitting data to Equation 1. The best-fit value of Ks_B was 0.05 g/L (r^2 = 0.83). Since stationary phase *P. putida* cells were used in predation experiments, these growth parameters (other than k_{d_B}) are not required for modeling of the batch experimental obtained data for *T. thermophila* and Pb; however, the parameters are reported here since they are of use in model simulations of conditions where *P. putida* growth occurs.

T. thermophila growth parameters

The growth curve for *T. thermophila* feeding on *P. putida* is shown in Figure 3.1. The experimental control (*T. thermophila* with no prey) usually did not show significant growth. In the cases where there was some growth in the control reactor,

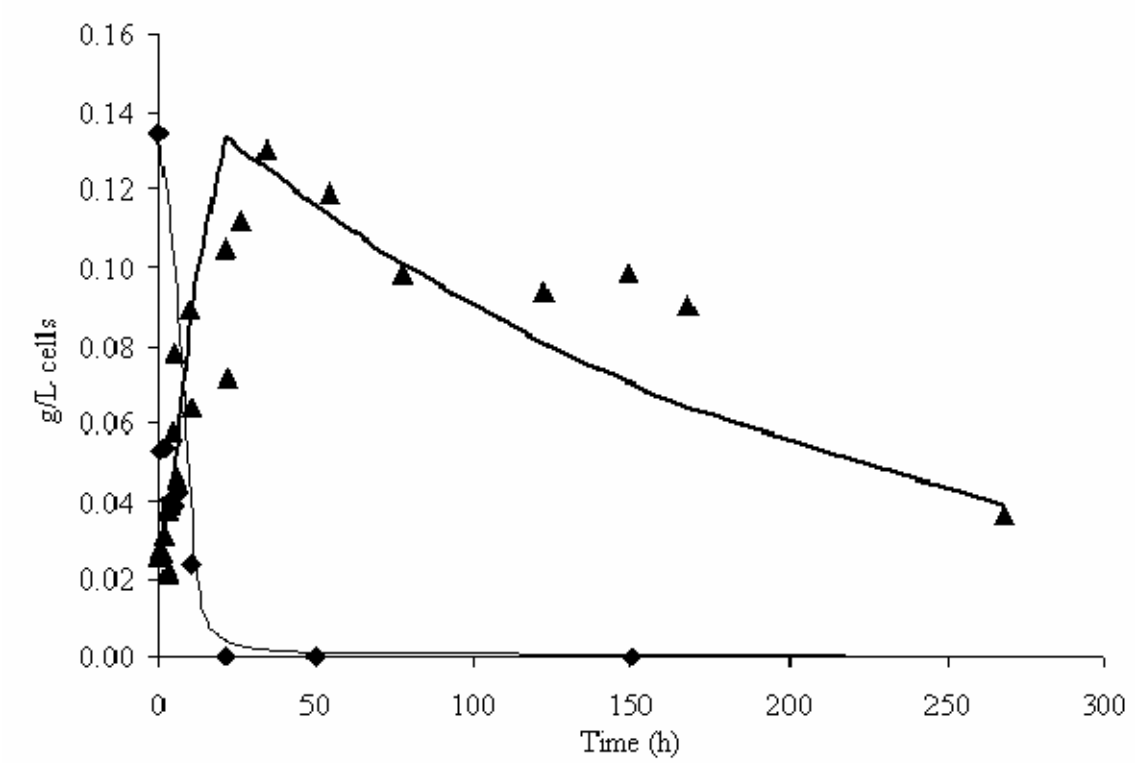

Figure 3.1. Growth of *T. thermophila* on *P. putida.* Symbols represent data points and lines represent model predictions:

▲ g/L *T. thermophila*

◆ g/L *P. putida*

Model fit of *T. thermophila* data

Model fit of *P. putida* data

predation-related growth was corrected for the control. The maximum growth rate of *T. thermophila* (μ_{max_P}) growing on *P. putida* was 0.16/h. This result is consistent with that reported in studies by other investigators of *T. thermophila* growing on *P. putida* in a batch culture, where the maximum observed growth rates ranged from 0.16/h (Hauptmann University 2000; http://bibd.uni-giessen.de/ghtm/2000/uni/d000050b.htm) to approximately 0.22/h [7]. The intrinsic death rate of the xenic population (k_{d_P}) was 0.005/hour ($r^2 = 0.85$). The saturation constant Ks_p was found to be 0.028 g/L ($r^2 = 0.79$) using the Monod model and 0.001 g^2/L^2 ($r^2 = 0.86$) with the double saturation model. Fits of the Monod and double saturation model to the data for the specific growth rate of the predator are shown in Figure 3.2. While both models were satisfactory, the double saturation model was selected as a model for *T. thermophila* growth in subsequent experiments because it better minimized the residual squared error between the data and model.

Measurements of the true yield of *T. thermophila* growing on *P. putida* (Y_P) were confounded by an apparent growth on something else besides *P. putida.* For instance, *Tetrahymena thermophila* cells may also have re-ingested excreted material, their own dead cell material and dead *P. putida* cells. The value for Y_P was found to be 0.8 g/g ($r^2 = 0.71$) by minimizing error between the data and the logistic growth curve. A model simulation using the measured or fitted parameters is shown in Figure 3.2 along with the experimental observations.

Effects of Pb on T. thermophila growth parameters

The effects of the three concentrations of Pb on the growth parameters of *T. thermophila* are summarized in Table 3.1. For each initial dissolved Pb concentration and for the control containing no Pb, *T. thermophila* growth was better fit by the

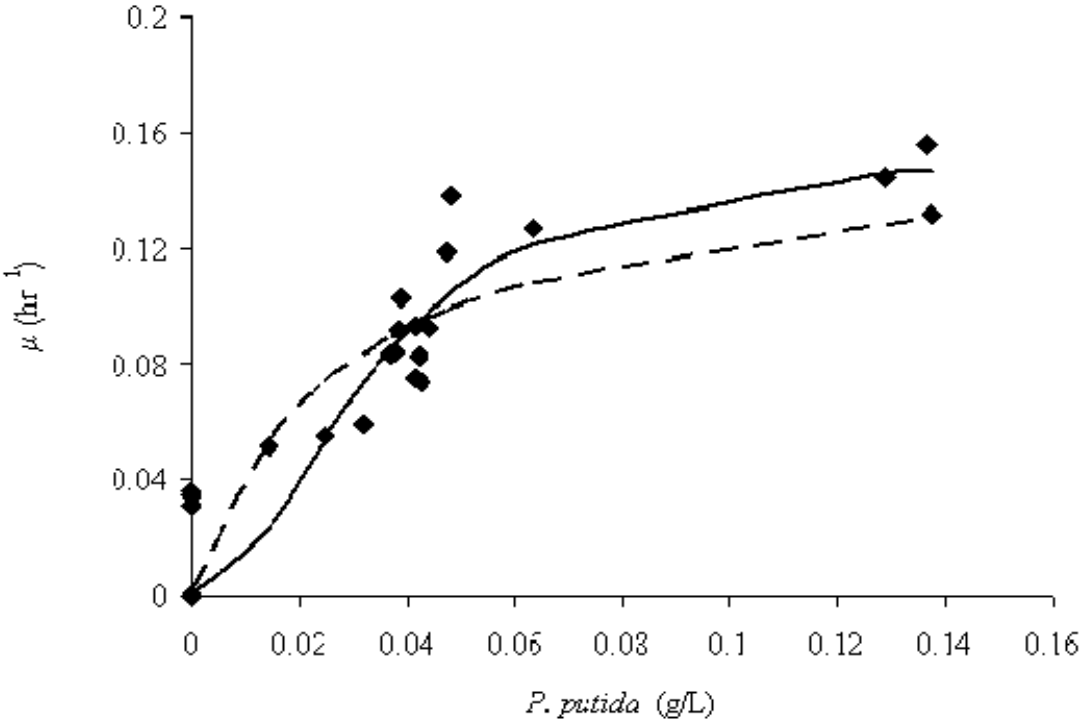

Figure 3.2. Effect of *P. putida* concentration on the specific growth rate of *T. thermophila*. Symbols represent data points and lines represent model predictions:

- ◆ *T. thermophila* specific growth rate
- ——— Double saturation model of specific growth rate
- – – – Monod model of specific growth rate

Table 3.1. The effect of Pb on *Tetrahymena thermophila* growth parameters.[a] NA = not applicable, no growth observed.

Initial dissolved Pb (μM)	μ_{maxp} (/h)	Ks_p (g^2/L^2)	Y_p (g/g)	k_{dp} (/h)
0	0.16	0.001	0.8	0.005
0.3	0.23	0.0003	0.8	0.034
0.7	0.03	0.0001	0.69	0.035
1.8	NA	NA	NA	0.036

[a] μ_{maxp} = maximum specific growth rate of predator; Ks_p = saturation constant of predator; Y_p = yield coefficient of predator growing on prey; k_{dp} = intrinstic death rate of predator.

double saturation model than the Monod model (e.g., r^2= 0.88 vs 0.94 for the Monod versus double saturation model fit for the lowest Pb concentration). Lead had a dose-dependent effect on the maximum growth rate, with *T. thermophila* growing more slowly at higher Pb concentrations: μ_{max_P} decreased linearly as the initial concentration of dissolved Pb increased, so that μ_{max_P} = -.09 • $[Pb]_{initial\ dissolved}$ +0.16 (r^2 = 0.60). At the highest Pb concentration, there was no observed growth. Pb slightly altered the saturation coefficient (Ks_P), as described by the relationship: Ks_P = -0.0015• $[Pb]_{initial\ dissolved}$ +0.001(r^2 = 0.82).

There was an indication that the yield coefficient (Y_p) decreased with Pb concentration when dissolved Pb concentration was equal to or less than 0.7 μM so that Y_p= -0.4•$[Pb]_{dissolved}$ +0.8 (r^2 = 0.89; at the highest dissolved Pb concentration there was no cell growth). However, this change was confounded by the experimental difficulty associated with the measurement of yield (see above discussion) and may not be significant. The death rate (k_{dp}), increased with initial dissolved Pb concentration. Intrinsic death rate without Pb was 0.005/h, and with Pb, even at the lowest dissolved Pb concentration of 0.3 μM, k_{dp} increased to 0.035/h. The coefficient describing Pb excretion from *T. thermophila* (k_w) also showed a linear relationship to initial dissolved Pb concentration, so that k_w = -0.025•$[Pb]_{initial\ dissolved}$ +0.11 (r^2 = 0.93).

The above relationships between model parameters and dissolved Pb concentration are approximations, since dissolved Pb varied somewhat from the initial concentration during each batch experiment. These relationships could be refined by conducting future experiments in chemostats, where steady state conditions in Pb concentration could be achieved.

Effect of prey concentration on predation and fate of Pb

Figure 3.3 shows the growth of *T. thermophila* at the three different initial prey densities. All experiments had the same initial Pb level (0.5 μM). The rate and amount of growth increased with starting prey density. Therefore, any toxic effect resulting from the increased uptake of cell-bound Pb was not as important as the positive effect on growth of the increased prey concentration.

The initial concentration of prey did not impact the temporal pattern of Pb fractionation. For example, Figure 3.4 shows the change over time in the fraction of ingested Pb, for different initial prey densities. A lower percentage of Pb was ingested by the end of the experiment for the highest prey density. If the predator were accumulating Pb in proportion to the number of prey cells it ate, we would expect to see the opposite trend. Instead, more Pb was adsorbed to the surface of predator cells because their concentration was higher as a result of growth on the prey. Initially, *P. putida* cells were in equilibrium with dissolved Pb. Upon addition of predator (immediately following the initial observation), the fraction of Pb_{total} associated with *P. putida* decreased as the cells were removed by predation (compared to the amount of Pb ingested, the adsorption of Pb to *T. thermophila* had a negligible effect on the fraction of dissolved Pb). Lead associated with *T. thermophila* increased with ingestion of *P. putida* and then decreased, presumably as ingested Pb was excreted. It should be noted that the Pb adsorbed to and internalized by the *P. putida* prey was not differentiated. Although this distinction should not make a difference in the total concentration of Pb ingested via predation, it could possibly affect the excretion and assimilation of the metal by the predator. For example, the process of digestion in the predator gut could result in a different fate for prey-bound metals versus prey-assimilated metals and the ratio of adsorbed to internal Pb could change with the external Pb concentration and/or time. Studies comparing assimilation of metals from

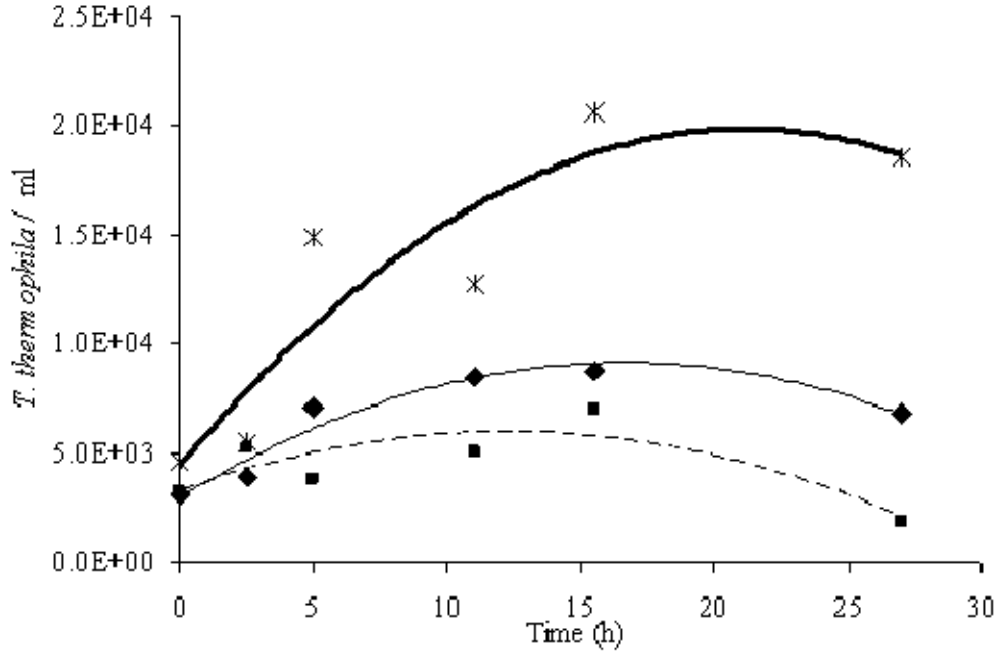

Figure 3.3. Effect of initial prey density on *T. thermophila* growth. Symbols represent data points and lines represent model predictions:

- ■ 1x (Initial *P. putida*- 0.01 g/l)
- ◆ 3x (Initial *P. putida*- 0.03 g/l)
- * 10x (Initial *P. putida*-0.13 g/l)
- _____ Polynomial model fit of 1x data
- _____ Polynomial model fit of 3x data
- _____ Polynomial model fit of 10x data

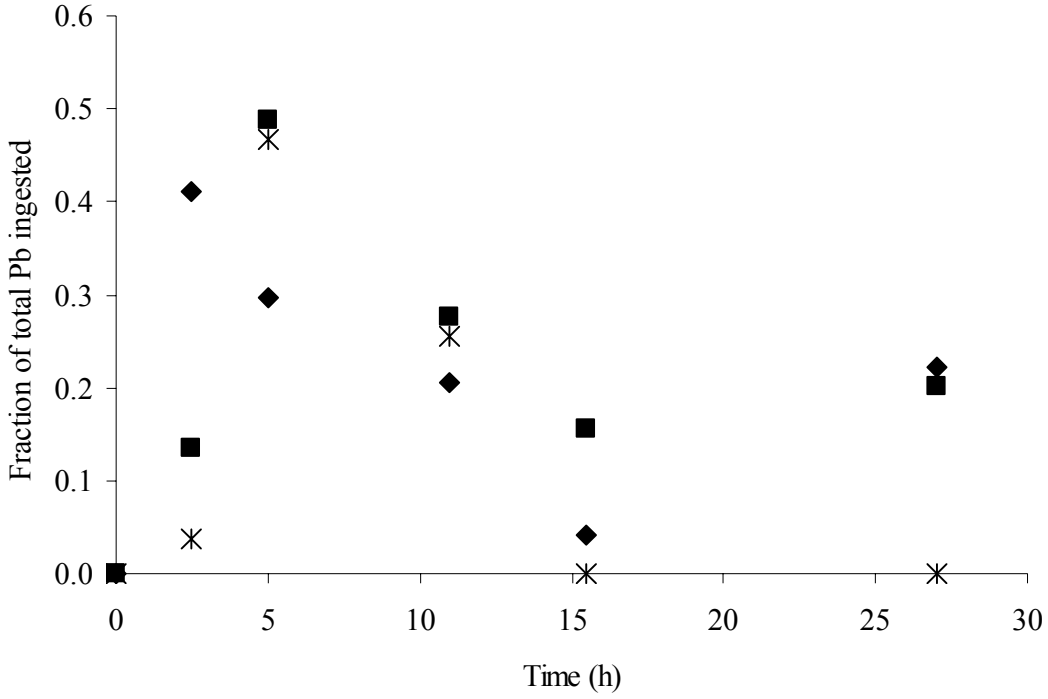

Figure 3.4. Fraction of Pb ingested over time for three different prey densities

■ 1x *Pseudomonas putida*

◆ 3x *P. putida*

* 10x *P. putida*

phytoplankton prey into bivalve larvae indicate that more assimilation occurs of metal originating in the cytoplasm of the prey, versus that adsorbed to prey cells [16]. It would be of interest in future experiments to distinguish these two pools of prey-associated Pb to extend our understanding of the factors regulating Pb excretion in this model system.

Exposure of *Tetrahymena* to sublethal concentrations of Pb has been shown to postpone growth phase, increase doubling time, and decrease or stop endocytosis (the formation of food vacuoles) [17]. The severity of such effects depends on factors other than the total concentration of Pb, notably Pb speciation and phase distribution. For example, pH strongly affects toxicity by changing the fraction of total Pb that is in the form of the free ion, Pb^{+2}, which (based on the preponderance of research related to microbial response to metal ions) controls the metal uptake rate. Nilsson reported an initial lag time in the growth of *Tetrahymena* exposed to 2.6 mM Pb at a pH of 6.8. At 3.9 and 5.2 mM Pb, the generation time was prolonged by a factor of 1.2 and 1.5, respectively [17]. All other factors being equal, Pb toxicity increases as pH decreases, and more of Pb_{total} exists as Pb^{+2}. However, at high pH, *Tetrahymena* may actually receive an increased dose of Pb, because it feeds on the Pb adsorbed to prey, and at very high lead concentrations the Pb dose may be increased by feeding on precipitated Pb minerals. Once inside *Tetrahymena* cells, in cases where normal cell functioning continues, Pb is found sequestered in dense granules, small vesicles, and mitochondria [9].

Toxicity is also affected by media composition. For the same Pb_{total}, a medium low in metal binding ligands (such as dissolved organic matter) will have a higher concentration of Pb^{+2}, and hence higher metal toxicity. The rate of *Tetrahymena* phagocytosis was observed to decrease by 52, 37, and 0% when the concentration of proteose peptone/liver extract media was 0.5, 1, and 2%, respectively [18]. In another

study, the 20-h LD-50 (i.e., dose resulting in 50% mortality to test organisms) for *Tetrahymena* exposed to $PbNO_3$ increased significantly with the addition of calcium carbonate [19]. This was likely the result of higher levels of inorganic ligands (HCO_3^-, CO_3^{-2}) and/or cation competition between Ca^{+2} and Pb^{+2}.

In the experiment with 10x *P. putida*, *T. thermophila* was exposed to a lower level of Pb^{+2}, since more of the added Pb was adsorbed to prey cells (relative to the 1x and 3x prey levels). However, if Pb is desorbed from ingested prey cells inside the acid environment of the food vacuoles, it is conceivable that adverse affects of Pb on *Tetrahymena* would appear after digestion of prey. Indeed, during excretion, the cytoproct, the region of the cell from which digested food is expelled, is reported to be high in Pb [18].

The experimental Pb concentrations used in this research are in the same range as soluble Pb in the mixed liquor of activated sludge plants, where levels are as high as 500 μg Pb /L (~2.4 μM; [4]) are reported. However, the experimental Pb concentrations are high compared with those found in natural waters. For example, Benoit [20] reports total Pb levels of approximately 2 ppb in the urbanized reach of the Quinnipiac River, Connecticut, USA, or roughly a factor of 40 below the lowest total Pb level used in this research. The Pb levels selected for use in our experiments permitted precise and accurate GFAAS analysis of Pb in samples without requiring use of ultra clean techniques. The experimental Pb levels also did not exceed the solubility product of any Pb solid phases and, as noted above, the solution speciation was dominated by the free ion. Lead was also not toxic to the prey at the levels used. Since adsorption of Pb to the prey obeyed a linear isotherm and adsorption to the predator was negligible, it is reasonable to expect that the results obtained can be extrapolated to lower Pb levels. Under conditions where Pb binding to prey follows a linear isotherm, the experimental use of elevated Pb levels has the net effect of

accelerating the time course of Pb uptake that would otherwise be observed for predators in the field.

Model predictions

Using kinetic parameters related to growth of *T. thermophila* on *P. putida* obtained in these laboratory experiments and previously determined Pb adsorption isotherms for the predator and prey, a computer model for Pb behavior was developed using Stella 8.0 modeling software (High Performance Systems, Lebanon, NH, USA). Figure 3.5 shows the observed effect of Pb on *T. thermophila* cell growth over time and the model predictions. Growth model predictions were based on the effects of Pb on growth parameters summarized in Table 3.1. The model effectively captures the temporal trends of the observations with the exception of the cell yield (Y_P). Model predictions of cell growth underestimated data for all Pb concentrations. As noted previously, there may be another energy source that predator cells were using for growth. The question of alternate food sources will be explored further in the next model and the next chapter of this dissertation.

Using these growth parameters and previously reported Pb adsorption isotherms [6], independent predictions (with no adjustments to model parameters) can be made for the behavior of Pb over time in the model predator-prey system at different Pb levels. The results of model predictions are shown in Figure 3.6 for the experiment at low Pb (initial dissolved Pb of 0.3 μM). The model predicts that the dissolved Pb and prey-bound Pb concentrations decrease upon addition of predator cells, since predators are consuming the bacterial prey and Pb is adsorbing to predator cells. After approximately 10 h, Pb begins to be excreted by *T. thermophila*. The predictions from the model effectively capture the observed trends in Pb adsorbed to cell surfaces and Pb associated with waste material, but underestimate Pb ingested,

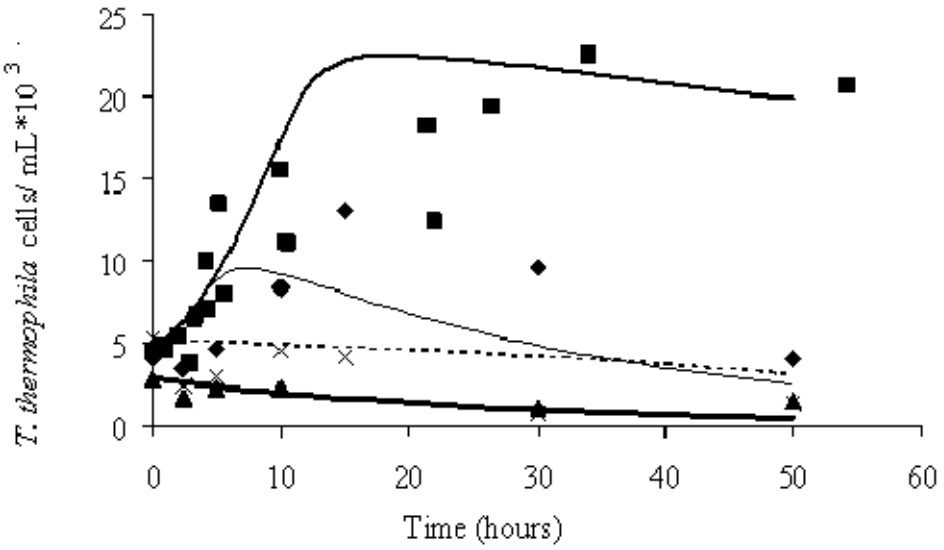

Figure 3.5. Growth of *T. thermophila* under three Pb concentrations. Symbols represent data points and lines represent model predictions:

- ■ No Pb
- ◆ Low Pb (0.3 μM)
- X Medium Pb (0.7 μM)
- ▲ High Pb (1.8 μM)
- ——— Model fit of *T. thermophila* growth with no Pb
- ——— Model fit of *T. thermophila* growth with low Pb
- – – – Model fit of *T. thermophila* growth with medium Pb
- ——— Model fit of *T. thermophila* growth with high Pb

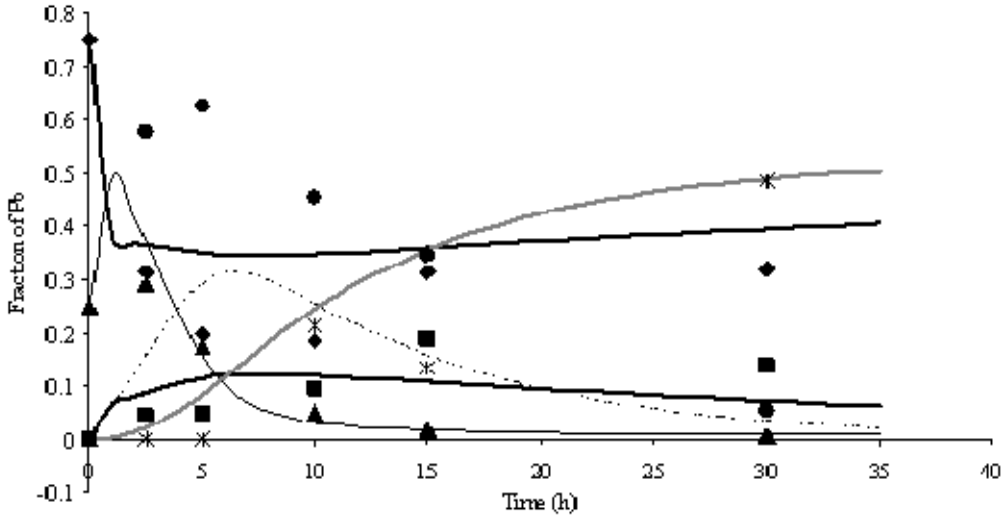

Figure 3.6. The fate of Pb when initial dissolved Pb = 0.3 μM. Symbols represent data points and lines represent model predictions:

♦ Dissolved Pb

■ Pb adsorbed to *T. thermophila*

● Pb ingested by *T. thermophila*

▲ Pb adsorbed to *P. putida*

* Pb adsorbed to waste material

——— Model fit of $[Pb]_{dissolved}$

——— Model fit of $[Pb]_{adsorbed_P}$

- - - - - Model fit of $[Pb]_{ingested}$

——— Model fit of $[Pb]_{adsorbed_B}$

— — — Model fit of $[Pb]_{adsorbed\ waste\ material}$

and consequently overestimate dissolved Pb. The model predicts that the concentration of ingested Pb peaks at around 15 h, and then decreases again as it is excreted. This prediction did not match the data. Instead, ingested Pb increased immediately (at the first measurement taken at 2.5 h) and began to decrease again soon after.

Model predictions and observations of Pb behavior in the high lead experiment (in which cells were exposed to an initial dissolved Pb concentration = 1.8 μM) are shown in Figure 3.7. Lead toxicity is much more evident under these conditions (see cell growth in Figure 3.5). The model predicts that Pb primarily remained bound to prey cells or in the dissolved state, since there was little *T. thermophila* growth or predation. Model predictions that negligible Pb is adsorbed to *T. thermophila* or associated with waste material were consistent with observations; however, there is a discrepancy again between the model simulation for ingested Pb and dissolved Pb versus observations.

It should be noted that the concentration of ingested Pb was measured as the difference in total Pb associated with *T. thermophila* cells (as determined by filtration through 5 μm filters) and the concentration adsorbed to the outside of the cells (based on the Pb isotherm for *T. thermophila*). However, the model calculations of ingested Pb are related to the number of prey cells eaten by predators and the Pb adsorption isotherm of the prey. Thus, one explanation for the discrepancy between the model simulation and experimental observation is that measurements of ingested Pb include a form or forms of particulate Pb different from that calculated by the model. This could occur if some waste material or lysed cells present in the original inoculum of *T. thermophila* were captured by the 5.0-μm filters used to separate *T. thermophila* from the waste- or bacteria-associated Pb. A large presence of such debris has been observed in the *Tetrahymena* pellet following the multiple centrifugations necessary to

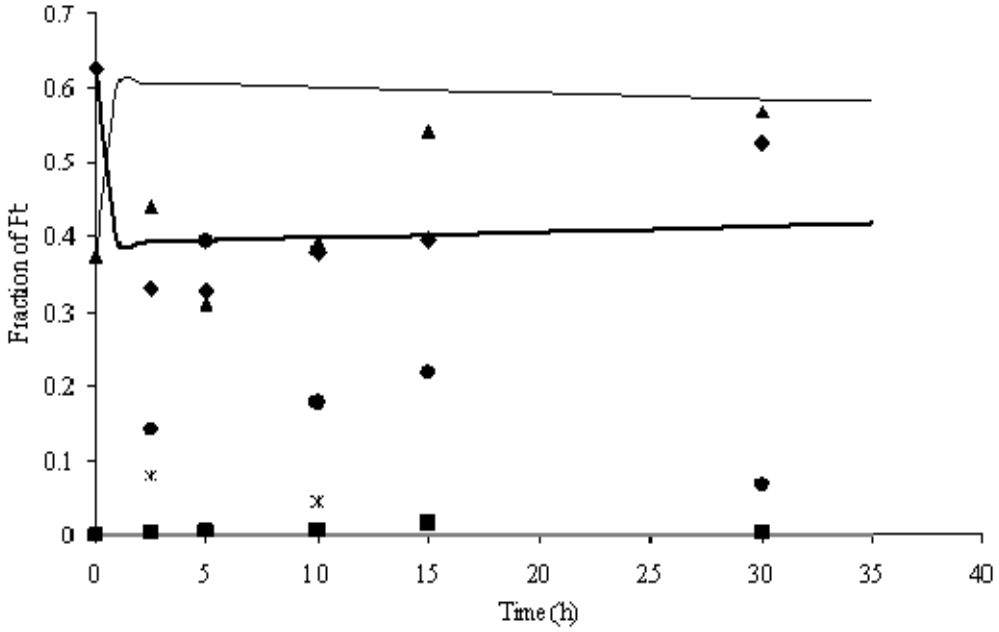

Figure 3.7. The fate of Pb when initial dissolved Pb = 1.8 μM.

◆ Dissolved Pb

■ Pb adsorbed to *T. thermophila*

● Pb ingested by *T. thermophila*

▲ Pb adsorbed to *P. putida*

* Pb adsorbed to waste material

—— Model fit of $[Pb]_{dissolved}$

—— Model fit of $[Pb]_{adsorbed_P}$

- - - - - Model fit of $[Pb]_{ingested}$

—— Model fit of $[Pb]_{adsorbed_B}$

– – Model fit of $[Pb]_{adsorbed\ waste\ material\ *}$

*Line is obscured by x-axis.

wash the cells prior to the inoculation [21]. Filter capture of particles other than the predator would inflate the concentration of Pb considered to be ingested. The plausibility of this hypothesis was tested through a model simulation in which it wasassumed that lysed cells and waste matter (called "debris" in the model) were added in addition to the *T. thermophila* inoculum. These particulates would adsorb Pb, but not consume prey. Lead adsorbed by the debris would be measured along with Pb associated with the predator, and the sum (determined in the simulation) can be compared to the experimental observations in which we speculate this occurred. Since debris would likely have a greater specific surface area than the predator cells, it would be expected to have a greater affinity (per unit mass) for Pb, and it was assigned an adsorption constant of 100 L/g (this value is arbitrary and is selected for purposes of illustration). Also, it was assumed that the ingestion of Pb via debris was first order with respect to the concentration of debris and was assigned a rate constant of 0.8/h. The initial density of debris was assumed to be equal to the initial *Tetrahymena* cell density.

Figure 3.8 shows the revised simulation for the low Pb case (initial dissolved Pb = 0.3 μM) and demonstrates that the presence of debris under these conditions could account for some of the discrepancy between experimental observations and the initial model simulation (in which no inert particles are assumed to be present).

An alternative explanation for the difference between the experimental data and the initial model simulations is that the model description is missing one or more Pb interactions that affect the observations. For example, we do not consider how the ingestion of decomposed predator cells by *T. thermophila* will affect the fate of Pb in this system. While the model could be readily modified to include this possibility and to assess its importance, this and other scenarios with a modified model would be best performed after the needed parameters were obtained from additional experiments. In

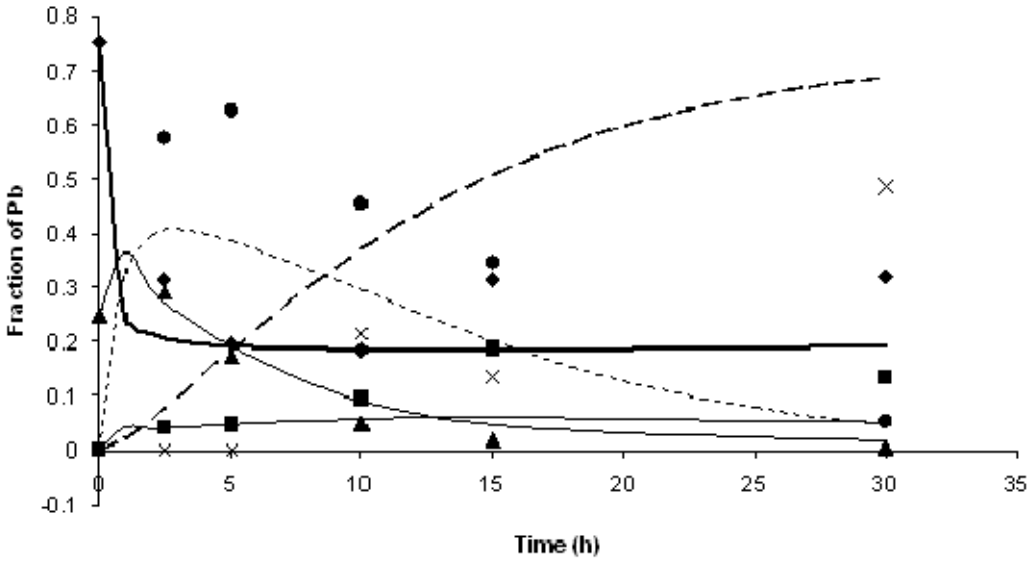

Figure 3.8. Result of model simulations of the fate of Pb when initial dissolved Pb = 0.3 μM and hypothetical inert particles that adsorb Pb are present. Symbols and lines are the same as in Figure 3.6.

cases where differences in observations and model simulations occur, observations can guide the evolution of a model towards a set of constitutive equations that are adequate to render predictions consistent with observations. Changes in the model, in turn, stimulate new experiments to obtain the needed additional model parameters and to verify predictions of the modified model.

In summary, results demonstrated that some kinetic parameters related to prey consumption and growth of *T. thermophila* are altered by Pb concentration. Upon addition of predator to prey cells in equilibrium with dissolved Pb, dissolved and prey-bound Pb became associated with the predator through ingestion and adsorption. Ingested Pb was later excreted as a bound metal associated with *T. thermophila* waste matter. A preliminary mathematical model was developed to describe predator-prey dynamics and their influence on the behavior and fate of Pb. Differences in model predictions and observations suggest possibilities for model alterations that can result in a closer approximation to experimental observations. Additional experiments are required to resolve whether differences in the model and observations result from measurement artifacts or missing processes in the model, or both.

References

1. Sieburth JM. 1979. *Sea Microbes*. Oxford University Press, New York, NY, USA.

2. Curds CR, Cockburn A.1971. A continuous monoxenic culture of *Tetrahymena pyriformis. J Gen Microbio* 66:95-108.

3. Madoni P, Davoli D, Gorbi G. 1993. Acute toxicity of cadmium, copper, mercury, and zinc to ciliates from activated sludge plants. *Bull Environ Contam Toxicol* 53:420-425.

4. Madoni P, Davoli D, Gorbi G, Vescovi L. 1996. Toxic effects of heavy metals on the activated sludge protozoan community. *Water Res* 30:135-141.

5. Morgan GB, Lackey JB. 1958. BOD determinations in wastes containing chelated copper and chromium. *Sewage Ind Wastes* 30:283-286.

6. Patton LE, Shuler ML, Lion LW. 2004. Development of a model microbial predator-prey system suitable for studies of the behavior of toxic trace metals. *Environ Toxicol Chem* 23:292-297.

7. Curds CR, Cockburn A. 1971. A continuous monoxenic culture of *Tetrahymena pyriformis. J Gen Microbiol* 66:95-108.

8. Barbeau K, Moffet J, Caron D, Croot PL, Erdner DL. 1996. Role of protozoan grazing in relieving iron limitation of phytoplankton. *Nature* 380:61-63.

9. Nilsson JR. 1989. *Tetrahymena* in cytotoxicology: With special reference to effects of heavy metals and selected drugs. *Eur J Protistol* 25:2-25.

10. Piccinni E, Irato P, Coppellotti O, Guidolin L. 1987. Biochemical and ultrastructural data on *Tetrahymena pyriformis* treated with copper and cadmium. *J Cell Sci* 88:283-293.

11. Bergquist BL, Bovee EL. 1973. Some adverse effects of cadmium on growth and locomotion of *Tetrahymena pyriformis. J Protozool* 20:497.

12. Sauvant MP, Pepin D, Piccinni E. 1999. *Tetrahymena pyriformis*: A tool for toxicological studies. A review. *Chemosphere* 38:1631-1669.

13. Nicolau A, Mota M, Lima N. 1999. Physiological responses of *Tetrahymena pyriformis* to copper, zinc, cycloheximde and Triton X-100. *FEMS Microbiol Ecol* 30:209-216.

14. Fleischer WR. 1970. *Standard Methods in Clinical Chemistry*. Academic, New York, NY, USA.

15. Jost JL, Drake JF, Tsuchiya HM, Fredrickson AG. 1973. Microbial food chains and food webs. *J Theor Biol* 41:461-484.

16. Reinfelder JR, Fisher NS. 1994. The assimilation of elemets ingested by marine planktonic bivalve larvae. *Limnol Oceanogr* 39(1):12-20.

17. Nilsson JR. 1978. Retention of lead within digestive vacuoles in *Tetrahymena pyriformis* GL. *Protoplasma* 95:163-173.

18. Nilsson JR. 1979. Intracellular distribution of lead in *Tetrahymena* during continuous exposure to the metal. *J Cell Sci* 39:383-396.

19. Carter JW, Cameron IL. 1973. Toxicity bioassay of heavy metals in water using *Tetrahymena pyriformis*. *Water Res* 7:951-961.

20. Benoit G. 1994. Clean technique measurement of Pb, Ag, and Cd in freshwater: A redefinition of metal pollution. *Environ Sci Technol* 28:1987-1991.

21. Zeiner C. 2004. Cycling of Biogenic Manganese Oxides in a Model Microbial Predator-Prey System. M.S. thesis; Cornell University, School of Civil and Environmental Engineering. Ithaca, NY. 110 pp.

CHAPTER IV

ADDITIONAL MODEL PREDICTIONS

Bioavailability of a toxic metal is an important determinant of the extent to which the metal (often the free ion) can adversely affect an ecosystem. Bioavailability is determined by metal speciation [1] and the phase distribution of the metal. It is the dissolved species of metal rather than its absolute concentration that has the greatest effect on toxicity and bioavailability [1]. Metal speciation and phase distribution are governed by the interactions of a host of environmental conditions and processes. The proceeding chapter explores the phase distribution of Pb in experimental and model-simulated microbial predator-prey systems and illustrates how Pb phase distribution is influenced by predation of bacteria and bacterially associated Pb. An experimental condition of interest would be the case where a continuous flow reactor (i.e., a chemostat) is used for experiments. Expected results for this type of experiment are obtained in this chapter through model simulations in which terms are added for continuous addition of a carbon/energy source for bacteria, and for advective loss of the dissolved and suspended constituents in the reactor vessel. A listing of the parameter values used in the chemostat model is provided in Table 4.1.

As an aid to readers, models used in this thesis have been numbered beginning with the models presented in Chapter 3. Model 1 corresponds to the originally proposed predator-prey model for the experimental batch reactor systems where waste matter did not adsorb Pb, Pb was ingested by predators only via predation, and neither waste matter nor dead cells acted as a food source. Model 2 corresponds to the modification of the batch reactor simulation suggested in Chapter 3, i.e., the addition of a component to simulate inert particles that might be captured on filters with the protozoan prey. Model 3 corresponds to additional changes in the batch reactor system

Table 4.1. Default parameters and equations.

Parameter	Value (no Pb)	Value with Pb if different	Basis for parameter determination
$\mu_{maxp}\ (hr^{-1})$	0.16	$0.16-[Pb_{dissolved}]*0.1$	Measured
$Ks_p\ (g^2/L^2)$	0.001	$0.001-[Pb_{dissolved}]*0.0015$ (if $Pb_{dissolved} \geq 0.66\mu M$, $Ks_p=0.0001$)	Best fit
$Y_p\ (g/g)$	0.8	$0.8-[Pb_{dissolved}]*0.47$ (if $Pb_{dissolved} \geq 0.8\mu M$, $Y_p=0$)	Best-fit
$k_{dp}\ (hr^{-1})$	0.005	$0.005+\left[\frac{0.035*[Pb_{dissolved}]}{0.047+[Pb_{dissolved}]}\right]$	Measured
$k_w\ (hr^{-1})$	0.11	$0.11-[Pb_{dissolved}]*0.02$	Measured indirectly
$\mu_{maxb}\ (hr^{-1})$	0.4		Measured
$Ks_b\ (g/L)$	0.05		Best fit
$Y_b\ (g/g)$	0.2		Measured
$k_{db}\ (hr^{-1})$	0.003		Measured
Adsorption constant prey (L/g)	25		Measured
Predator Γ_{max} (μmol/g)	1.3		Measured
Adsorption constant predator (L/μmol)	17.0		Measured
Adsorption constant debris (L/g)	100		Estimated
Debris k (hr^{-1})	0.8		Estimated
Adsorption constant waste matter (L/g)	50		Estimated
$Y_{P\ dead\ pred}$ (g/g)	0.5		Estimated
$Y_{P\ dead\ prey}$ (g/g)	0.5		Estimated
$IE_{excretion}$ (g/g)	0.1		Estimated

discussed here. In the first model described in this chapter, Model 3, the inert particles discussed in Chapter 3 are referred to as "debris". In Model 3 additional food sources for the predator are introduced. The addition of alternate food sources for the predator may also change the fate of Pb associated with the predators in simulations where Pb is present (see discussion below). As noted in Chapter 3, the predictions made by the initial formulation of Model 1 for ingested Pb in batch growth were always lower than what was observed in the laboratory experiments. Additional explanations for this discrepancy are explored here using model simulations. Potential sources of ingested Pb that were not previously considered could include via ingestion of the dead bodies of other predators (which had decomposed into the size range preferred by predators), the ingestion of dead bacteria, and the ingestion of waste material, all of which would contain adsorbed Pb. These effects will be first considered in a batch reactor (Model 3) model to serve as a comparison to Model 2, and then they will be modeled in a chemostat (Model 4). A summary of the models and how they differ from one another is given in Table 4.2. Also, the STELLA equations for each model are given in Appendix I.

In Model 3 the growth and death parameters used for predator and prey are those previously established for *T. thermophila* and *P. putida*, respectively, and are given in Chapter 3 and Table 4.1. In the simulations shown here, the initial concentrations of predator and prey are assumed to be 0.02 g/L and 0.06 g/L, respectively, and are typical of those used in the laboratory experiments previously presented in this thesis. The growth of predators on dead predators was assumed to follow double saturation kinetics (as with predator growth on prey), and the corresponding ingestion of dead predators, was assumed equal to the additional growth divided by a yield coefficient. The yield coefficient ($Y_{P_{dead\ pred}}$) was assumed to be 0.5 gram of predators per gram of dead predators consumed. Thus the ingestion rate

Table 4.2. Summary of models developed in this thesis.

Model	New assumptions	Changes in initial conditions?
1.	• Batch reactor (original model from Chapter 3).	
2.	• Inert particles ("debris") added to batch reactors along with predator cells. • Debris can adsorb Pb. • Predators can eat debris.	
3.	• Predators can eat other dead predator cells. • Pb adsorbing to dead predators has same Pb adsorption isotherm as that for live predators. • Predators can eat dead prey cells. • Pb adsorbed to dead prey has same Pb adsorption isotherm as that for live prey. • Predator excretes everything it ingests by 1st order kinetics with rate constant k_w. • Pb excreted is all adsorbed to excretion. • Predator can re-ingest what it excretes (with an ingestion efficiency ($IE_{excretion}$) of 0.1 grams of excretion per gram of predator) and all associated Pb and subsequently re-excrete it. • Adsorption constant for excretion = 50 L/g.	Initial concentration of dissolved Pb set to 1.0 μM.
4.	• Reactor from Model 3 is continuous flow.	Q=0.4 /hour V=1.0 L Pyruvate feed concentration = 0.5 g
Twiss	• Batch reactor • Debris excluded from model. • Metal is excreted in the dissolved form.	All metal is added to reactors as metal previously ingested by prey.

of dead predators was equal to:

$$\frac{1}{Y_{P_{dead\ pred}}}\left(\frac{\mu_{max_P}(Dead\ predator)^2 * Predator}{K_{S_P}+(Dead\ predator)^2}\right)$$

Death of predators over time in the reactor provides a contribution to the dead predator pool. Furthermore, some "debris" consisting of dead predators and fecal material was assumed to accompany the initial inoculum of live predators (see Chapter 3 and Model 2). The initial mass of debris is set (for purposes of illustration) to one half of the initial predator concentration. As in previous models debris adsorbs Pb and is eaten by the predator. In consideration of the presence of waste matter in the debris, predator's growth was assumed to not occur as a consequence of debris consumption.

It is also assumed that the predators can eat prey that have died of causes not related to predation (i.e. as a consequence of intrinsic cell death). The ingestion of dead prey was assumed to follow double saturation kinetics and the yield for dead prey was set equal to 0.8. The half velocity coefficient (K_{S_P}) and maximum specific rate (μ_{max_P}) for consumption of dead prey was assumed to be the same as that for consumption of dead predators. Therefore the ingestion rate for dead prey was equal to:

$$\frac{1}{Y_{P_{dead\ prey}}}\left(\frac{\mu_{max_P}(Dead\ prey)^2 * Predator}{K_{S_P}+(Dead\ prey)^2}\right)$$

In Chapter 3 model simulations for batch reactors predicted that the ultimate sink for Pb was the predator's excreted waste material. *T. thermophila* (and many other protozoan predators) discriminate in their consumption of particles based on particle size (*vs.* composition). Thus, it is likely that the reingestion of waste material and the associated Pb might also occur and would contribute to the higher "ingested" Pb observed in experiments. Model 3 therefore includes the cyclic outcome of predators excreting waste material, reingesting some of it and excreting it again.

Excretion of ingested material is modeled with a first order dependence on the amount of ingested material with an excretion rate constant k_w. The excretion constant, k_w = 0.1/hour, was taken from the measurement of the decrease in predator-associated Pb concentration over time following predation on Pb-covered prey (see Chapter 3). The predator's ingestion of excreted waste material was modeled in a manner similar to the uptake of dead predators and prey but was assumed to follow Monod kinetics because use of double saturation kinetics was presumed to be restricted to the predator growth on food that itself requires a food source (or did at one time, as in the case of dead prey). The waste material was assumed to not contribute to the growth of the predator therefore no yield coefficient was necessary. However, a coefficient for waste material ingestion efficiency, ($IE_{excretion}$, grams of waste material ingested per gram of predator) was introduced to account for the fact that all waste material was not in a size range amenable to ingestion. Consumption of excreted waste material (termed "Excretion" in the model) was therefore described by the following relationship:

$$IE_{excretion}\left(\frac{\mu_{max_P}(Excretion)*Predator}{K_{S_P}+(Excretion)}\right)$$

An assumed value of $IE_{excretion}$ equal to 0.1 was used for the simulations discussed below. An increase in this value would result in assigning greater importance to Pb uptake through the mechanism of assimilation of waste material.

Figure 4.1 compares predator growth in Models 2 and 3, the two batch reactors. Model 3 appears to fit the original population data as well or better than Model 2 did. Keeping in mind that Pb has not yet been introduced, the major difference between these models is the addition of dead prey and predator cells which live predators can consume *and grow* on. Figure 4.1 illustrates the significant effect on predator population that this extra food source provides over time. The dead cells

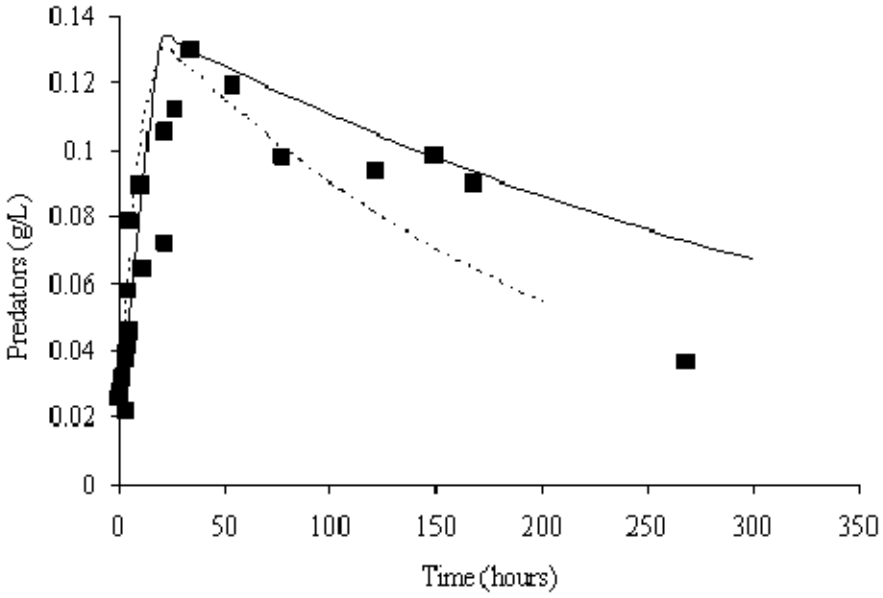

Figure 4.1. Predator population in Model 2 versus 3 and experimental data.

..... Model 2

____ Model 3

■ *T. thermophila* (g/L)

enable the population of predators to sustain themselves longer even as their live prey dies out.

The dynamics described above (Model 3) were used to consider the response of the predator/prey reactor system when Pb was introduced. Experimentally, the effects of Pb on cell growth were assessed in relation to the *initial* dissolved Pb concentration (see Chapter 3). In Model 3 and the subsequent chemostat model discussed below, it is assumed that the relationships of growth to Pb are the same, but the growth parameters are treated as responding to the *actual* instantaneous dissolved Pb concentration rather than the initial value. These relationships are listed in Table 4.1. The intrinsic death rate of predators (k_{dp}) increased with the introduction of Pb. In the absence of Pb the value of k_{dp} was 0.005/ hour and when Pb was added it rose to 0.035/ hour. This increase was seen at the lowest levels of Pb used. The hyperbolic relationship shown below was utilized to provide a smooth transition in k_{dp} values (*vs.* a step change) over the range of k_{dp}= 0.005/hr to 0.035/hr. The sensitivity of k_{dp} to the Pb concentration was controlled through the selection of the constant in the denominator. The selected value of 0.047 μmol/L is low relative to the initial dissolved Pb level used in Model 3 (0.3 μM) and to the 0.5 and 1.0 μM Pb levels used for the input concentration in the chemostat simulations described below.

New assumptions for Model 3 are summarized in Table 4.2 and include the assumption that the concentrations of Pb adsorbed to the predator, prey and waste matter are controlled by the concentrations of dissolved Pb and predator cells, prey cells and waste matter, respectively. Dead predator cells and dead prey cells are assumed to obey the same Pb adsorption isotherms as their live counterparts. Instantaneous equilibrium is assumed for all adsorption reactions. [Note that the instantaneous adsorption equilibrium between dissolved Pb and Pb bound to a surface is actually modeled in the STELLA programming environment as a very fast reaction

with first order forward rate (adsorption) and backward rates (desorption), where the ratio of the forward and backward rate constants is set equal to the equilibrium constant.] Association of Pb to waste matter was assumed to obey a linear isotherm with an adsorption constant of 50 L/g. The value of 50 L/g is two-times the adsorption constant used for prey, and was chosen based on the assumption that the specific surface area of waste matter is higher than that of prey.

Before considering the behavior of Pb in this model, the relative importance of various sources of ingested Pb was analyzed for the purpose of simplifying the model. The sources of ingested Pb are waste material, debris, dead predator cells, dead prey cells and live prey cells. Figure 4.2 shows the concentration of ingested Pb over time when each Pb source is systematically removed.

In each of the five scenarios shown in Figure 4.2, the predator is eating live prey. When predators are eating waste matter, debris, and dead predator and prey cells (i.e. all sources), ingested Pb is highest. When waste matter is removed as a food source there is a decrease in the concentration of Pb ingested. When the model is altered so that predators also cannot eat dead prey and dead predator cells there is no significant change in the Pb ingested. The contribution of debris in the inoculum to ingested Pb is noticeable for approximately 20 hours of the simulation (Figure 4.2; gray dotted line). So as to the original question in Chapter 3/Model 2 of why the ingested Pb always tended to be underestimated by the model, the ingestion by the predator of Pb-adsorbing waste matter is indicated to be a likely explanation. The ingestion of debris, while contributing to predator Pb-load early on, would not

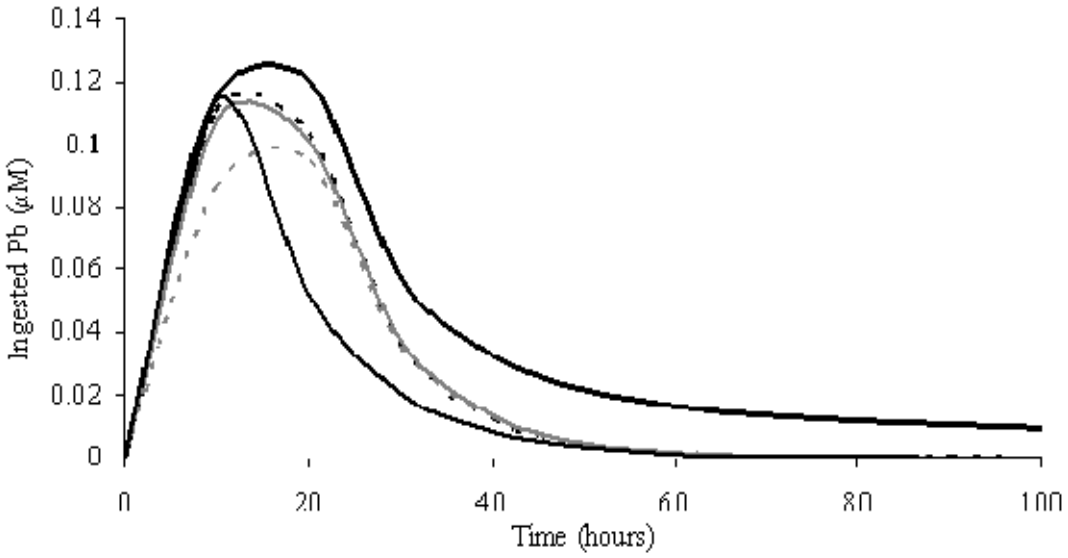

Figure 4.2. Ingested Pb in Model 3.

——— Everything eaten

..... Waste material not eaten

——— Waste material, dead cells not eaten

_ _ _ _ _ Waste material, dead cells, debris not eaten

——— $[Pb]_{ingested}$ in Model 2

ultimately help answer this question. However, it was retained in the models because of its early effect. Ingestion of dead cells was retained in subsequent model modifications because of its effect on predator growth (see Figure 4.1).

Model 4 has the same properties as Model 3 except that it has been modified to simulate a continuous flow reactor (i.e., a chemostat). For purposes of illustration the carbon/energy source, pyruvate, is assumed to be fed into the system at a constant rate; the reactor volume (V) is set equal to 1.0 L, the volumetric flow in and out of the reactor (Q) is 0.04/hour (giving a hydraulic residence time of 25 hr) and the pyruvate feed concentration, is assumed to be 0.5 g/L. Pyruvate either washes out of the reactor or is consumed by the bacterial prey. The prey grows on pyruvate according to Monod kinetics. The prey population decreases in one of three ways: prey can be consumed by predators, prey can die (intrinsic prey death), and prey can wash out of the reactor. As in previous simulations, predator growth on prey is modeled according to double saturation kinetics. Predator numbers decrease as they die (intrinsic predator death) and wash out of the reactor.

Figure 4.3 shows model results for the cell populations and pyruvate concentration in the simulated chemostat over time for the case where Pb is not present. The prey population initially increases, peaks during the interval that predator concentrations are low, and then begins to decline as the predator population increases. The predator concentration reaches a maximum value and shortly thereafter prey is at its minimum cell density. In response to the decrease in prey concentration, the predator population declines. After additional minor fluctuations, both predator and prey populations as well as the concentration of pyruvate stabilize and the chemostat system attains a steady state. Increasing or decreasing the initial prey or predator concentration has no effect on the final system composition other than

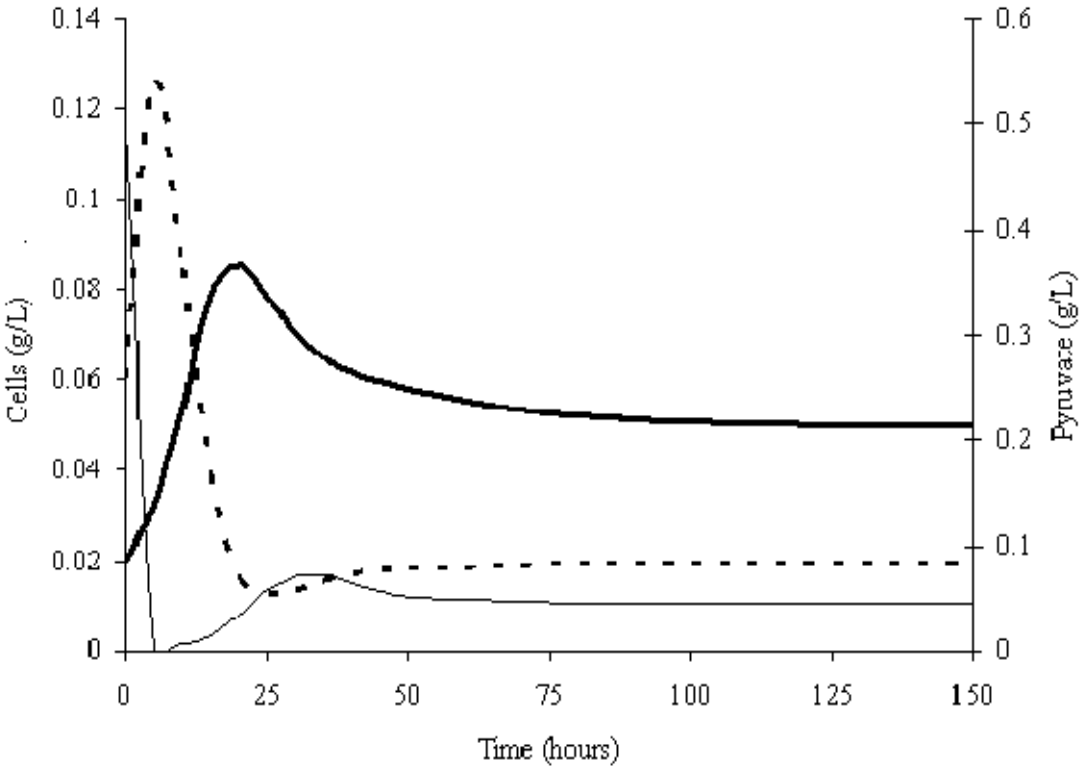

Figure 4.3. Cell density and pyruvate concentration over time in Model 4 when no Pb is present.

Predator

Prey

Pyruvate

delaying or hastening the approach to steady state. Figure 4.4 shows the same scenario but in this case, the flow rate into the chemostat (Q) is tripled so that residence time is decreased by one third to 8⅓ hours. At the shorter residence time, the concentration of the predator is reduced and therefore predation does not impact the bacterial population to the same extent. The reduced degree of predation results in prey, not predator, being the dominant biological component of the chemostat reactor.

Upon introduction of Pb into the reactor the fate of added Pb becomes of interest and an impact is expected on the predator-prey dynamics through the toxic effect of Pb on the predator. In the first scenario where Pb is introduced, dissolved Pb flows continuously into the reactor at a concentration of 1.0 μM. Figure 4.5 shows the temporal variation of five Pb compartments for this simulation: Pb adsorbed to predator, ingested Pb, Pb adsorbed to excreted waste material, dissolved Pb, and Pb adsorbed to prey.

The adsorption of Pb to waste material is the dominant sink for Pb in this continuous flow simulation, as it was in the batch reactor. The importance of waste matter as a Pb adsorbent is dependent upon the Pb adsorption distribution coefficient. As noted above, the adsorption constant for waste matter was set equal to 50 L/g under the assumption that the specific surface area of waste material would be higher than that of prey (25 L/g). Results for the simulation shown in Figure 4.5 with the adsorption constant for waste matter set equal to 25 L/g are shown in Figure 4.6; waste matter remains an important Pb sink under these conditions. If the adsorption constant for waste matter is set to 1 L/g then much of the excreted Pb is desorbed into the dissolved phase as is shown in Figure 4.7. [Note: regeneration of Cd associated with prey as dissolved Cd was observed by Twiss and Campbell [2]].

These simulations illustrate the importance of the Pb sequestration by waste matter in the model predictions. In the remaining simulations discussed below an

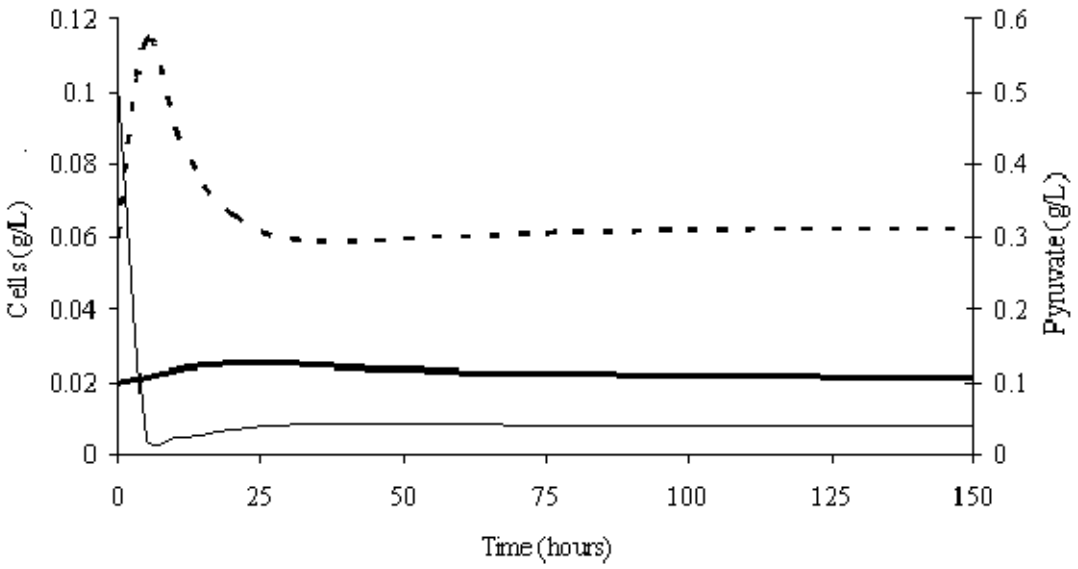

Figure 4.4. Cell density and pyruvate concentration when flow rate (Q) is tripled.

Predator

Prey

Pyruvate

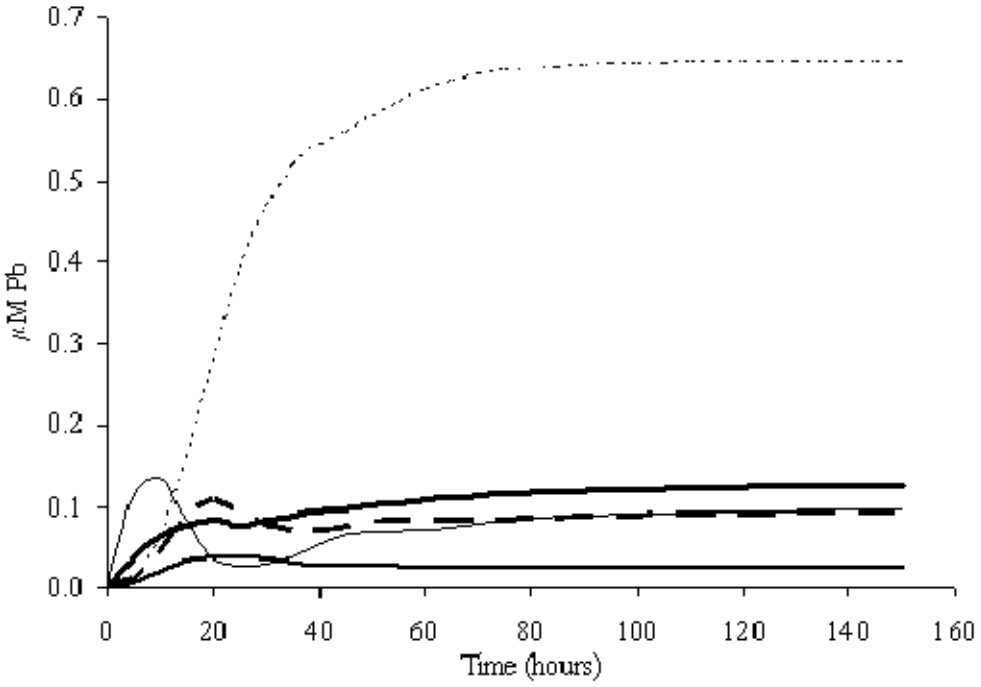

Figure 4.5. Temporal Pb distribution in Model 4.

——— $[Pb]_{adsorbed\ to\ predator}$
– – – $[Pb]_{ingested}$
..... $[Pb]_{adsorbed\ to\ waste\ material}$
——— $[Pb]_{dissolved}$
——— $[Pb]_{adsorbed\ to\ prey}$

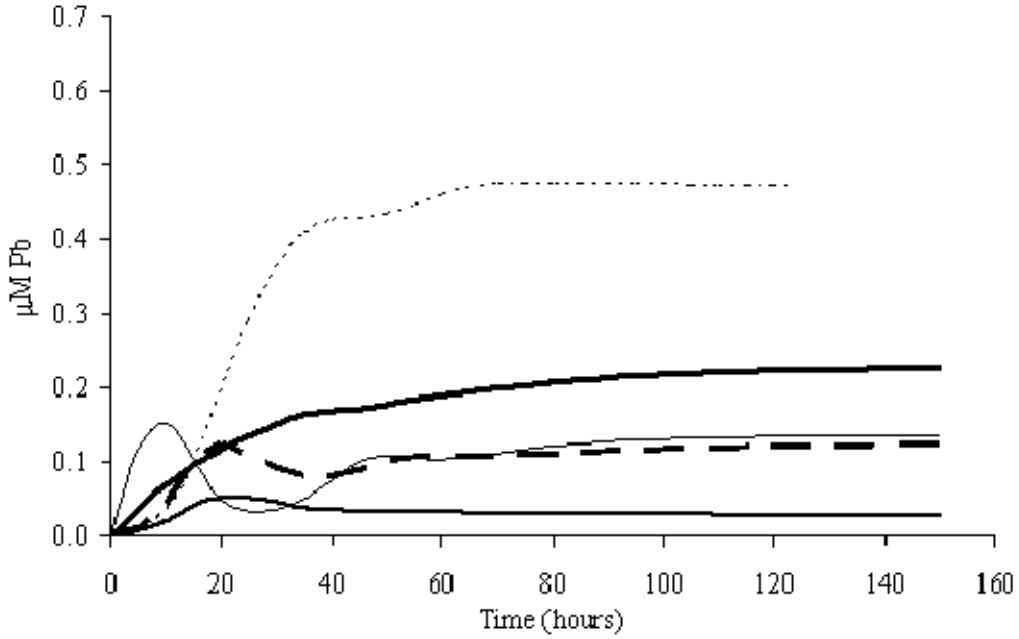

Figure 4.6. Model 4 Pb distribution where adsorption constant for Pb binding to waste matter is 25 L/g.

——— $[Pb]_{adsorbed\ to\ predator}$
– – – $[Pb]_{ingested}$
..... $[Pb]_{adsorbed\ to\ waste\ material}$
▬▬ $[Pb]_{dissolved}$
——— $[Pb]_{adsorbed\ to\ prey}$

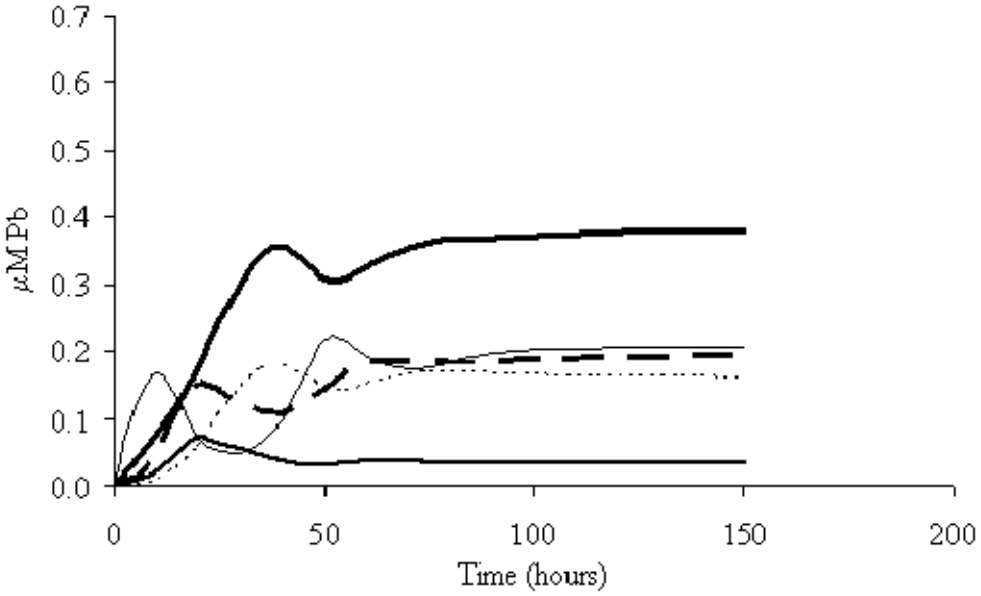

Figure 4.7. Model 4 Pb distribution where adsorption constant for Pb binding to waste matter is 1.0 L/g.

——— $[Pb]_{adsorbed\ to\ predator}$
– – – $[Pb]_{ingested}$
..... $[Pb]_{adsorbed\ to\ waste\ material}$
——— $[Pb]_{dissolved}$
——— $[Pb]_{adsorbed\ to\ prey}$

adsorption constant of 50 L/g was used for Pb onto waste material. The concentration of Pb adsorbed on the prey and predator change in Figures 4.5 through 4.7 in response to changes in the numbers of prey and predator which in turn are interdependent, as previously discussed. These cell dynamics approach a steady state at around 75 hours as shown in Figure 4.8.

In the next set of simulations the addition of Pb is delayed until after predator and prey cells have approached steady state (at 75 hours). In the first scenario, Pb is a continuous input. Figure 4.9 compares the changes in predator cell populations over time with no Pb, 0.5 or 1.0 μM Pb added continuously to the chemostat after populations have stabilized in the absence of Pb (the onset of the Pb addition is indicated by the arrow on the X axis). The overall effect of the Pb is a lower predator population at steady state. This makes sense based on the fact that predator growth parameters are negatively influenced by Pb (see Chapter 3). The decrease in the predator population occurs over a time frame of 30 hours after the onset of the Pb addition and is sensitive to the concentration of the Pb input.

The temporal distribution of Pb resulting from the continuous flow of 1.0 μM Pb into the chemostat starting after approaching steady state of the cell population is shown in Figure 4.10. As in the case where Pb was added at time 0, the pool of Pb adsorbed to waste material dominates over the other four pools. As noted above, the importance of waste material as a Pb sink is dependent upon the adsorption constant for that solid phase.

If the same mass of Pb is pulsed into the reactor at a regular interval of 20 hours, a similar pattern emerges but with oscillations corresponding to the addition of each pulse. The overall concentration of Pb is lower than in the continuous scenario since it partially washes out of the reactor between pulses (Figure 4.11).

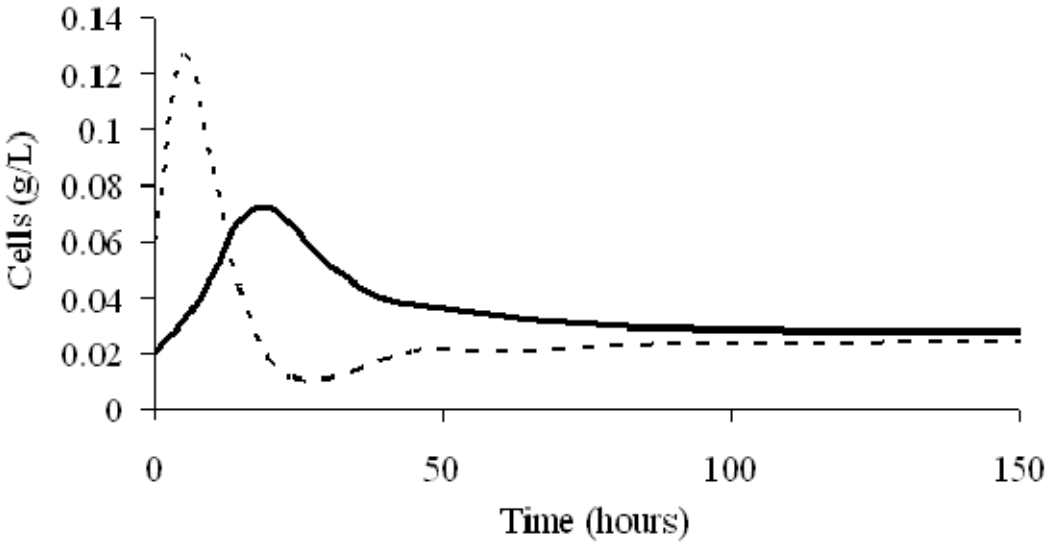

Figure 4.8. Cell densities when 1.0 μM Pb is added continuously to model reactors.

——— Predator

..... Prey

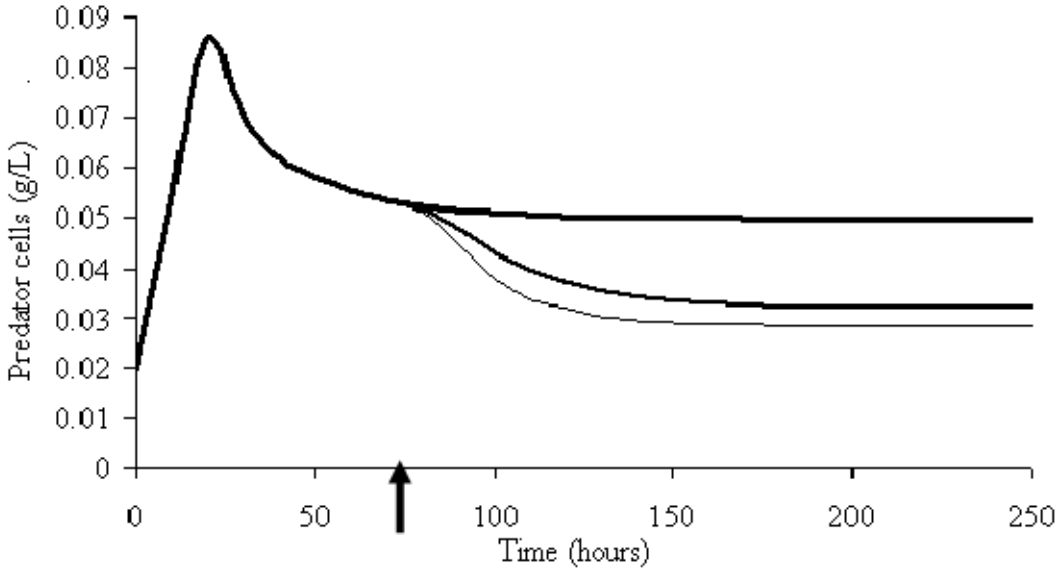

Figure 4.9. Effect of Pb on predator cell density over time.

No Pb

Constant flow of 0.5 μM Pb

Constant flow of 1.0 μM Pb

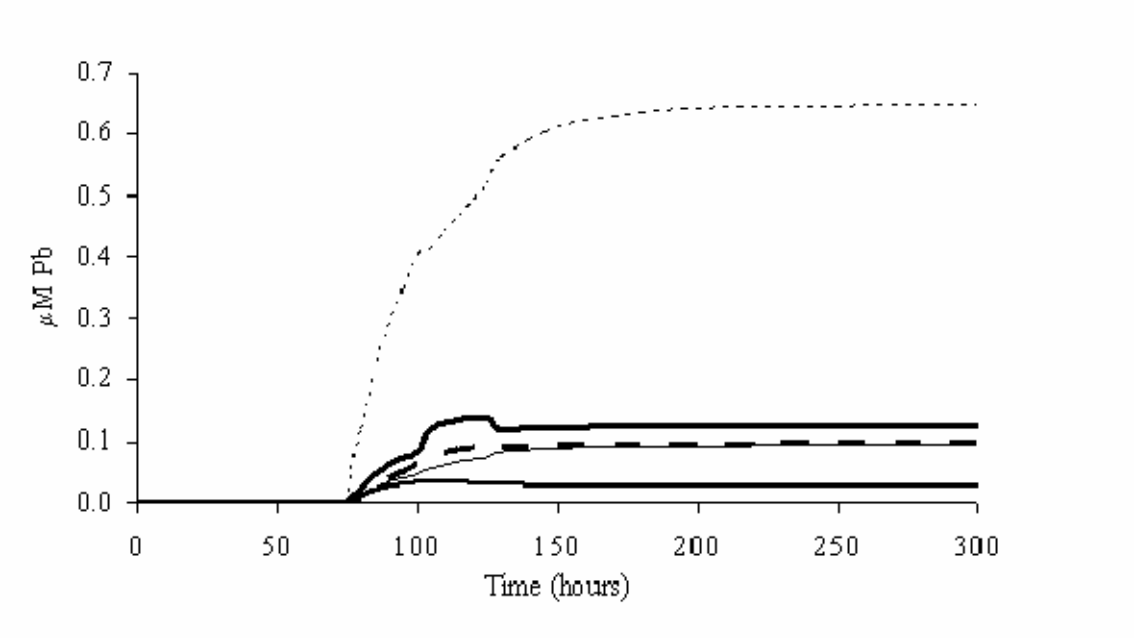

Figure 4.10. Temporal Pb distribution when Pb is added after cells have reached equilibrium.

——— $[Pb]_{adsorbed\ to\ predator}$
– – $[Pb]_{ingested}$
..... $[Pb]_{adsorbed\ to\ waste\ material}$
▬▬ $[Pb]_{dissolved}$
——— $[Pb]_{adsorbed\ to\ prey}$

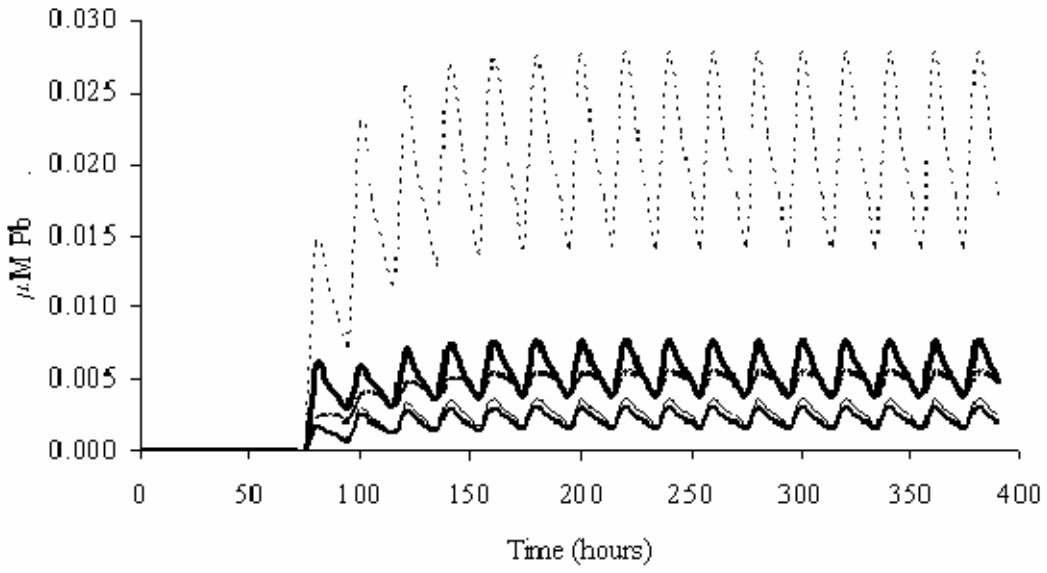

Figure 4.11. Temporal Pb distribution when Pb is added as a pulse every 20 hours.

——— $[Pb]_{adsorbed\ to\ predator}$
– – $[Pb]_{ingested}$
..... $[Pb]_{adsorbed\ to\ waste\ material}$
▬▬ $[Pb]_{dissolved}$
——— $[Pb]_{adsorbed\ to\ prey}$

The ability of Model 4 to predict metal partitioning in other systems was tested using data from the research of Michael Twiss and Peter G.C. Campbell in their paper "Regeneration of trace metals from picoplankton by nanoflagellate grazing" [2]. This study assessed metal partitioning between the dissolved phase, a cyanobacterium (*Synechococcus leopoliensis*) and a nanoflagellate bacterivore (*Ochromonas danica)* in a batch reactor. Bacteria were pretreated with radioactive metal (Gd, Zn, Cd, or Cs), rinsed with EDTA to remove extracellular adsorbed metals, and introduced to the predator for a 43-hour grazing experiment during which periodic metal analyses and cells counts were conducted. Metal partitioning was assessed using a serial filtration system to separate predator-sized particles (>3.0 μm) from prey-sized particles (0.2-3.0 μm) from the dissolved phase (<0.2 μm). The authors also measured the regeneration of metals from predator biomass to the dissolved phase following grazing.

Model 4 was modified to accommodate differences in experimental set-up, species growth parameters and metal properties. The modified model, referred to here as the "Twiss model" is for their batch system. New cell growth parameters were calculated using data given in Twiss & Campbell's Figure 2 and in the text of that paper. In-depth calculations relating to the Twiss model can be found in Appendix II. The simulations performed with the revised model that are presented here focus on Twiss and Campbell's results for Cd partitioning and regeneration. Table 4.3 summarizes values for initial conditions given by the authors.

Since the cell densities were given in units of cells/ml, dry weights for prey and predator were estimated. The average dry weight of *Synechococcus* cells was estimated to be 2.5×10^{-12} g/cell. The dry weight of *O. danica* was calculated to be 3×10^{-11} g/cell based on its cell volume (119 μm^3; [3] and conversion factors of 8.3 μm^3 cell/ pg carbon and a dry weight to carbon conversion factor of 0.45 [4]). Note

Table 4.3. Initial conditions given by Twiss & Campbell.

	Prey control	**Predator control**	**Prey (xenic)**	**Predator (xenic)**
Initial cell density (cells/ml)	1.20E+06	5.50E+03	2.00E+06	1.00E+04
Net growth (d^{-1})	7.30E-01	5.50E-01	-1.73E+00	8.60E-01
Initial [Cd] (μM)	6.90E-04	0.00E+00	6.90E-04	0.00E+00

that contrary to the previous Model 4, there was no added debris in the reactor as the authors made no mention of such particles in their inoculum at the start of the experiment. Because the contribution to ingested metal via dead cells was small in Model 4 it was not added to this model for the sake of simplicity.

Table 4.4 gives cell densities in units of cells/ml based on Figure 2 in the Twiss & Campbell paper. Growth/death rates were calculated as the difference in cell densities over time (Δ ln cells mL^{-1} /Δ t) and these are given in Table 4.5.

The maximum growth rate of *O. danica* (μ_{max_p}) was 0.17/hr (see Table 4.5) and the intrinsic death rate (k_{dp}) was calculated as the difference between net growth (given by the authors) and the overall growth rate (over the entire 43-hour experiment) and equaled 0.003/hr. A saturation constant (K_{Sp}) equal to $1.5x10^{-5}$ g^2/L^2 was calculated using least-squares regression to the double saturation model ($R^2 = 0.83$). The yield of predator cells growing on prey cells (Y_P) was calculated to be 0.27 g/g. The yields for predator growth on dead prey cells and dead predator cells were both assigned a value of 0.1 g/g. The intrinsic death rate for *Synechococcus* (k_{d_B}) was estimated as with k_{dp} to be 0.003/ hour. Details and examples of all calculations are given in Appendix II to this thesis.

Figure 4.12 shows the result of the model's simulation of predator and prey populations. The data are represented by symbols and the model simulations are lines. The model predicts cell numbers well.

The adsorption of Cd to *Synechococcus* cells was estimated using data in Table 2 of Twiss & Campbell's paper. The authors calculated that 2.2% of the 9.0 nM Cd was adsorbed to cell surfaces. The initial prey density in this experiment was $3.4x10^5$ cells/ml. Assuming no cell death over the 24-hour period of Cd exposure, and assuming a linear isotherm (the isotherm for Pb adsorption to *P. putida* is linear) the

Table 4.4. Cell densities in units of cells/ml. Data from Twiss & Campbell Figure 2.

Time (hours)	Prey control	Predator control	Prey (xenic)	Predator (xenic)
0	1.20E+06	5.50E+03	2.00E+06	1.00E+04
4	1.40E+06	1.00E+04	1.39E+06	2.00E+04
9	1.80E+06	1.75E+04	1.10E+06	2.50E+04
23	4.00E+06	2.10E+04	8.00E+05	4.00E+04
43	5.00E+06	1.90E+04	8.00E+04	5.25E+04

Table 4.5. Growth and death rates of cells (hour^{-1}).

Time interval (hours)	Prey control	Predator control	Prey (xenic)	Predator (xenic)
0 to 4	0.039	0.149	-0.091	0.173
4 to 9	0.050	0.112	-0.047	0.045
9 to 23	0.057	0.013	-0.023	0.034
23 to 43	0.011	-0.005	-0.115	0.014
0 to 43	*0.033*	*0.029*	*-0.075*	*0.039*

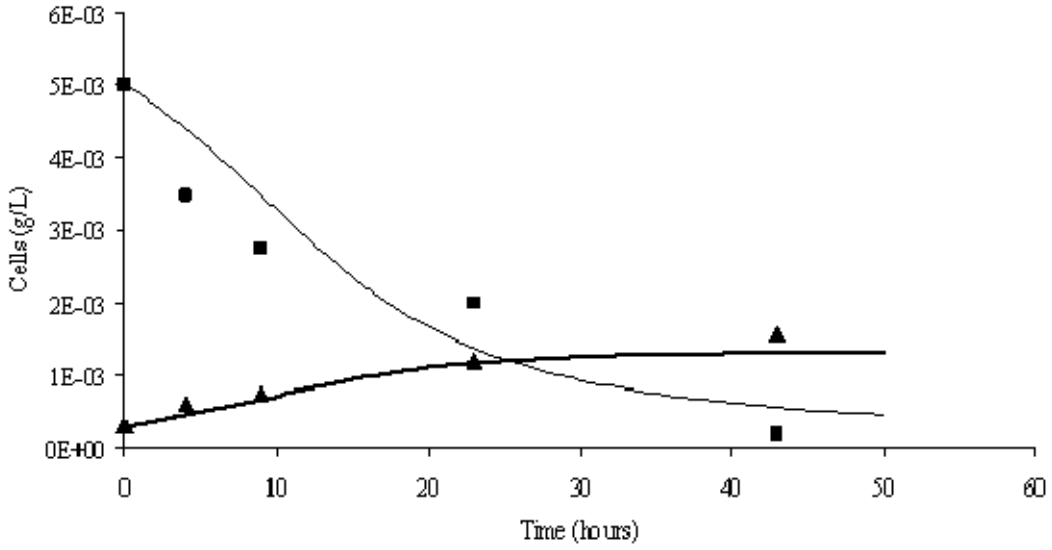

Figure 4.12. Model data fit with data from Twiss & Campbell (1995)

▲ Predator

——— Predator (model)

■ Prey

——— Prey (model)

adsorption constant for Cd binding to the surface of *Synechococcus* cells is 26 L/g (see Appendix II for details). This value is higher than adsorption constants for Cd binding to other bacteria cell surfaces, which are in the range 0.04 L/g (*Citrobacter*) [5] to 6.85 L/g (*Pseudomonas putida*) [6]. Therefore, a range of adsorption constants will be used in the model to find the best fit. The adsorption of Cd to *O. danica* was not discussed by Twiss and Campbell. The adsorption constant for Cd binding to *Pavlova viridis,* another alga, was 0.27 L/g (approximate value; [7]). Values for adsorption constants in this range were tested as with *Synechococcus* cells.

Twiss & Campbell showed that Cd regenerated from predators to the dissolved phase (up to 40% of the total Cd consumed, according to their Figure 4) and the regeneration rate increased with grazing rate. In Model 4 metal ingested by predators exited predators as metal adsorbed to excretion but could result in some metal regeneration to the dissolved phase through desorption. In the Twiss model, the metal is assumed to leave the predator in the dissolved phase. To account for the metal solubilization upon excretion, the release of dissolved metal via excretion was modeled as a first order rate dependent on the internal concentration of metal in the predator using a rate constant of $k_r = 0.28$/hr. This value was calculated from data given in the Twiss and Campbell paper and is the maximum increase in dissolved metal concentration over time ($\Delta \ln [Cd]_{dissolved} / \Delta t$).

In Twiss and Campbell, the partitioning of metal between the dissolved phase (<0.2-μm) and two particle size ranges: 0.2-3.0 μm (metal sorbed and ingested by bacteria as well as any associated with waste matter or other debris) and >3.0-μm (all predator-associated metal) was considered. In Model 4 particles included in the prey-sized range would also include dead prey cells and waste matter ("excretion" in the model equations). These data (from Twiss & Campbell Figure 3 for Cd) and results of

the first model simulation of the distribution of Cd over time are given in Figure 4.13 (solid lines).

The model predicts the metal in the prey size range relatively well in terms of both concentration and temporal trend. The binding constant for Cd and prey cells was set to 1.0 L/g but using a constant as high as 26 L/g did not change the model predictions significantly because metal in the prey size range was primarily internalized in prey cells, not adsorbed to their surface. Using a Cd-predator binding constant of 1.0 L/g, the metal in the predator size range is modeled fairly accurately until around 20 hours when the model predicts a decrease in the metal in this size range but the data show this concentration continuing to increase. Changing the Cd-predator binding constant from 0.27 to 26.0 L/g did not improve the fit to the data so the value of 1.0 L/g was retained.

Another factor influencing the overall phase distribution of metals is the distribution of those metals in the prey. For example, the degree of trace metal assimilation in bivalve larvae and copepods was directly related to the fraction of that metal originating in the cytoplasm of the phytoplankton prey [8]. Generally, metals and nonmetals with a necessary physiological function were found in the cytoplasmic fraction of prey organisms and were more available to predators via digestion. Metals like Cd that were nonessential tended to be associated with prey abiotically and had lower assimilation efficiencies in the predators [8]. In this study all metal presented to predators was associated with the cytoplasm of the prey. However, upon regeneration of dissolved metals some adsorption to cell surfaces takes place. Therefore there may be more than one regeneration constant necessary in this model: one for regeneration of the Cd originating from inside the prey (lower regeneration/ more assimilation) and one for Cd that was adsorbed to the prey surface (higher regeneration/less assimilation). Figure 4.13 (dotted lines) shows the simulation results when the

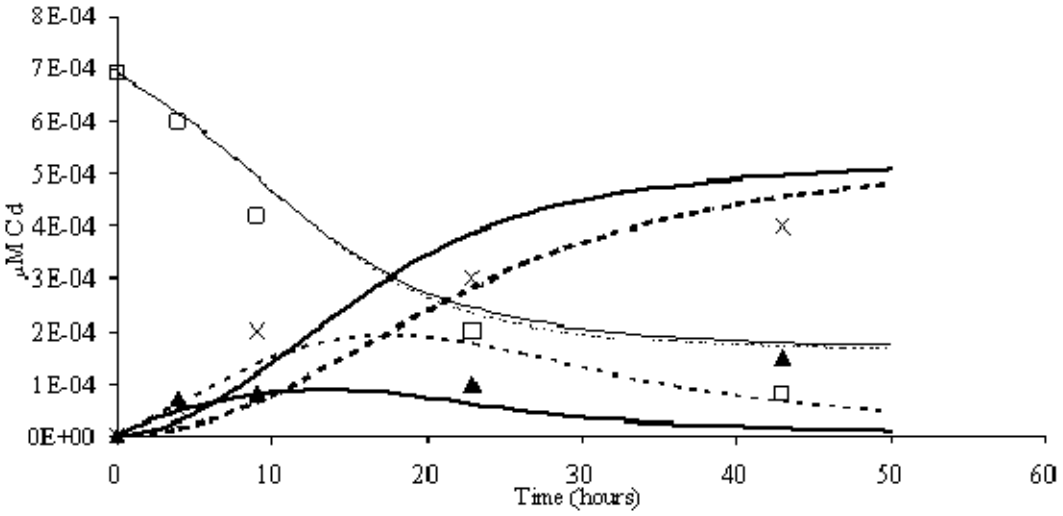

Figure 4.13. Temporal Cd distribution in Twiss & Campbell data and model predictions with a single versus multiple metal regeneration constant.

X Dissolved metal

Model fit of dissolved metal

Model fit of dissolved metal (multiple k_r)

□ Prey-sized metal (0.2-3.0 µm)

Model fit of prey-sized metal

Model fit of prey-sized metal (multiple k_r)

▲ Predator-sized metal (>3.0 µm)

Model fit of prey-sized metal

Model fit of prey-sized metal (multiple k_r)

regeneration constant (k_r) for metals originally adsorbed to prey was 0.28/ hr and k_r for metals originally internalized by prey cells was 0.1/ hr. These model results reflect the fact that more metal was assimilated into predator biomass and less was ultimately dissolved. This manipulation did not improve the model's fit to the data, however, particularly in the predator size range where model Cd concentrations are too high early on and too low after about 25 hours. Twiss and Campbell noted a correlation between the regeneration efficiency and the predation rate. The fit between the data and the model improves when k_r is modeled as a linear function of the predation rate. (Figure 4.14).

Through the research described in the second two chapters of this dissertation, a model was developed for the purpose of predicting Pb distribution in a predator-prey system. As shown in this chapter the model, with relatively minor modifications, can be extended to consider other reactor types, parameter values, and regimes of Pb-dosing. The model also appears to be suitable for describing the uptake and release of other trace metals. A key variable indicated by the model simulation is whether metal is excreted in dissolved or particulate form by the predator. In addition, the importance of waste matter as an adsorptive sink will be controlled by its isotherm for metal binding, and determination of metal equilibria with waste mater would be a fruitful area for future research.

The modeling approach presented here serves as a prototype for models that may eventually guide environmental management strategies in which an understanding is needed of the interplay between chemical and biological factors governing metal uptake and phase distribution, including prediction of toxic metal bioaccumulation in aquatic communities. Such applications include risk assessments, design of dredging and remediation practices, and the setting of future water quality criteria for metal discharge limits. This model would also be useful for predicting

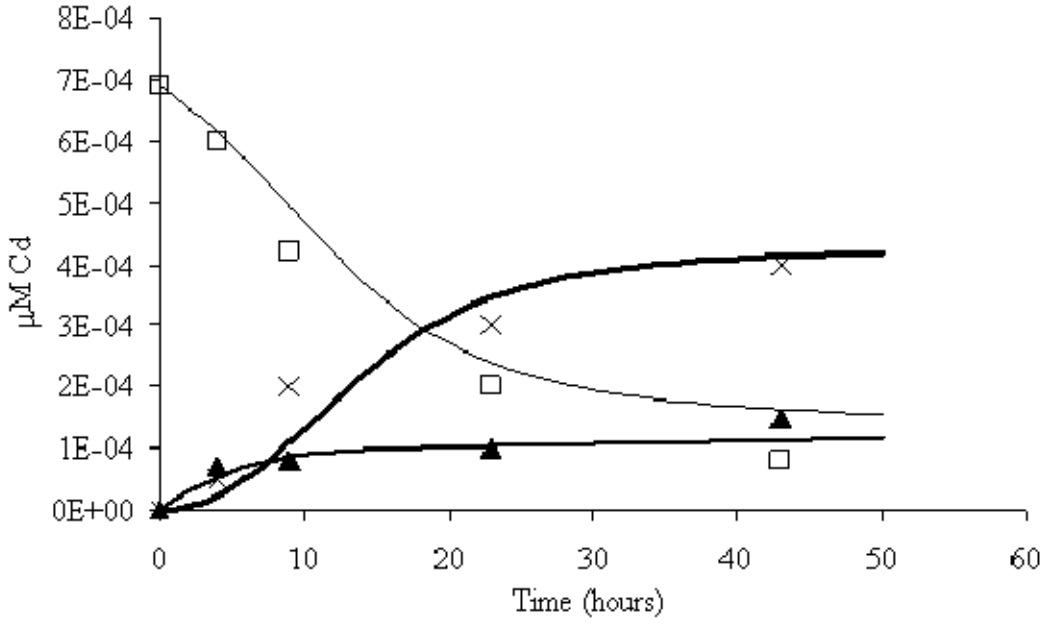

Figure 4.14. Temporal Cd distribution in Twiss & Campbell data and model predictions when k_r is dependent on the predation rate.

X Dissolved metal

Model fit of dissolved metal

□ Prey-sized metal (0.2-3.0 µm)

Model fit of prey-sized metal

▲ Predator-sized metal (>3.0 µm)

Model fit of prey-sized metal

metal removal in wastewater treatment systems such as activated sludge, for predicting bioaccumulation of metals in aerobic sediment, soil, and aquifer systems, and for predicting the fate of toxic metals in land-applied biosolids.

References

1. Hodson PV, Borgmann U, Shear H. 1979. Toxicity of copper to aquatic biota. In Nriagu, JO, ed, *Copper in the Environment Part II Health Effects*. Wiley-Interscience, New York, NY, USA.

2. Twiss MR, Campbell PGC. 1995. Regeneration of trace metals from picoplankton by nanoflagellate grazing. *Limnol Oceanogr* 40(8):1418-1429.

3. Chrzanowski T, Simek K. 1990. Prey-size selection by freshwater flagellated protozoa. Limnol Oceanogr 35(7):1429-1436.

4. Hansen B, Bjornsen PK, Hansen PJ. 1994. The size ratio between planktonic predators and their prey. Limnol Oceanogr 39(2):395-403.

5. Puranik PR, Paknikar KM. 1999. Biosorption of Lead, Cadmium, and Zinc by *Citrobacter* Strain MCMB-181: Characterization Studies. *Biotechnol Prog 15:* 228-237.

6. Pardo R, Herguedas M, Barrado E, Vega M. 2003. Biosorption of cadmium, copper, lead and zinc by inactive biomass of Pseudomonas putida. *Anal Bioanal Chem* 376:26-32.

7. Chen B, Huang Q, Lin X, Shi Q, Wu S. 1998. Accumulation of Ag, Cd, Co, Cu, Hg, Ni and Pb in *Pavlova viridis* Tseng (Haptophyceae*). J Appl Phycol* 10:371-376.

8. Reinfelder JR, Fisher NS. 1994. The assimilation of elemets ingested by marine planktonic bivalve larvae. *Limnol Oceanogr* 39(1):12-20.

CHAPTER V

CONCLUSIONS AND RECOMMENDATIONS FOR FUTURE RESEARCH

This dissertation consisted of the design and testing of a microbial predator-prey system for modeling the fate of Pb in the aquatic ecosystem. The first part of the research focused on the development of methods to differentiate processes for Pb uptake: adsorption, predation (phagocytosis), and pinocytosis. Experimental results showed relative contributions of prey and predator to metal sorption could be discerned using size selective filtration in combination with centrifugation. Other methods developed included the use of fluorescent microspheres as a suitable proxy for bacteria cells in a predator-prey model based on similar adsorption properties and the lack of preference of the predator *T. thermophila* to consume the microspheres versus actual bacteria.

In the second phase of the research a laboratory-scale model was implemented to assess the kinetics of microbial growth and predation and the effect of Pb on these parameters. Results demonstrated that some kinetic parameters related to prey consumption and growth of *T. thermophila* are altered by Pb concentration. Upon addition of predator to prey cells in equilibrium with dissolved Pb, dissolved and prey-bound Pb became associated with the predator through ingestion and adsorption. Ingested Pb was later excreted as a bound metal associated with *T. thermophila* waste matter. A preliminary mathematical model was developed to describe predator-prey dynamics and their influence on the behavior and fate of Pb. This preliminary model accurately fit *T. thermophila* growth curves under a range of Pb concentrations. Differences in independent model predictions and observations for the concentration of ingested Pb suggested the experimental methods used to quantify ingested Pb may have included another source of Pb such as debris (lysed cells, waste material) from

the initial inoculum of *T. thermophila* cells or another adsorptive surface in the reactor such as dead predator cells or predator waste material.

Additional exploration of the predator-prey system was accomplished in the next phase of the research using mathematical models. New model simulations evaluated the potential effect of predator ingestion of dead cells along with any associated metal, and the excretion and the reconsumption of waste material with adsorbed Pb. These simulations indicate that the consumption of waste matter is a likely explanation for the underestimation by the original model of the ingested Pb level.

The model for the predator prey system also permitted the consideration of replacing the batch predator-prey reactor with a continuous flow reactor. The overall temporal pattern of Pb distribution was not altered by changes in the timing of Pb exposure (Pb added at the time predators were introduced versus at the time when predator and prey popultions reached a steady state) or by repeated versus one-time Pb-exposures. Adsorption to waste matter was indicated to be an important contribution to phase distribution of Pb even when the originally estimated binding constant for Pb to waste was decreased by a factor of two. However, when the constant was lowered by a factor of fifty, the major component of total Pb was calculated to be the dissolved phase. This result underscores the importance of the metal-waste binding constant as a determinant of the phase distribution for Pb. This point is worth bearing in mind in light of experimental results of Twiss and Campbell who demonstrated that Cd associated with prey was regenerated to the dissolved phase following predation [1].

Results from this Twiss and Campbell paper were used as a test of the model developed in Chapter 4 to predict metal fate in other predator-prey systems. The

model was suitable for describing the uptake and release of Cd under the assumption that Cd was excreted in the dissolved form.

The modeling approach presented in this thesis serves as a prototype for models that may eventually guide environmental management strategies in which an understanding is needed of the interplay between chemical and biological factors governing metal uptake and phase distribution, including prediction of toxic metal bioaccumulation in aquatic communities. Such applications include risk assessments, design of dredging and remediation practices, and the setting of future water quality criteria for metal discharge limits. This model would also be useful for predicting metal removal in wastewater treatment systems such as activated sludge, for predicting bioaccumulation of metals in aerobic sediment, soil, and aquifer systems, and for predicting the fate of toxic metals in land-applied biosolids.

Areas for future research include more accurate estimations of certain predator growth parameters, particularly yield (Y_P) and the saturation constant (K_{Sp}), by using chemostats to evaluate these constants. Additionally, as mentioned above, the determination of metal equilibria with waste matter would be a worthwhile area for future research since the ultimate fate of metal in model simulations is dependent on the form in which metal is excreted and the adsorption of metal to waste matter.

The interaction of biogeochemical factors in the environment determines metal bioavailability and therefore metal fate in the predator-prey food web. A study of any of these interactions would enhance this model and extend its scope. Examples include changing the concentration of organic and inorganic ligands in the medium, addition of metal chelating agents, or addition of another adsorbent metal sink such as iron or manganese-oxides.

References

1. Twiss, Michael R and Campbell, Peter GC. Regeneration of trace metals from picoplankton by nanoflagellate grazing. *Limnol. Oceanogr*. 40(8) 1995, 1418-1429.

APPENDIX I

EQUATIONS FOR THE MODELS DESCRIBED IN THIS THESIS

Model 1

Dead_predator(t) = Dead_predator(t - dt) + (Pred_death) * dt
INIT Dead_predator = 0

INFLOWS:
Pred_death = Predator*kdp
Dissolved_pb(t) = Dissolved_pb(t - dt) + (- adsorb_desorb - adsorb_desorb2) * dt
INIT Dissolved_pb = .3

OUTFLOWS:
adsorb_desorb = Dissolved_pb*fast_adsorption_pred-
Pb_adsorbed_to_pred*fast_desorption_pred
adsorb_desorb2 = Dissolved_pb*fast_adsorption_prey-
Pb_adsorbed_to_prey*fast_desorption_prey
Ingested_Pb(t) = Ingested_Pb(t - dt) + (Ingestion_of_Pb_from_prey -
Pb_excretion_rate) * dt
INIT Ingested_Pb = 0

INFLOWS:
Ingestion_of_Pb_from_prey = predation_death_rate*umol_g_sorbed_to_prey
OUTFLOWS:
Pb_excretion_rate = Ingested_Pb*kw
Pb_adsorbed_to_pred(t) = Pb_adsorbed_to_pred(t - dt) + (adsorb_desorb) * dt
INIT Pb_adsorbed_to_pred = 0

INFLOWS:
adsorb_desorb = Dissolved_pb*fast_adsorption_pred-
Pb_adsorbed_to_pred*fast_desorption_pred
Pb_adsorbed_to_prey(t) = Pb_adsorbed_to_prey(t - dt) + (adsorb_desorb2 -
Ingestion_of_Pb_from_prey) * dt
INIT Pb_adsorbed_to_prey = .0992

INFLOWS:
adsorb_desorb2 = Dissolved_pb*fast_adsorption_prey-
Pb_adsorbed_to_prey*fast_desorption_prey
OUTFLOWS:
Ingestion_of_Pb_from_prey = predation_death_rate*umol_g_sorbed_to_prey
Pb_excreted(t) = Pb_excreted(t - dt) + (Pb_excretion_rate) * dt
INIT Pb_excreted = 0

INFLOWS:
Pb_excretion_rate = Ingested_Pb*kw
Predator(t) = Predator(t - dt) + (Pred_birth - Pred_death) * dt
INIT Predator = .024

INFLOWS:
Pred_birth = (umaxp*Prey*Prey*Predator)/(Ksp+Prey*Prey)
OUTFLOWS:
Pred_death = Predator*kdp
Prey(t) = Prey(t - dt) + (Prey_growth - predation_death_rate - intrinsic_prey_death) * dt
INIT Prey = .06

INFLOWS:
Prey_growth = ((umaxb*Pyruvate*Prey)/(Ksb+Pyruvate))
OUTFLOWS:
predation_death_rate = if Y_p=0 then Pred_birth/.0001 else Pred_birth/Y_p
intrinsic_prey_death = kdb*Prey
Pyruvate(t) = Pyruvate(t - dt) + (- pyruvate_depletion_by_prey) * dt
INIT Pyruvate = 0

OUTFLOWS:
pyruvate_depletion_by_prey = Prey_growth/Y_b
adsorption_constant_prey = 25
conc_diss_pb = Dissolved_pb/V
fast_adsorption_pred = adsorption_constant_pred*fast_desorption_pred*Predator
fast_adsorption_prey = adsorption_constant_prey*fast_desorption_prey*Prey
fast_desorption_pred = 100
fast_desorption_prey = 100
kdb = .003
kdp = .034
Ksb = .05
Ksp = .0003
kw = if (dissolved_pb) = 0 then 0 else -.0248*(dissolved_pb)+.113
tetra_per_ml_x1000 = (Predator*1.73*10^8)/(1000*1000)
umaxb = .4
umaxp = .23
umol_g_ingested = Ingested_Pb/Predator
umol_g_sorbed_to_pred = Pb_adsorbed_to_pred/Predator
umol_g_sorbed_to_prey = if Prey=0 then 0 else Pb_adsorbed_to_prey/Prey
V = 1
Y_b = .2
Y_p = .8

adsorption_constant_pred = GRAPH(conc_diss_pb) where the points on the graph are (x [dissolved Pb conc],y [adsorption constant predator]):
(0.01, 6.46), (0.0884, 6.46), (0.167, 6.46), (0.245, 4.72), (0.324, 4.12), (0.402, 3.58), (0.481, 3.04), (0.559, 2.51), (0.637, 1.97), (0.716, 1.43), (0.794, 0.889), (0.873, 0.346), (0.951, 0.2), (1.03, 0.01), (1.11, 0.005), (1.19, 0.005), (1.26, 0.005), (1.34, 0.005), (1.42, 0.005), (1.50, 0.005)

Model 2

added_debris(t) = added_debris(t - dt) + (- debris_eaten) * dt
INIT added_debris = INIT(Predator)
OUTFLOWS:
debris_eaten = debris_k*added_debris

Dissolved_pb(t) = Dissolved_pb(t - dt) + (- adsorb_desorb - adsorb_desorb2 - ads_des_debris) * dt
INIT Dissolved_pb = .3
OUTFLOWS:
adsorb_desorb = Dissolved_pb*fast_adsorption_pred-
Pb_adsorbed_to_pred*fast_desorption_pred
adsorb_desorb2 = Dissolved_pb*fast_adsorption_prey-
Pb_adsorbed_to_prey*fast_desorption_prey
ads_des_debris = Dissolved_pb*fast_ads_debris
-Pb_adsorbed_to_debris*fast_desorb_debris

excreted_debris(t) = excreted_debris(t - dt) + (excretion) * dt
INIT excreted_debris = 0
INFLOWS:
excretion = kw*ingested_debris

excreted_Pb(t) = excreted_Pb(t - dt) + (Pb_excretion_rate) * dt
INIT excreted_Pb = 0
INFLOWS:
Pb_excretion_rate = Ingested_Pb*kw

Excreted_prey(t) = Excreted_prey(t - dt) + (prey_excretion) * dt
INIT Excreted_prey = 0
INFLOWS:
prey_excretion = Ingested_prey*kw

ingested_debris(t) = ingested_debris(t - dt) + (debris_eaten - excretion) * dt
INIT ingested_debris = 0
INFLOWS:
debris_eaten = debris_k*added_debris
OUTFLOWS:
excretion = kw*ingested_debris

Ingested_Pb(t) = Ingested_Pb(t - dt) + (Ingestion_of_Pb_from_prey + debris_pb_ingested - Pb_excretion_rate) * dt
INIT Ingested_Pb = 0
INFLOWS:
Ingestion_of_Pb_from_prey = predation_death_rate*umol_g_sorbed_to_prey

```
debris_pb_ingested = debris_k*Pb_adsorbed_to_debris
OUTFLOWS:
Pb_excretion_rate = Ingested_Pb*kw

Ingested_prey(t) = Ingested_prey(t - dt) + (predation_death_rate - prey_excretion) * dt
INIT Ingested_prey = 0
INFLOWS:
predation_death_rate = if Y_p=0 then Pred_birth/.0001 else Pred_birth/Y_p
OUTFLOWS:
prey_excretion = Ingested_prey*kw

Pb_adsorbed_to_debris(t) = Pb_adsorbed_to_debris(t - dt) + (ads_des_debris -
debris_pb_ingested) * dt
INIT Pb_adsorbed_to_debris = 0
INFLOWS:
ads_des_debris = Dissolved_pb*fast_ads_debris
-Pb_adsorbed_to_debris*fast_desorb_debris
OUTFLOWS:
debris_pb_ingested = debris_k*Pb_adsorbed_to_debris

Pb_adsorbed_to_pred(t) = Pb_adsorbed_to_pred(t - dt) + (adsorb_desorb) * dt
INIT Pb_adsorbed_to_pred = 0
INFLOWS:
adsorb_desorb = Dissolved_pb*fast_adsorption_pred-
Pb_adsorbed_to_pred*fast_desorption_pred
Pb_adsorbed_to_prey(t) = Pb_adsorbed_to_prey(t - dt) + (adsorb_desorb2 –

Ingestion_of_Pb_from_prey) * dt
INIT Pb_adsorbed_to_prey = .0992
INFLOWS:
adsorb_desorb2 = Dissolved_pb*fast_adsorption_prey-
Pb_adsorbed_to_prey*fast_desorption_prey
OUTFLOWS:
Ingestion_of_Pb_from_prey = predation_death_rate*umol_g_sorbed_to_prey

Predator(t) = Predator(t - dt) + (Pred_birth - Pred_death) * dt
INIT Predator = .024
INFLOWS:
Pred_birth = (umaxp*Prey*Prey*Predator)/(Ksp+Prey*Prey)
OUTFLOWS:
Pred_death = Predator*kdp

Prey(t) = Prey(t - dt) + (Prey_growth - predation_death_rate - intrinsic_prey_death) *
dt
INIT Prey = .0636
```

INFLOWS:
Prey_growth = ((umaxb*Pyruvate*Prey)/(Ksb+Pyruvate))
OUTFLOWS:
predation_death_rate = if Y_p=0 then Pred_birth/.0001 else Pred_birth/Y_p
intrinsic_prey_death = kdb*Prey

Pyruvate(t) = Pyruvate(t - dt) + (- pyruvate_depletion_by_prey) * dt
INIT Pyruvate = 0
OUTFLOWS:
pyruvate_depletion_by_prey = Prey_growth/Y_b

adsorption_constant_prey = 25
adsorption_const_debris = 100
conc_diss_pb = Dissolved_pb/V
debris_k = 0.8
fast_adsorption_pred = adsorption_constant_pred*fast_desorption_pred*Predator
fast_adsorption_prey = adsorption_constant_prey*fast_desorption_prey*Prey
fast_ads_debris = adsorption_const_debris*fast_desorb_debris*added_debris
fast_desorb_debris = 100
fast_desorption_pred = 100
fast_desorption_prey = 100
kdb = .003
Ksb = .05
Ksp = if Dissolved_pb <0.66 then (0.001-Dissolved_pb*0.0015) else 1000
kw = if (dissolved_pb) = 0 then 0 else -.0248*(dissolved_pb)+.113
umaxb = .4
umol_g_debris = Pb_adsorbed_to_debris/added_debris
umol_g_ingested = Ingested_Pb/Predator
umol_g_sorbed_to_pred = Pb_adsorbed_to_pred/Predator
umol_g_sorbed_to_prey = if Prey=0 then 0 else Pb_adsorbed_to_prey/Prey
V = 1
Y_b = .2
adsorption_constant_pred = GRAPH(conc_diss_pb) where the points on the graph are (x [dissolved Pb conc],y [adsorption constant predator):
(0.01, 6.46), (0.0884, 6.46), (0.167, 6.46), (0.245, 4.72), (0.324, 4.12), (0.402, 3.58), (0.481, 3.04), (0.559, 2.51), (0.637, 1.97), (0.716, 1.43), (0.794, 0.889), (0.873, 0.346), (0.951, 0.2), (1.03, 0.01), (1.11, 0.005), (1.19, 0.005), (1.26, 0.005), (1.34, 0.005), (1.42, 0.005), (1.50, 0.005)
kdp = GRAPH(Dissolved_pb) where the points on the graph are (x [dissolved Pb conc],y [kdp):
(0.00, 0.005), (0.143, 0.035), (0.286, 0.035), (0.429, 0.035), (0.571, 0.035), (0.714, 0.0348), (0.857, 0.035), (1, 0.0348), (1.14, 0.0348), (1.29, 0.035), (1.43, 0.0348), (1.57, 0.0348), (1.71, 0.0348), (1.86, 0.0348), (2.00, 0.0348)
umaxp = GRAPH(Dissolved_pb) where the points on the graph are (x [dissolved Pb conc],y [umaxp]):

(0.00, 0.156), (0.357, 0.128), (0.714, 0.096), (1.07, 0.064), (1.43, 0.031), (1.79, 0.00), (2.14, 0.00), (2.50, 0.00), (2.86, 0.00), (3.21, 0.00), (3.57, 0.00), (3.93, 0.00), (4.29, 0.00), (4.64, 0.00), (5.00, 0.00)
Y_p = GRAPH(Dissolved_pb) where the points on the graph are (x [dissolved Pb conc],y [Y_p]):
(0.00, 0.8), (0.263, 0.695), (0.526, 0.59), (0.789, 0.486), (1.05, 0.00), (1.32, 0.00), (1.58, 0.00), (1.84, 0.00), (2.11, 0.00), (2.37, 0.00), (2.63, 0.00), (2.89, 0.00), (3.16, 0.00), (3.42, 0.00), (3.68, 0.00), (3.95, 0.00), (4.21, 0.00), (4.47, 0.00), (4.74, 0.00), (5.00, 0.00)

Model 3

added_debris(t) = added_debris(t - dt) + (- debris_eaten) * dt
INIT added_debris = .5*INIT(Predator)
OUTFLOWS:
debris_eaten = debris_k*added_debris

Dead_predator(t) = Dead_predator(t - dt) + (Pred_death - Pred_eats_pred) * dt
INIT Dead_predator = 0
INFLOWS:
Pred_death = Predator*kdp
OUTFLOWS:
Pred_eats_pred =
(umaxp*Dead_predator*Dead_predator*Predator)/(Ksp+Dead_predator^2)/Yp_dead_
pred

Dead_prey(t) = Dead_prey(t - dt) + (intrinsic_prey_death - pred_eat_dead_prey) * dt
INIT Dead_prey = 0
INFLOWS:
intrinsic_prey_death = kdb*Prey
OUTFLOWS:
pred_eat_dead_prey =
((umaxp*Dead_prey*Dead_prey*Predator)/(Ksp+Dead_prey*Dead_prey))/Ydead_pre
y

Dissolved_pb(t) = Dissolved_pb(t - dt) + (- adsorb_desorb - adsorb_desorb2 -
ads_des_excretion - ads_des_dead_pred - ads_des_debris - ads_des_dead_prey) * dt
INIT Dissolved_pb = .3
OUTFLOWS:
adsorb_desorb = Dissolved_pb*fast_adsorption_pred-
Pb_adsorbed_to_pred*fast_desorption_pred
adsorb_desorb2 = Dissolved_pb*fast_adsorption_prey-
Pb_adsorbed_to_prey*fast_desorption_prey
ads_des_excretion = Dissolved_pb*fast_adsorption_excreted
-fast_desorp_excreted*Pb_adsorbed_to_excretion
ads_des_dead_pred = Dissolved_pb*fast_adsorb_dead_pred-
Pb_adsorbed_to_dead_predators*fast_desorb_dead_pred
ads_des_debris = Dissolved_pb*fast_ads_debris
-Pb_adsorbed_to_debris*fast_desorb_debris
ads_des_dead_prey = Dissolved_pb*fast_ads_dead_prey
-Pb_ads_to_dead_prey*fast_desorption_prey

Excretion_in_water(t) = Excretion_in_water(t - dt) + (prey_excretion +
dead_predator_excretion + re_excreting + debris_excretion - eating_excretion) * dt
INIT Excretion_in_water = 0
INFLOWS:

```
prey_excretion = Ingested_prey*kw
dead_predator_excretion = kw*Ingested_predator
re_excreting = kw*Reingested_excretion
debris_excretion = ingested_debris*kw
OUTFLOWS:
eating_excretion =
IE*((umaxp*Excretion_in_water*Predator)/(Ksp+Excretion_in_water))

ingested_debris(t) = ingested_debris(t - dt) + (debris_eaten - debris_excretion) * dt
INIT ingested_debris = 0
INFLOWS:
debris_eaten = debris_k*added_debris
OUTFLOWS:
debris_excretion = ingested_debris*kw

Ingested_Pb(t) = Ingested_Pb(t - dt) + (Ingestion_of_Pb_from_prey +
pb_on_reingested_excretion + ingestion_of_pb_from_dead_preds +
debris_pb_ingested + ingestion_of_Pb_from_dead_prey - Pb_excretion_rate) * dt
INIT Ingested_Pb = 0
INFLOWS:
Ingestion_of_Pb_from_prey = predation_death_rate*umol_g_sorbed_to_prey
pb_on_reingested_excretion = eating_excretion*umol_g_on_excretion
ingestion_of_pb_from_dead_preds = Pred_eats_pred*umol_g_dead_pred
debris_pb_ingested = debris_k*Pb_adsorbed_to_debris
ingestion_of_Pb_from_dead_prey =
pred_eat_dead_prey*umol_g_sorbed_to_dead_prey
OUTFLOWS:
Pb_excretion_rate = Ingested_Pb*kw

Ingested_predator(t) = Ingested_predator(t - dt) + (Pred_eats_pred -
dead_predator_excretion) * dt
INIT Ingested_predator = 0
INFLOWS:
Pred_eats_pred =
(umaxp*Dead_predator*Dead_predator*Predator)/(Ksp+Dead_predator^2)/Yp_dead_
pred
OUTFLOWS:
dead_predator_excretion = kw*Ingested_predator

Ingested_prey(t) = Ingested_prey(t - dt) + (predation_death_rate +
pred_eat_dead_prey - prey_excretion) * dt
INIT Ingested_prey = 0
INFLOWS:
predation_death_rate = if Y_p=0 then Pred_birth/.0001 else Pred_birth/Y_p
```

pred_eat_dead_prey =
((umaxp*Dead_prey*Dead_prey*Predator)/(Ksp+Dead_prey*Dead_prey))/Ydead_pre
y
OUTFLOWS:
prey_excretion = Ingested_prey*kw

Pb_adsorbed_to_dead_predators(t) = Pb_adsorbed_to_dead_predators(t - dt) +
(ads_des_dead_pred - ingestion_of_pb_from_dead_preds) * dt
INIT Pb_adsorbed_to_dead_predators = 0
INFLOWS:
ads_des_dead_pred = Dissolved_pb*fast_adsorb_dead_pred-
Pb_adsorbed_to_dead_predators*fast_desorb_dead_pred
OUTFLOWS:
ingestion_of_pb_from_dead_preds = Pred_eats_pred*umol_g_dead_pred

Pb_adsorbed_to_debris(t) = Pb_adsorbed_to_debris(t - dt) + (ads_des_debris -
debris_pb_ingested) * dt
INIT Pb_adsorbed_to_debris = 0
INFLOWS:
ads_des_debris = Dissolved_pb*fast_ads_debris
-Pb_adsorbed_to_debris*fast_desorb_debris
OUTFLOWS:
debris_pb_ingested = debris_k*Pb_adsorbed_to_debris

Pb_adsorbed_to_excretion(t) = Pb_adsorbed_to_excretion(t - dt) + (Pb_excretion_rate
+ ads_des_excretion - pb_on_reingested_excretion) * dt
INIT Pb_adsorbed_to_excretion = 0
INFLOWS:
Pb_excretion_rate = Ingested_Pb*kw
ads_des_excretion = Dissolved_pb*fast_adsorption_excreted
-fast_desorp_excreted*Pb_adsorbed_to_excretion
OUTFLOWS:
pb_on_reingested_excretion = eating_excretion*umol_g_on_excretion

Pb_adsorbed_to_pred(t) = Pb_adsorbed_to_pred(t - dt) + (adsorb_desorb) * dt
INIT Pb_adsorbed_to_pred = 0
INFLOWS:
adsorb_desorb = Dissolved_pb*fast_adsorption_pred-
Pb_adsorbed_to_pred*fast_desorption_pred

Pb_adsorbed_to_prey(t) = Pb_adsorbed_to_prey(t - dt) + (adsorb_desorb2 –
Ingestion_of_Pb_from_prey) * dt
INIT Pb_adsorbed_to_prey = .0992
INFLOWS:

```
adsorb_desorb2 = Dissolved_pb*fast_adsorption_prey-
Pb_adsorbed_to_prey*fast_desorption_prey
OUTFLOWS:
Ingestion_of_Pb_from_prey = predation_death_rate*umol_g_sorbed_to_prey

Pb_ads_to_dead_prey(t) = Pb_ads_to_dead_prey(t - dt) + (ads_des_dead_prey -
ingestion_of_Pb_from_dead_prey) * dt
INIT Pb_ads_to_dead_prey = 0
INFLOWS:
ads_des_dead_prey = Dissolved_pb*fast_ads_dead_prey
-Pb_ads_to_dead_prey*fast_desorption_prey
OUTFLOWS:
ingestion_of_Pb_from_dead_prey =
pred_eat_dead_prey*umol_g_sorbed_to_dead_prey

Predator(t) = Predator(t - dt) + (Pred_birth - Pred_death) * dt
INIT Predator = .02
INFLOWS:
Pred_birth = (umaxp*Prey*Prey*Predator)/(Ksp+Prey*Prey)+
Pred_eats_pred*Yp_dead_pred+
pred_eat_dead_prey*Y_p
OUTFLOWS:
Pred_death = Predator*kdp

Prey(t) = Prey(t - dt) + (Prey_growth - predation_death_rate - intrinsic_prey_death) *
dt
INIT Prey = .06
INFLOWS:
Prey_growth = ((umaxb*Pyruvate*Prey)/(Ksb+Pyruvate))
OUTFLOWS:
predation_death_rate = if Y_p=0 then Pred_birth/.0001 else Pred_birth/Y_p
intrinsic_prey_death = kdb*Prey

Pyruvate(t) = Pyruvate(t - dt) + (- pyruvate_depletion_by_prey) * dt
INIT Pyruvate = 0.5
OUTFLOWS:
pyruvate_depletion_by_prey = Prey_growth/Y_b

Reingested_excretion(t) = Reingested_excretion(t - dt) + (eating_excretion -
re_excreting) * dt
INIT Reingested_excretion = 0
INFLOWS:
eating_excretion =
IE*((umaxp*Excretion_in_water*Predator)/(Ksp+Excretion_in_water))
OUTFLOWS:
```

re_excreting = kw*Reingested_excretion

adsorption_constant_prey = 25
adsorption_const_debris = 100
ads_const_excretion = 50
conc_diss_pb = Dissolved_pb/V
debris_k = .8
fast_adsorb_dead_pred =
adsorption_constant_pred*fast_desorb_dead_pred*Dead_predator
fast_adsorption_excreted =
Excretion_in_water*ads_const_excretion*fast_desorp_excreted
fast_adsorption_pred = adsorption_constant_pred*fast_desorption_pred*Predator
fast_adsorption_prey = adsorption_constant_prey*fast_desorption_prey*Prey
fast_ads_dead_prey = adsorption_constant_prey*fast_desorption_prey*Dead_prey
fast_ads_debris = adsorption_const_debris*fast_desorb_debris*added_debris
fast_desorb_dead_pred = 100
fast_desorb_debris = 100
fast_desorption_pred = 100
fast_desorption_prey = 100
fast_desorp_excreted = 100
IE = 0.1
kdb = .003
Ksb = .05
Ksp = if Dissolved_pb <0.66 then (0.001-Dissolved_pb*0.0015) else 1000
kw = -.0248*(Dissolved_pb)+.113
umaxb = .4
umol_g_dead_pred = if Dead_predator=0 then 0 else
Pb_adsorbed_to_dead_predators/Dead_predator
umol_g_debris = Pb_adsorbed_to_debris/added_debris
umol_g_ingested = Ingested_Pb/Predator
umol_g_on_excretion = if Excretion_in_water=0 then 0 else
Pb_adsorbed_to_excretion/Excretion_in_water
umol_g_sorbed_to_dead_prey = if Dead_prey=0 then 0 else
Pb_ads_to_dead_prey/Dead_prey
umol_g_sorbed_to_pred = Pb_adsorbed_to_pred/Predator
umol_g_sorbed_to_prey = if Prey=0 then 0 else Pb_adsorbed_to_prey/Prey
V = 1
Ydead_prey = .5
Yp_dead_pred = .5
Y_b = .2
adsorption_constant_pred = GRAPH(conc_diss_pb) where the points on the graph are
(x [dissolved Pb conc],y [adsorption constant predator]):
(0.01, 6.46), (0.0884, 6.46), (0.167, 6.46), (0.245, 4.72), (0.324, 4.12), (0.402, 3.58),
(0.481, 3.04), (0.559, 2.51), (0.637, 1.97), (0.716, 1.43), (0.794, 0.889), (0.873, 0.346),

(0.951, 0.2), (1.03, 0.01), (1.11, 0.005), (1.19, 0.005), (1.26, 0.005), (1.34, 0.005), (1.42, 0.005), (1.50, 0.005)
kdp = GRAPH(Dissolved_pb) where the points on the graph are (x [dissolved Pb conc],y [kdp]):
(0.00, 0.005), (0.143, 0.035), (0.286, 0.035), (0.429, 0.035), (0.571, 0.035), (0.714, 0.0348), (0.857, 0.035), (1, 0.0348), (1.14, 0.0348), (1.29, 0.035), (1.43, 0.0348), (1.57, 0.0348), (1.71, 0.0348), (1.86, 0.0348), (2.00, 0.0348)
umaxp = GRAPH(Dissolved_pb) where the points on the graph are (x [dissolved Pb conc],y [umaxp]):
(0.00, 0.156), (0.357, 0.128), (0.714, 0.096), (1.07, 0.064), (1.43, 0.031), (1.79, 0.00), (2.14, 0.00), (2.50, 0.00), (2.86, 0.00), (3.21, 0.00), (3.57, 0.00), (3.93, 0.00), (4.29, 0.00), (4.64, 0.00), (5.00, 0.00)
Y_p = GRAPH(Dissolved_pb) where the points on the graph are (x [dissolved Pb conc],y [Y_p]):
(0.00, 0.8), (0.263, 0.695), (0.526, 0.59), (0.789, 0.486), (1.05, 0.00), (1.32, 0.00), (1.58, 0.00), (1.84, 0.00), (2.11, 0.00), (2.37, 0.00), (2.63, 0.00), (2.89, 0.00), (3.16, 0.00), (3.42, 0.00), (3.68, 0.00), (3.95, 0.00), (4.21, 0.00), (4.47, 0.00), (4.74, 0.00), (5.00, 0.00)

Model 4

added_debris(t) = added_debris(t - dt) + (- debris_eaten) * dt
INIT added_debris = .5*INIT(Predator)
OUTFLOWS:
debris_eaten = debris_k*added_debris

Dead_predator(t) = Dead_predator(t - dt) + (Pred_death - Pred_eats_pred - Dead_pred_out) * dt
INIT Dead_predator = 0
INFLOWS:
Pred_death = Predator*kdp
OUTFLOWS:
Pred_eats_pred = (umaxp*Dead_predator*Dead_predator*Predator)/(Ksp+Dead_predator^2)/Yp_dead_pred
Dead_pred_out = (Q/V)*Dead_predator

Dead_prey(t) = Dead_prey(t - dt) + (intrinsic_prey_death - pred_eat_dead_prey - dead_prey_OUT) * dt
INIT Dead_prey = 0
INFLOWS:
intrinsic_prey_death = kdb*Prey
OUTFLOWS:
pred_eat_dead_prey = ((umaxp*Dead_prey*Dead_prey*Predator)/(Ksp+Dead_prey*Dead_prey))/Yp_dead_prey
dead_prey_OUT = (Q/V)*Dead_prey

Dissolved_pb(t) = Dissolved_pb(t - dt) + (add_pb - adsorb_desorb - adsorb_desorb2 - diss_Pb_out - ads_des_excretion - ads_des_dead_pred - ads_des_dead_prey) * dt
INIT Dissolved_pb = 0
INFLOWS:
add_pb = Delayed_continuous_pb_feed*Q/V
OUTFLOWS:
adsorb_desorb = Dissolved_pb*fast_adsorption_pred-Pb_adsorbed_to_pred*fast_desorption_pred
adsorb_desorb2 = Dissolved_pb*fast_adsorption_prey-Pb_adsorbed_to_prey*fast_desorption_prey
diss_Pb_out = Dissolved_pb*(Q/V)
ads_des_excretion = Dissolved_pb*fast_adsorption_excreted
-fast_desorp_excreted*Pb_adsorbed_to_excretion
ads_des_dead_pred = Dissolved_pb*fast_adsorb_dead_pred-Pb_adsorbed_to_dead_predators*fast_desorb_dead_pred
ads_des_dead_prey = Dissolved_pb*fast_ads_dead_prey
-Pb_ads_to_dead_prey*fast_desorption_prey

Excretion_in_water(t) = Excretion_in_water(t - dt) + (prey_excretion + dead_predator_excretion + re_excreting + debris_excretion - eating_excretion - excretion_out) * dt
INIT Excretion_in_water = 0
INFLOWS:
prey_excretion = Ingested_prey*kw
dead_predator_excretion = kw*Ingested_predator
re_excreting = kw*Reingested_excretion
debris_excretion = ingested_debris*kw
OUTFLOWS:
eating_excretion = IE*((umaxp*Excretion_in_water*Predator)/(Ksp+Excretion_in_water))
excretion_out = (Q/V)*Excretion_in_water

ingested_debris(t) = ingested_debris(t - dt) + (debris_eaten - debris_excretion) * dt
INIT ingested_debris = 0
INFLOWS:
debris_eaten = debris_k*added_debris
OUTFLOWS:
debris_excretion = ingested_debris*kw

Ingested_Pb(t) = Ingested_Pb(t - dt) + (Ingestion_of_Pb_from_prey + pb_on_reingested_excretion + ingestion_of_pb_from_dead_preds + ingestion_of_Pb_from_dead_prey - Pb_excretion_rate - Ingested_Pb_OUT) * dt
INIT Ingested_Pb = 0
INFLOWS:
Ingestion_of_Pb_from_prey = predation_death_rate*umol_g_sorbed_to_prey
pb_on_reingested_excretion = eating_excretion*umol_g_on_excretion
ingestion_of_pb_from_dead_preds = Pred_eats_pred*umol_g_dead_pred
ingestion_of_Pb_from_dead_prey = pred_eat_dead_prey*umol_g_sorbed_to_dead_prey
OUTFLOWS:
Pb_excretion_rate = Ingested_Pb*kw
Ingested_Pb_OUT = umol_g_ingested*Pred_out

Ingested_predator(t) = Ingested_predator(t - dt) + (Pred_eats_pred - dead_predator_excretion - Ingested_pred_out) * dt
INIT Ingested_predator = 0
INFLOWS:
Pred_eats_pred = (umaxp*Dead_predator*Dead_predator*Predator)/(Ksp+Dead_predator^2)/Yp_dead_pred
OUTFLOWS:
dead_predator_excretion = kw*Ingested_predator

Ingested_pred_out = Ingested_predator*Flow_out_w_predator

Ingested_prey(t) = Ingested_prey(t - dt) + (predation_death_rate +
pred_eat_dead_prey - prey_excretion - ingested_prey_out) * dt
INIT Ingested_prey = 0
INFLOWS:
predation_death_rate = if Y_p=0 then Pred_birth/.0001 else Pred_birth/Y_p
pred_eat_dead_prey =
((umaxp*Dead_prey*Dead_prey*Predator)/(Ksp+Dead_prey*Dead_prey))/Yp_dead_
prey
OUTFLOWS:
prey_excretion = Ingested_prey*kw
ingested_prey_out = Ingested_prey*Flow_out_w_predator

Pb_adsorbed_to_dead_predators(t) = Pb_adsorbed_to_dead_predators(t - dt) +
(ads_des_dead_pred - ingestion_of_pb_from_dead_preds - Pb_on_dead_preds_OUT)
* dt
INIT Pb_adsorbed_to_dead_predators = 0
INFLOWS:
ads_des_dead_pred = Dissolved_pb*fast_adsorb_dead_pred-
Pb_adsorbed_to_dead_predators*fast_desorb_dead_pred
OUTFLOWS:
ingestion_of_pb_from_dead_preds = Pred_eats_pred*umol_g_dead_pred
Pb_on_dead_preds_OUT = umol_g_dead_pred*Dead_pred_out

Pb_adsorbed_to_excretion(t) = Pb_adsorbed_to_excretion(t - dt) + (Pb_excretion_rate
+ ads_des_excretion - pb_on_reingested_excretion - Excretion_Pb_OUT) * dt
INIT Pb_adsorbed_to_excretion = 0
INFLOWS:
Pb_excretion_rate = Ingested_Pb*kw
ads_des_excretion = Dissolved_pb*fast_adsorption_excreted
-fast_desorp_excreted*Pb_adsorbed_to_excretion
OUTFLOWS:
pb_on_reingested_excretion = eating_excretion*umol_g_on_excretion
Excretion_Pb_OUT = umol_g_on_excretion*excretion_out

Pb_adsorbed_to_pred(t) = Pb_adsorbed_to_pred(t - dt) + (adsorb_desorb -
Pb_on_pred_OUT) * dt
INIT Pb_adsorbed_to_pred = 0
INFLOWS:
adsorb_desorb = Dissolved_pb*fast_adsorption_pred-
Pb_adsorbed_to_pred*fast_desorption_pred
OUTFLOWS:
Pb_on_pred_OUT = Pred_out*umol_g_sorbed_to_pred

Pb_adsorbed_to_prey(t) = Pb_adsorbed_to_prey(t - dt) + (adsorb_desorb2 - Ingestion_of_Pb_from_prey - Pb_on_prey_OUT) * dt
INIT Pb_adsorbed_to_prey = 0
INFLOWS:
adsorb_desorb2 = Dissolved_pb*fast_adsorption_prey-
Pb_adsorbed_to_prey*fast_desorption_prey
OUTFLOWS:
Ingestion_of_Pb_from_prey = predation_death_rate*umol_g_sorbed_to_prey
Pb_on_prey_OUT = umol_g_sorbed_to_prey*Prey_out

Pb_ads_to_dead_prey(t) = Pb_ads_to_dead_prey(t - dt) + (ads_des_dead_prey - ingestion_of_Pb_from_dead_prey - Pb_on_dead_prey_out) * dt
INIT Pb_ads_to_dead_prey = 0
INFLOWS:
ads_des_dead_prey = Dissolved_pb*fast_ads_dead_prey
-Pb_ads_to_dead_prey*fast_desorption_prey
OUTFLOWS:
ingestion_of_Pb_from_dead_prey =
pred_eat_dead_prey*umol_g_sorbed_to_dead_prey
Pb_on_dead_prey_out = umol_g_sorbed_to_dead_prey*dead_prey_OUT

Predator(t) = Predator(t - dt) + (Pred_birth - Pred_death - Pred_out) * dt
INIT Predator = .02
INFLOWS:
Pred_birth = (umaxp*Prey*Prey*Predator)/(Ksp+Prey*Prey)+
Pred_eats_pred*Yp_dead_pred+
pred_eat_dead_prey*Y_p
OUTFLOWS:
Pred_death = Predator*kdp
Pred_out = (Q/V)*Predator

Prey(t) = Prey(t - dt) + (Prey_growth - predation_death_rate - Prey_out - intrinsic_prey_death) * dt
INIT Prey = .06
INFLOWS:
Prey_growth = ((umaxb*Pyruvate*Prey)/(Ksb+Pyruvate))
OUTFLOWS:
predation_death_rate = if Y_p=0 then Pred_birth/.0001 else Pred_birth/Y_p
Prey_out = (Q/V)*Prey
intrinsic_prey_death = kdb*Prey

Pyruvate(t) = Pyruvate(t - dt) + (pyruvate_in - pyruvate_depletion_by_prey - pyruvate_out) * dt
INIT Pyruvate = 0.5
INFLOWS:

pyruvate_in = Q*pyruvate_feed_conc/V
OUTFLOWS:
pyruvate_depletion_by_prey = Prey_growth/Y_b
pyruvate_out = (Q/V)*Pyruvate

Reingested_excretion(t) = Reingested_excretion(t - dt) + (eating_excretion - re_excreting - reing_excretion_OUT) * dt
INIT Reingested_excretion = 0
INFLOWS:
eating_excretion = IE*((umaxp*Excretion_in_water*Predator)/(Ksp+Excretion_in_water))
OUTFLOWS:
re_excreting = kw*Reingested_excretion
reing_excretion_OUT = Reingested_excretion*Flow_out_w_predator

adsorption_constant_prey = 25
ads_const_excretion = 50
conc_diss_pb = Dissolved_pb/V
continuous_pb_feed = 1
debris_k = .8
Delayed_continuous_pb_feed = (delay(0,75,0))
delayed_pulse_pb_feed = (pulse (Q/V*1*20,75,20))
fast_adsorb_dead_pred = adsorption_constant_pred*fast_desorb_dead_pred*Dead_predator
fast_adsorption_excreted = Excretion_in_water*ads_const_excretion*fast_desorp_excreted
fast_adsorption_pred = adsorption_constant_pred*fast_desorption_pred*Predator
fast_adsorption_prey = adsorption_constant_prey*fast_desorption_prey*Prey
fast_ads_dead_prey = adsorption_constant_prey*fast_desorption_prey*Dead_prey
fast_desorb_dead_pred = 100
fast_desorption_pred = 100
fast_desorption_prey = 100
fast_desorp_excreted = 100
Flow_out_w_predator = Pred_out*Predator
IE = 0.1
kdb = .003
Ksb = .05
Ksp = if Dissolved_pb <0.66 then (0.001-Dissolved_pb*0.0015) else 1000
kw = -.0248*(Dissolved_pb)+.113
pyruvate_feed_conc = 0.5
Q = .04
umaxb = .4
umol_g_dead_pred = if Dead_predator=0 then 0 else Pb_adsorbed_to_dead_predators/Dead_predator
umol_g_ingested = Ingested_Pb/Predator

umol_g_on_excretion = if Excretion_in_water=0 then 0 else
Pb_adsorbed_to_excretion/Excretion_in_water
umol_g_sorbed_to_dead_prey = if Dead_prey=0 then 0 else
Pb_ads_to_dead_prey/Dead_prey
umol_g_sorbed_to_pred = Pb_adsorbed_to_pred/Predator
umol_g_sorbed_to_prey = if Prey=0 then 0 else Pb_adsorbed_to_prey/Prey
V = 1
Yp_dead_pred = .5
Yp_dead_prey = .5
Y_b = .2
adsorption_constant_pred = GRAPH(conc_diss_pb) where the points on the graph are (x [dissolved Pb conc],y [adsorption constant predator]):
(0.01, 6.46), (0.0884, 6.46), (0.167, 6.46), (0.245, 4.72), (0.324, 4.12), (0.402, 3.58), (0.481, 3.04), (0.559, 2.51), (0.637, 1.97), (0.716, 1.43), (0.794, 0.889), (0.873, 0.346), (0.951, 0.2), (1.03, 0.01), (1.11, 0.005), (1.19, 0.005), (1.26, 0.005), (1.34, 0.005), (1.42, 0.005), (1.50, 0.005)
kdp = GRAPH(Dissolved_pb) where the points on the graph are (x [dissolved Pb conc],y [kdp]):
(0.00, 0.005), (0.143, 0.035), (0.286, 0.035), (0.429, 0.035), (0.571, 0.035), (0.714, 0.0348), (0.857, 0.035), (1, 0.0348), (1.14, 0.0348), (1.29, 0.035), (1.43, 0.0348), (1.57, 0.0348), (1.71, 0.0348), (1.86, 0.0348), (2.00, 0.0348)
umaxp = GRAPH(Dissolved_pb) where the points on the graph are (x [dissolved Pb conc],y [umaxp]):
(0.00, 0.156), (1.61, 0.00115), (3.23, 0.00), (4.84, 0.00), (6.45, 0.00), (8.06, 0.00), (9.68, 0.00), (11.3, 0.00), (12.9, 0.00), (14.5, 0.00), (16.1, 0.00), (17.7, 0.00), (19.4, 0.00), (21.0, 0.00), (22.6, 0.00), (24.2, 0.00), (25.8, 0.00), (27.4, 0.00), (29.0, 0.00), (30.6, 0.00), (32.3, 0.00), (33.9, 0.00), (35.5, 0.00), (37.1, 0.00), (38.7, 0.00), (40.3, 0.00), (41.9, 0.00), (43.5, 0.00), (45.2, 0.00), (46.8, 0.00), (48.4, 0.00), (50.0, 0.00), (51.6, 0.00), (53.2, 0.00), (54.8, 0.00), (56.5, 0.00), (58.1, 0.00), (59.7, 0.00), (61.3, 0.00), (62.9, 0.00), (64.5, 0.00), (66.1, 0.00), (67.7, 0.00), (69.4, 0.00), (71.0, 0.00), (72.6, 0.00), (74.2, 0.00), (75.8, 0.00), (77.4, 0.00), (79.0, 0.00), (80.6, 0.00), (82.3, 0.00), (83.9, 0.00), (85.5, 0.00), (87.1, 0.00), (88.7, 0.00), (90.3, 0.00), (91.9, 0.00), (93.5, 0.00), (95.2, 0.00), (96.8, 0.00), (98.4, 0.00), (100.0, 0.00)
Y_p = GRAPH(Dissolved_pb) where the points on the graph are (x [dissolved Pb conc],y [Y_p]):
(0.00, 0.8), (0.263, 0.695), (0.526, 0.59), (0.789, 0.486), (1.05, 0.00), (1.32, 0.00), (1.58, 0.00), (1.84, 0.00), (2.11, 0.00), (2.37, 0.00), (2.63, 0.00), (2.89, 0.00), (3.16, 0.00), (3.42, 0.00), (3.68, 0.00), (3.95, 0.00), (4.21, 0.00), (4.47, 0.00), (4.74, 0.00), (5.00, 0.00)

Twiss Model

adsorbed_M_ingested_by_predator(t) = adsorbed_M_ingested_by_predator(t - dt) + (ingestion_of_adsorbed_M + Noname_1 - M_regeneration_high) * dt
INIT adsorbed_M_ingested_by_predator = 0
INFLOWS:
ingestion_of_adsorbed_M = predation_rate*umol_g_sorbed_to_prey
Noname_1 = eating_fecal_matter*umol_g_on_FM
OUTFLOWS:
M_regeneration_high = if kr2<0 then 0 else
adsorbed_M_ingested_by_predator*kr2

Dead_predator(t) = Dead_predator(t - dt) + (Pred_death - Pred_eats_pred) * dt
INIT Dead_predator = 0
INFLOWS:
Pred_death = Predator*kdp
OUTFLOWS:
Pred_eats_pred =
(umaxp*Dead_predator*Dead_predator*Predator)/(Ksp+Dead_predator^2)/Yp_dead_pred

Dead_prey(t) = Dead_prey(t - dt) + (intrinsic_prey_death - pred_eat_dead_prey) * dt
INIT Dead_prey = 0
INFLOWS:
intrinsic_prey_death = kdb*Prey
OUTFLOWS:
pred_eat_dead_prey =
((umaxp*Dead_prey*Dead_prey*Predator)/(Ksp+Dead_prey*Dead_prey))/Yp_dead_prey

Dissolved_M(t) = Dissolved_M(t - dt) + (M_regeneration_low + M_regeneration_high - ads_des_pred - adsorb_desorb_prey - ads_des_fecal - ads_des_dead_prey - ads_des_dead_pred) * dt
INIT Dissolved_M = 0
INFLOWS:
M_regeneration_low = internalized_ingested_metal*kr
M_regeneration_high = if kr2<0 then 0 else
adsorbed_M_ingested_by_predator*kr2
OUTFLOWS:
ads_des_pred = Dissolved_M*fast_adsorption_pred-
M_adsorbed_to_pred*fast_desorption_pred
adsorb_desorb_prey = Dissolved_M*fast_adsorption_prey-
M_adsorbed_to_prey*fast_desorption_prey
ads_des_fecal = Dissolved_M*fast_adsorption_FM
-fast_desorp_FM*M_on_fecal_matter
ads_des_dead_prey = Dissolved_M*fast_ads_dead_prey

-M_ads_to_dead_prey*fast_desorption_prey
ads_des_dead_pred = Dissolved_M*fast_adsorb_dead_pred-
M_adsorbed_to_dead_pred*fast_desorb_dead_pred

Fecal_matter_in_water(t) = Fecal_matter_in_water(t - dt) + (re_excreting_FM +
prey_excretion + dead_predator_excretion - eating_fecal_matter) * dt
INIT Fecal_matter_in_water = 0
INFLOWS:
re_excreting_FM = kw*Reingested_FM
prey_excretion = Ingested_prey*kw
dead_predator_excretion = kw*Ingested_predator
OUTFLOWS:
eating_fecal_matter =
IE*((umaxp*Fecal_matter_in_water*Predator)/(Ksp+Fecal_matter_in_water))

Ingested_predator(t) = Ingested_predator(t - dt) + (Pred_eats_pred -
dead_predator_excretion) * dt
INIT Ingested_predator = 0
INFLOWS:
Pred_eats_pred =
(umaxp*Dead_predator*Dead_predator*Predator)/(Ksp+Dead_predator^2)/Yp_dead_
pred
OUTFLOWS:
dead_predator_excretion = kw*Ingested_predator

Ingested_prey(t) = Ingested_prey(t - dt) + (predation_rate + pred_eat_dead_prey -
prey_excretion) * dt
INIT Ingested_prey = 0
INFLOWS:
predation_rate = Pred_birth/Y_p
pred_eat_dead_prey =
((umaxp*Dead_prey*Dead_prey*Predator)/(Ksp+Dead_prey*Dead_prey))/Yp_dead_
prey
OUTFLOWS:
prey_excretion = Ingested_prey*kw

internalized_ingested_metal(t) = internalized_ingested_metal(t - dt) +
(ingestion_of_internalized_M - M_regeneration_low) * dt
INIT internalized_ingested_metal = 0
INFLOWS:
ingestion_of_internalized_M = umol_g_inside_of_prey*predation_rate
OUTFLOWS:
M_regeneration_low = internalized_ingested_metal*kr

M_adsorbed_to_dead_pred(t) = M_adsorbed_to_dead_pred(t - dt) +
(ads_des_dead_pred) * dt
INIT M_adsorbed_to_dead_pred = 0
INFLOWS:
ads_des_dead_pred = Dissolved_M*fast_adsorb_dead_pred-
M_adsorbed_to_dead_pred*fast_desorb_dead_pred

M_adsorbed_to_pred(t) = M_adsorbed_to_pred(t - dt) + (ads_des_pred) * dt
INIT M_adsorbed_to_pred = 0
INFLOWS:
ads_des_pred = Dissolved_M*fast_adsorption_pred-
M_adsorbed_to_pred*fast_desorption_pred

M_adsorbed_to_prey(t) = M_adsorbed_to_prey(t - dt) + (adsorb_desorb_prey -
ingestion_of_adsorbed_M) * dt
INIT M_adsorbed_to_prey = 0
INFLOWS:
adsorb_desorb_prey = Dissolved_M*fast_adsorption_prey-
M_adsorbed_to_prey*fast_desorption_prey
OUTFLOWS:
ingestion_of_adsorbed_M = predation_rate*umol_g_sorbed_to_prey

M_ads_to_dead_prey(t) = M_ads_to_dead_prey(t - dt) + (ads_des_dead_prey) * dt
INIT M_ads_to_dead_prey = 0
INFLOWS:
ads_des_dead_prey = Dissolved_M*fast_ads_dead_prey
-M_ads_to_dead_prey*fast_desorption_prey

M_inside_prey(t) = M_inside_prey(t - dt) + (- ingestion_of_internalized_M) * dt
INIT M_inside_prey = .00069
OUTFLOWS:
ingestion_of_internalized_M = umol_g_inside_of_prey*predation_rate

M_on_fecal_matter(t) = M_on_fecal_matter(t - dt) + (ads_des_fecal - Noname_1) * dt
INIT M_on_fecal_matter = 0
INFLOWS:
ads_des_fecal = Dissolved_M*fast_adsorption_FM
-fast_desorp_FM*M_on_fecal_matter
OUTFLOWS:
Noname_1 = eating_fecal_matter*umol_g_on_FM

Predator(t) = Predator(t - dt) + (Pred_birth - Pred_death) * dt
INIT Predator = 3*10^-4
INFLOWS:
Pred_birth = (umaxp*Prey*Prey*Predator)/(Ksp+Prey*Prey)

OUTFLOWS:
Pred_death = Predator*kdp

Prey(t) = Prey(t - dt) + (- predation_rate - intrinsic_prey_death) * dt
INIT Prey = 5*10^-3
OUTFLOWS:
predation_rate = Pred_birth/Y_p
intrinsic_prey_death = kdb*Prey

Reingested_FM(t) = Reingested_FM(t - dt) + (eating_fecal_matter - re_excreting_FM) * dt
INIT Reingested_FM = 0
INFLOWS:
eating_fecal_matter = IE*((umaxp*Fecal_matter_in_water*Predator)/(Ksp+Fecal_matter_in_water))
OUTFLOWS:
re_excreting_FM = kw*Reingested_FM

adsorption_constant_PRED = 1
adsorption_constant_prey = 1
ads_const_FM = 50
conc_diss_M = Dissolved_M/V
fast_adsorb_dead_pred = adsorption_constant_PRED*fast_desorb_dead_pred*Dead_predator
fast_adsorption_FM = Fecal_matter_in_water*ads_const_FM*fast_desorp_FM
fast_adsorption_pred = adsorption_constant_PRED*fast_desorption_pred*Predator
fast_adsorption_prey = adsorption_constant_prey*fast_desorption_prey*Prey
fast_ads_dead_prey = adsorption_constant_prey*fast_desorption_prey*Dead_prey
fast_desorb_dead_pred = 100
fast_desorption_pred = 100
fast_desorption_prey = 100
fast_desorp_FM = 100
IE = 0.1
kdb = .003
kdp = .003
kr = 0.1
kr2 = .28
Ksp = 1.53*10^-5
kw = 0.1
predator_size_metal = M_adsorbed_to_pred+internalized_ingested_metal+M_adsorbed_to_dead_pred+adsorbed_M_ingested_by_predator
prey_sized_metal = M_inside_prey+M_adsorbed_to_prey+M_ads_to_dead_prey+M_on_fecal_matter

umaxp = .17
umol_g_inside_of_prey = M_inside_prey/Prey
umol_g_on_FM = if Fecal_matter_in_water=0 then 0 else
M_on_fecal_matter/Fecal_matter_in_water
umol_g_sorbed_to_dead_prey = if Dead_prey=0 then 0 else
M_ads_to_dead_prey/Dead_prey
umol_g_sorbed_to_prey = M_adsorbed_to_prey/Prey
V = 1
Yp_dead_pred = .1
Yp_dead_prey = .1
Y_p = .27

APPENDIX II

CALCULATIONS BASED ON DATA FROM TWISS AND CAMPBELL PAPER REFERENCED IN CHAPTER 4

Growth/death parameter calculations

1. Growth rate

Example calculation for data in Table 4.5:

Growth rate of control predators from 0-4 hours

$= (\ln 1x10^4 - \ln 5.5x10^3)/(4-0)$

$=0.149/$ hour

2. $\mu_{max_P} = 0.17$/hour based on the highest growth rate of xenic predators in Table 4.5.

3. $k_{dP} = 0.003$/hour

Calculation of k_{dp}:

(Overall growth for prey/ hour from 0-43 hrs as shown in Table 4.5)*24 hrs = Overall growth rate/day.

0.039*24 = 0.93 /d

Overall growth rate/ d – Net growth/ d = Death rate/ d

0.93 – 0.86 = 0.07 /d

= 0.003/hour

4. $k_{dB} = 0.003$/hour (see calculation for k_{dP} for details)

5. $K_{SP} = 1.5x10^{-5}\ g^2/L^2$

Calculated using least squares regression of growth rate of predator on prey to the Monod and double saturation equations (see Figure A2.1).

6. $Y_P = 0.28$ g/g (see Figure A2.2).

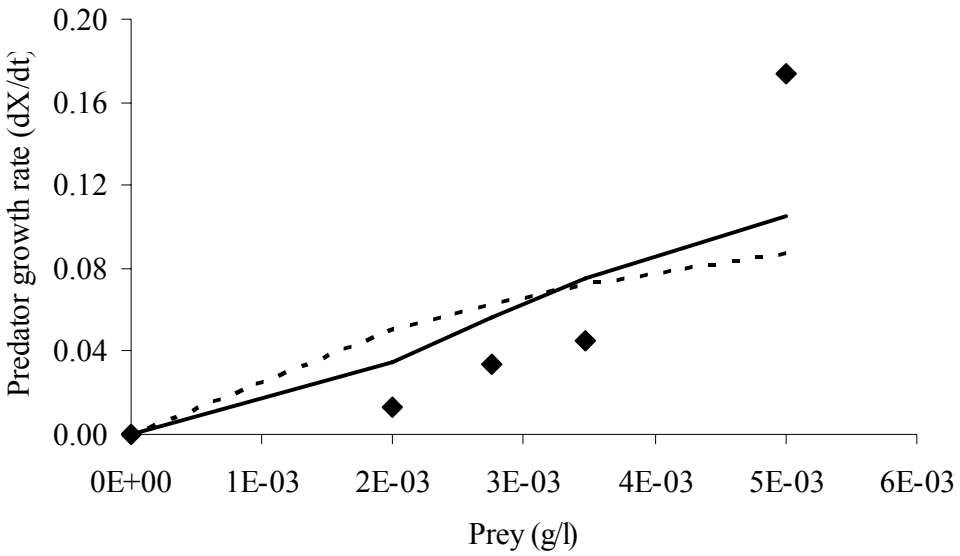

Figure A2.1. Calculation of the saturation constant for predator cells (K_{Sp}) in Twiss model. Symbols represent data points and lines represent model predictions:

♦ Predator growth rate

——— Monod model fit of predator growth rate

– – – Double saturation model fit of predator growth rate

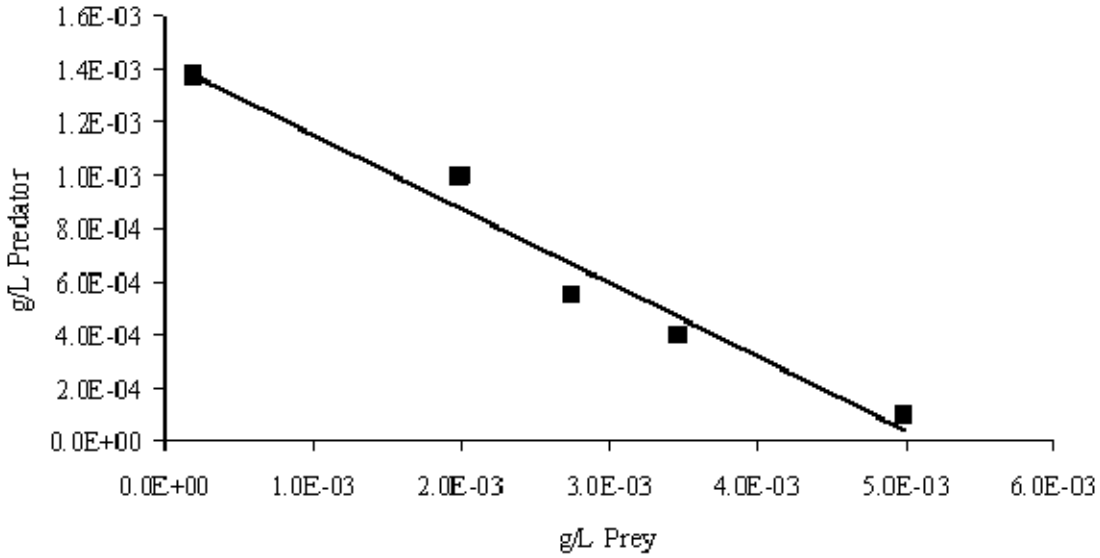

Figure A2.2. Calculation of yield for predator cells growing on prey cells (Y_P) in the Twiss model. Diamonds are data and line is linear fit of data.

Calculation of Cd-Synechococcus adsorption isotherm.

Given: $3.4*10^{-5}$ cells/ml were exposed to 9.0 nM Cd and that 2.2% (0.198 nM) of that Cd became adsorbed to cells when equilibrium Cd concentration = 0.0088 μM. Therefore the concentration of Cd adsorbed/g dry wt. cells

= (0.198 nmol Cd/L) / ($2.5*10^{-12}$grams dry wt./cell) / ($3.4*10^{-5}$cell/ml) / (1000 ml/L) / (1000 nmol/μmol)

= 0.23 μmol Cd/g adsorbed to *Synechococcus* cells and the linear adsorption constant is 26.5 L/g (see Figure A2.3).

Estimation of Cd regeneration rate constant (k_r)

Table data from Twiss & Campbell Figure 3:

Time	Dissolved Cd (μM) in xenic reactor
0	0.0E+00
4	5.0E-05
9	2.0E-04
23	3.0E-04
43	4.0E-04

$k_r = (\ln [Cd]_{dissolved\ @\ T9} - \ln [Cd]_{dissolved\ @\ T4})/9 - 4$ hrs

$= \ln (2*10^{-4}) - \ln (5*10^{-5})$ / 5 hrs

= 0.28/hour

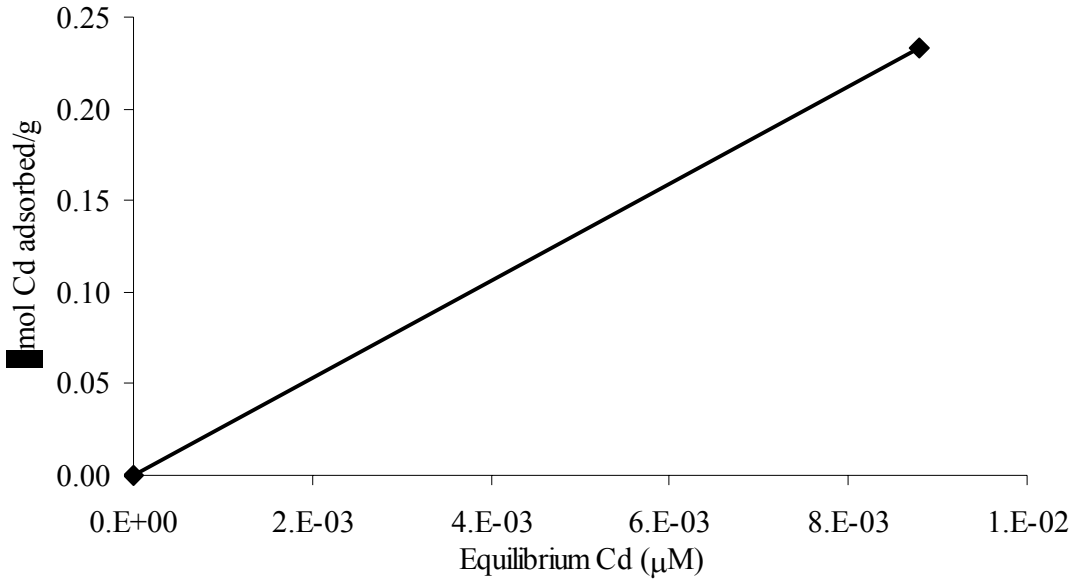

Figure A2.3. Calculation of Cd-Synechococcus adsorption isotherm